Clin Exp Nephrol
DOI 10.1007/s10157-015-1180-5

ORIGINAL ARTICLE

Clinical and genetic characteristics of Japanese nephronophthisis patients

Keisuke Sugimoto[1] · Tomoki Miyazawa[1] · Takuji Enya[1] · Hitomi Nishi[1] · Kohei Miyazaki[1] · Mitsuru Okada[1] · Tsukasa Takemura[1]

Received: 30 August 2015 / Accepted: 4 October 2015

Abstract
Background Nephronophthisis (NPH) accounts for 4–5 % of end-stage renal disease occurring in childhood.
Method We investigated the clinical context and characteristics of renal and extrarenal symptoms, as well as the *NPHP* genes, in 35 Japanese patients with clinical and histologic features suggesting NPH.
Results NPH occurred fairly uniformly throughout Japan irrespective of region or gender. In three families, NPH affected siblings. The median age of patients was 12.5 years. Renal abnormalities attributable to NPH discovered through mass screening, such as urine tests in school. However, NPH accounted for less than 50 % of children with abnormal findings, including incidentally discovered renal dysfunction during evaluation of extrarenal symptoms or during routine check-ups. Typical extrarenal manifestations leaded to discovery including anemia and delayed physical development. The urine often showed low gravity specific density and low molecular weight proteinuria. Frequent renal histologic findings included cystic dilation of tubules, mainly in the medulla, and irregularity of tubular basement membranes. Genetically abnormalities of *NPHP1* were not common, with large deletions frequently noted. Compound heterozygotes showing single abnormalities in each of *NPHP1*, *NPHP3*, and *NPHP4* were observed.
Conclusions Our findings resemble those reported in Western populations.

✉ Keisuke Sugimoto
ksugimo@med.kindai.ac.jp

[1] Department of Pediatrics, Kinki University Faculty of Medicine, 377-2 Ohno-higashi, Osaka-Sayama 589-8511, Japan

Keywords End-stage renal disease · Renal cysts · *NPHP* genes · Children · Renal tubules

Introduction

Nephronophthisis (NPH) is a disease characterized by renal medullary cyst formation. Additional histologic findings include tubulointerstitial nephritis accompanied by progressive sclerosis and hyaline glomeruli. Although NPH characteristically shows autosomal recessive inheritance, it may occur sporadically [1]. NPH accounts for approximately 4–5 % of end-stage renal disease (ESRD) in childhood. Disease subtypes include: infantile NPH (NPH2), which progresses to ESRD around the age of 5 years; juvenile NPH (NPH1), which develops from early childhood to school age and usually progresses to ESRD by an age of about 13 or 14 years; and adolescent NPH (NPH3), with development of ESRD at an average age of 19 years. Juvenile NPH is reported to be the most common subtype [1].

NPHP1, the gene most often responsible for juvenile nephronophthisis, encodes the nephrocystin-1 molecule. This gene has an extent of approximately 11 kbp, and is located on chromosome 2q12-13 [2]. The nephrocystin-1 protein consists of 677 amino acids and includes three coiled domains; two highly acidic negatively charged glutamic acid-rich domains; and an Src-homology 3 domain. Nephrocystin-1 has a molecular weight of 83 kD. As this protein is located in the transition zone of primary cilia of renal tubular epithelial cells, its abnormalities typically cause dysfunction of these primary cilia (ciliopathy) [1, 2].

NPHP4, whose abnormalities cause a second form of NPH1, is located on chromosome 1p36 and encodes the nephrocystin-4 (nephroretinin) molecule. Nephrocystin-4

Published online: 23 October 2015

Primers for *NPHP1*

exon	F primer	5′-nucleotide sequence -3′	R primer	5′-nucleotide sequence -3′	Amprified fragment length (bp)
exon1	NPHP1E01F010	GACCACCGCAAGAGAACATTT	NPHP1E01R010	AAGCTCCCAGGATTAGGTGGG	319
exon2	NPHP1E02F010	GGTATATGGGTTTTCACTGTA	NPHP1E02R010	TTCCATTTGATTCCAAAGGAC	319
exon3	NPHP1E03F010	TAATTGCCTTGCCTGCTCAAC	NPHP1E03R010	CAGACTTAGCAAGCCTGTTCG	320
exon4	NPHP1E04F010	GATAGGTGTAATGTCACACTG	NPHP1E04R010	CATGGGATCTAACACCTTCTA	418
exon5	NPHP1E05F010	CCAGCTCCAAATATGGGATAT	NPHP1E05R010	CAGGTGTACAGGCAGAGTTTTC	380
exon6	NPHP1E06F010	GGGAAGCTTTTGATAAACCTT	NPHP1E06R010	GTCATTCACTAGTCAACTGAC	349
exon7	NPHP1E07F010	GTTTTTGTTTTTACTGGAGGG	NPHP1E07R010	GTTGTCTCCATTTCAAGAAAG	306
exon8	NPHP1E08F010	CTCGTTTTCATCTGGAAACTG	NPHP1E08R010	GGAAAGCAGGATCAATGAGAA	443
exon9	NPHP1E09F010	CTTCCACTAAAGTCTGTATGT	NPHP1E09R010	GTGAGATTCAACATCTTCTTC	322
exon10	NPHP1E10F010	TTTGGAAGTGCCTGTACTCTA	NPHP1E10R010	GTCCAAATTCTGCCTTAGTTA	360
exon11	NPHP1E11F010	GCCTGCCAATATTTATTGTTCC	NPHP1E11R010	TACTCTCTTGGGAATTGGGGA	494
exon12	NPHP1E12F010	TCCTCACTTAGTGTAGCCACT	NPHP1E12R010	GTCCTCAAAGAACACCAAAGA	302
exon13	NPHP1E13F010	CACCTTCAACATTGGGATTAC	NPHP1E13R010	CATTCTCATTCCTCAAGGGAT	365
exon14	NPHP1E14F010	GCAAAATGAGATTCTACTGTG	NPHP1E14R010	AGTTATTGGCATGCTCATAGA	342
exon15	NPHP1E15F010	GGCATAAATGAAATGTCTGAG	NPHP1E15R010	GTCTCATATGTGTTACCAAGA	374
exon16	NPHP1E16F010	GCACTACTGGGTGGTATATTT	NPHP1E16R010	GGGAAGAATTAAAGAGGACAA	330
exon17	NPHP1E17F010	GAAGCAAAATTTGGGACTGTT	NPHP1E17R010	AAAGTCACAACCAGAAACAGA	316
exon18	NPHP1E18F010	CCTAGAAGTCAAAGTGTGTAG	NPHP1E18R010	GGAGACATCATCCTAGTAACA	326
exon19	NPHP1E19F010	CAGCATTTTTAACCCTGTCCA	NPHP1E19R010	GGGATTATGACTATGGCTACT	261
exon20	NPHP1E20F010	CCCTCCATCCTACCTCTTAGG	NPHP1E20R010	CTAAGTTGTAAAGTGACAGTG	478

Primers for *NPHP2*

exon	F primer	5′-nucleotide sequence -3′	R primer	5′-nucleotide sequence -3′	Amprified fragment length (bp)
5UTR	I5Uf1	TTTCCCATTGGGCTCTCGGCC	I5Ur1	TGAGTCTGCAGCAGGGGCCAA	366
exon1	IEx1F	CCCACTTGGAACTGATGAGAC	IEx1R	AACAAACTTCCTCAGGACAAAC	265
exon2	IEx2F	ATAATAAACAGCGAATATAGTTCCTAC	IEx2R	TGTCCATTGCATAGTTCCAC	327
exon3	IEx3F	GTGGAATTACAAGCATTTTTCC	IEx3R	AATTCAGGCCTTCTTCCTTG	411
exon4	IEx4F	TTGTTACTGTTGTTATTTCGAGAACC	IEx4R	ACTTCTTGGGGGATGAGTCC	356
exon5	IEx5F	CACCAAATGTAATTTATTGAGGATTC	IEx5R	AGTGGAAGGGAAGGCACAG	317
exon6	IEx6F	CTGCTGTTCAGAAACCGTTG	IEx6R	GGTGTAGGAGTGCAAAAAGC	421
exon7	IEx7F	AGGGGAAAATGCTTTGCTTC	IEx7R	AATTTTATAGCAACATCTACACTTTGG	351
exon8	IEx8F	GATGGGGAAATCAAGAGAGG	IEx8R	TGTGCAGCTTTCTGCTAAGG	348
exon9	IEx9F	CCATAAGAATAAAGCATTAAAGGAAC	IEx9R	TGTGGGTGATCTCTTCATCTTG	494
exon10	IEx10F	CCACATATCCAAAAATACTTACTCC	IEx10R	AGAAAGGATGTATGATAAAGAGCAC	528
exon11	IEx11F	TTCCACATCTTAGAATGAAGTTTCC	IEx11R	CTCATCTGTTTCCCTCTCCTG	427
exon12	IEx12F	CACACAGAGACTTGAGGAGGTG	IEx12R	CGGCAGAAGATGACAAAGG	382
exon13	IEx13F	TGTAACTGCCACTATTATGGTGATG	IEx13R	CACCACATGGAACTCACTGG	939
exon14	IEx14F	AATGGGAGCTTGAATGAACC	IEx14R	TGGTACTCTGGGGGTACTTG	410
exon15	IEx15F	CACACACCTGCAAGCTCAAG	IEx15R	TCTTTGGGGATGAAACAAAGG	255
exon16	IEx16F	CCAATGAACTATTCCCTTCAGC	IEx16R	GCAGAAAATCTGAACTCTGCAC	242

Fig. 1 Genomic DNA extraction, PCR, and determination of *NPHP1, 2, 3* and *4* gene sequence. PCR primers were prepared to amplify approximately 200–300 bp fragments based on *NPHP 1–4* gene sequences registered in GenBank, the following primers were used as shown

has been shown to carry out signal transmission between renal tubular epithelial cells, in cooperation with nephrocystin-1 [3].

NPHP2, the gene responsible for infantile NPH (NPH2), is located on 9q22-31 [4]. *NPHP2* encodes a protein termed inversin (INVS). An abnormality in INVS can cause situs inversus, pancreatic islet-cell dysplasia, cardiovascular abnormalities, and hepato-biliary disorders. In addition, INVS abnormalities can cause cyst formation resembling that in juvenile nephronophthisis. However, the renal prognosis is worse progression to ESRD in early childhood.

The gene responsible for adolescent NPH (NPH3), *NPHP3* is located on chromosome 3q21-22 [5]. *NPHP3* is believed to encode a protein involved in signal

Primers for *NPHP3*

exon	F primer	5′-nucleotide sequence -3′	R primer	5′-nucleotide sequence -3′	Amprified fragment length (bp)
exon1	NPHP4E01F010	ATGCAAATCAGGATGGGCCCG	NPHP4E01R010	AACCCACGTAGCCAAACGGCA	598
exon2	NPHP4E02F010	AGGTTCCTCTGGGATTTAGTG	NPHP4E02R010	AATCAAAGCATCGTAAGCCAG	373
exon3	NPHP4E03F010	TGATATCTGAGCGAGGTGGCC	NPHP4E03R010	AAGTCTGAGACGCGCTGTGAG	368
exon4	NPHP4E04F010	TGCTGTGGCACGTGTAGGAAG	NPHP4E04R010	ACTGCACTCTAGCCTGGTTGA	379
exon5	NPHP4E05F010	AAAGCTCTAGTGGGCGTGGTG	NPHP4E05R010	CAGATAGCAGTTTACACTGAG	273
exon6	NPHP4E06F010	CCTGTTTGTGGTGTTTCTAAC	NPHP4E06R010	TTCCATCCTCCTCCACTGTCC	426
exon7	NPHP4E07F030	TGGAGGAGGTTTGGGGTAGAT	NPHP4E07R020	AGGGGAAAAGACAGAACTACA	569
exon8	NPHP4E08F010	CTGCTCCAGTTTCTTCTCTCT	NPHP4E08R010	TCCCACGTGGGTGAGTCAACA	383
exon9	NPHP4E09F010	ACTTGCTGTTGCAGCAGCACC	NPHP4E09R010	CCATCTCATCTGTATCCTTTG	446
exon10	NPHP4E10F010	CACTGAGCTCTCGTTGAATTT	NPHP4E10R010	GGCATACCCATGACATGAAAA	420
exon11	NPHP4E11F010	GACTTTGTTTTAGGGCAGAGC	NPHP4E11R010	ATGTGGTGATTACCGTACTAG	339
exon12	NPHP4E12F010	AGACAAGGTGGTGAGGCCTGT	NPHP4E12R010	AAGCACGCAGGGATCCACTGT	274
exon13	NPHP4E13F010	TTGAGAAGCGGTCCCAGGTTC	NPHP4E13R010	TGCCACCTAACTAAGGACAGG	384
exon14	NPHP4E14F010	CCAGAGGCAATTAATCGATGA	NPHP4E14R010	ATTGATGCACCTCCCTGTGGA	354
exon15	NPHP4E15F010	CAGACTGTTGGACCTTGTGAA	NPHP4E15R010	TCAGCACAGACAGTTCTGCCA	392
exon16	NPHP4E16F010	GACTAAGGTGCCTGGACCATC	NPHP4E16R010	GGTCACCGTATGATTCTAATG	419
exon17	NPHP4E17F010	GTAGCTATGACAGAAGCAGAA	NPHP4E17R010	ACAAGTCCTGTGCGGGATAGC	392
exon18	NPHP4E18F010	AGGGTCTTATCCTGCGCACAC	NPHP4E18R010	ATTCTCCCGGTTTCCTCCTGG	441
exon19	NPHP4E19F010	AGGCCATTTGAAAGCCACAGC	NPHP4E19R010	CACATGCACACACGCATGCAC	326
exon20	NPHP4E20F010	CCCTCCCTATATAGGTGGTCC	NPHP4E20R010	AGGTAAGAGAGAATCATGTGG	404
exon21	NPHP4E21F010	AATGTCCTCTTCTGAGATCGC	NPHP4E21R010	AGAGAAGTCAAATCGCCCCGG	444
exon22	NPHP4E22F010	TCTCTCCCACTCCTCTGAGCA	NPHP4E22R010	TGCACAGGTAAGGGAGGGACA	391
exon23	NPHP4E23F010	TCAGTGTGAGAGGAGGCTGGT	NPHP4E23R010	AAAAGGCCATTCCCAGGCCCA	346
exon24	NPHP4E24F010	GTCTTGGCAACAGTGGAGATA	NPHP4E24R010	ACCAGGGCATGAAGCCATGAG	360
exon25	NPHP4E25F010	TGACGAGCCTGTCCTGTCCTA	NPHP4E25R010	CCTAAAATGAAGAGGATCCCA	286
exon26	NPHP4E26F010	AGATGCGTTCTGGGAGGGACT	NPHP4E26R010	TTTAGGAAGGGGCCAAGCCCA	308
exon27	NPHP4E27F010	TTTCCCTGCACAGCCTCCTGT	NPHP4E27R010	AAAAGCTGCTGTCAGGGCCAC	390
exon28	NPHP4E28F010	AACCACCCATGACCTTGGGCT	NPHP4E28R010	TGTATCCAGTGGTCCGAGTCA	392
exon29	NPHP4E29F010	TCTTATCTCTGTGGGGGTCCC	NPHP4E29R010	GCTGGTGATTTGAGGAACTCG	364
exon30	NPHP4E30F010	CAGCTCCCCTTGGAAATAAAC	NPHP4E30R020	AAACTGCCAAGGGAAGACGTG	768

Primers for *NPHP4*

exon	F primer	5′-nucleotide sequence -3′	R primer	5′-nucleotide sequence -3′	Amprified fragment length (bp)
exon1	NPHP3E01F020	TGCTCCGCCCAGTCCTGCTCT	NPHP3E01R020	GAGAATATGGCCTCTCAAATT	694
exon2	NPHP3E02F010	CATGAAGTTCCTGATAATTGG	NPHP3E02R010	GAATCCTACATGACTTACTTC	387
exon3	NPHP3E03F010	GAGGACCAAATGAATATTGGT	NPHP3E03R020	GCAGCTGACAGAGAGAACACA	420
exon4	NPHP3E04F020	CAGTATCTTTGAACTTTGCCA	NPHP3E04R020	GATGGTTTGTCAATGGAAAGC	459
exon5	NPHP3E05F020	GGTATGGCAGTATTAACATGT	NPHP3E05R020	GCTTCCTGTTCTTTAAGACAT	391
exon6	NPHP3E06F020	GTATTTGAGAGAAACTTGCCT	NPHP3E06R020	GCTATATTTGCCAAACTCTGA	595
exon7	NPHP3E07F020	GTTGGACCTTTTCTGGCCACT	NPHP3E07R020	GTTCCAGCCACACTGGTTTCT	401
exon8	NPHP3E08F010	CCTAAGGTTGTTGTGAAGATA	NPHP3E08R010	TTCAAAAAGACAAGCAAGTGG	320
exon9	NPHP3E09F020	AAGGCTGTATGTTTGAACTTG	NPHP3E09R020	CACATCTCAACATGGATAATC	440
exon10	NPHP3E10F010	CAGCTTTTCTCCAGTATTTTC	NPHP3E10R020	GGGCATGAACCTATTGTTTTA	350
exon11	NPHP3E11F020	AGTAACTGACCACCTGATTGC	NPHP3E11R020	GACCCGATTGTATCGAATATT	390
exon12	NPHP3E12F020	ATATTCGATACAATCGGGTCC	NPHP3E12R020	CTGTGGGCATACGATATATTT	458
exon13	NPHP3E13F010	CAGAGTTCAGATTGGTGATAA	NPHP3E13R010	CCTCACTGCAAGTTACATAAA	406
exon14	NPHP3E14F010	GTTGTGATTCATTGCTCAAAG	NPHP3E14R010	CCTTATAACAGATCCCCTATA	410
exon15	NPHP3E15F010	TTTCTGTCGGGGTACTTGTTG	NPHP3E15R010	CAGACTGGTGTAGTGATCAGT	283
exon16	NPHP3E16F020	TGACTCTAGCAGCCCCATAAA	NPHP3E16R020	GGCTATCAGCATTCCTGCATA	435
exon17	NPHP3E17F020	GTTATCTTTGGTGTGCTAGAT	NPHP3E17R010	CTTTGGCAGAAATAATCTTGC	487
exon18	NPHP3E18F010	CATTCCACACTTCTGAGATTT	NPHP3E18R010	GAATAGGGAGAGGATTTAATC	496
exon19	NPHP3E19F020	GGTTCTGCATATCACTGAATT	NPHP3E19R020	GGAAAAGCAGATCTAATAGAG	492
exon20	NPHP3E20F010	CAGTACTCGCCTACTAATAAA	NPHP3E20R020	GCAAGATCTGTCATCTGATTA	440
exon21	NPHP3E21F020	CTCTTCTCTTTTTCCAAGATG	NPHP3E21R020	CCACATGAAGACTAGGCACAG	497
exon22	NPHP3E22F020	CTAGACTTGCTTTGTTTTGTC	NPHP3E22R020	CTTTAAAGAACTGAGGTAGCT	614
exon23	NPHP3E23F010	GTTGCCATGTGGAAATATTTG	NPHP3E23R010	CATACATGAAATTTTGCGTGG	436
exon24	NPHP3E24F010	GGAAAGTAAGATTTTGAGCTG	NPHP3E24R020	GTTCTGCTCAGTTACTTGTTA	536
exon25	NPHP3E25F020	GCTTTTCTATACAGTGTAGCT	NPHP3E25R010	CCTTCATACAAGTCTAACTTC	485
exon26	NPHP3E26F010	CCCATCTTTTAGGAGGATATT	NPHP3E26R010	CCCCACTCTAAGAAAAAACAT	341
exon27	NPHP3E27F010	AGGGGAAATGGGCAAATATTT	NPHP3E27R020	CCTTGGATACCATATAATAGG	512

Fig. 1 continued

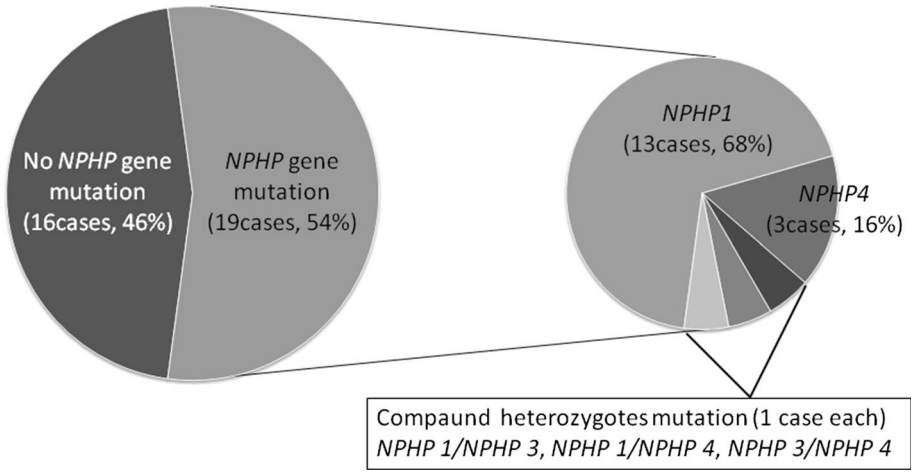

Fig. 2 Percentage of NPH patients with *NPHP* gene mutation. *NPHP* gene mutation was detected in 19 patients. No *NPHP* gene aberration detected within the sequences analyzed in the other 16 patients with suspicion of NPH clinicopathologically

transmission in renal tubular epithelial cells, such as signaling involving diacylglycerol kinase-zeta and receptor-like tyrosine kinase. Abnormalities of the protein disrupt urinary concentrating ability and the structure of cilia of renal tubules, as in the other types of NPH.

Previous reports describe occurrence of *NPHP1* mutations in approximately 30–50 % of juvenile nephronophthisis patients in Western countries [1, 6], where genetic analysis of *NPHP1* is performed initially when juvenile NPH is suspected. If mutation is detected, kidney biopsy usually is deferred [7]. Genetic diagnosis is made less frequently in Japan; so kidney biopsy often is performed to obtain a definitive diagnosis. Not infrequently, NPH is discovered in the advanced or end stage in many Japanese patients, in whom treatment no longer can slow progression. Unfortunately, symptoms typically seen in early stages are incompletely characterized.

In the present study, we investigated clinical, histologic, and genetic features in 35 Japanese patients clinically and histologically suspected to have NPH, aiming to promote early diagnosis. We studied many exons as many as 13 *NPHP* genes. Since such genetic analysis involves significant cost and time, we also screened biopsy specimens by immunohistologic methods employing antibodies against relevant peptides.

Methods

Patient registration and informed consent

Our subjects included 35 patients with clinicopathologic findings suggestive of NPH who were referred to our department from various regions of Japan. The study was performed following approval by the Ethics Committee of Kinki University Faculty of Medicine and acquisition of written informed consent from patients or their parents (Actual state of Japanese juvenile nephronophthisis patients and identification of gene aberrations; approval number 20–99).

Genomic DNA extraction, polymerase-chain reaction (PCR), and determination of *NPHP* gene sequence.

After approximately 5 mL of peripheral blood was collected from patients into tubes containing Na-EDTA, genomic DNA was extracted using NucleoSpin for Blood (TaKaRa Bio Inc, Shiga, Japan). Human genomic DNA (TaKaRa Clontech, code 636401; Shiga, Japan) was used as a control. Patient samples and control genomic DNA were diluted with sterile water to prepare 10 ng/μL solutions. PCR was performed using these as templates and TaKaRa PCR Thermal Cycler Dice Gradient (TaKaRa Bio Inc, Shiga, Japan). To determine extent of deletions and identify break points, PCR primers were prepared to amplify approximately 200–300 bp fragments based on *NPHP* gene sequences registered in GenBank (Fig. 1). For PCR, annealing temperatures and times were 63 °C and 15 s for *NPHP1* and *NPHP3*; 60 °C and 15 s for *NPHP2*; and 60 °C and 20 s for *NPHP4*, respectively. For sequence analysis, PCR products were purified by an enzyme reaction, and templates for sequencing were prepared. The sequencing reaction was carried out using the prepared template DNA and a BigDye Terminator v.3.1 Cycle Sequencing Kit (Applied Biosystems, CA, USA), employing the dye terminator method. Reaction products were purified by gel filtration, and sequence analysis was performed using a capillary-type sequencer, ABI3730xl (Applied Biosystems, CA, USA). The algorithm established by Salomon et al. [8]. was adapted for use in our analytical procedure. In children with renal dysfunction

Table 1 Characteristics of patients found to have NPHP gene mutations

Age/gender	Motive of discovery	BUN/Orn (mg/dL)[a]	UP	Urinary LMP	Low gravity urine	Extrarenal symptom	Diagnosis at first biopsy	*NPHP*/mutation	The other *NPHP* mutation	Consenguineous marriage	Family history of renal disease
14 years/M	Anemia	49/3.3	(−)	(−)	(−)	n.f	n.d	Large delation (>2.0kbp)		(−)	(−)
13 years/F	Nocturnal enuresis	27/1.3	(−)	(−)	(−)	n.f	n.d	Large delation		(−)	NPH (younger brother)
11 years/M	Sibling with NPH	17/0.6	(−)	(+)	(+)	n.f	n.d	Large delation		(−)	NPH (elder sister)
15 years/F	Protein uria (school urinalysis)	21.3/1.3	(±)	(−)	(−)	n.f	TIN	(−)	D1980G (*NPHP4*, hetero)	(−)	(−)
15 years/F	Protein uria (school urinalysis)	89.6/11.6	(−)	(+)	(+)	RP	NPH	Partial delation (=300bp)		(−)	Acute glomerulonephritis (mother)
14 years/M	Chance discovery of the RD (heatstroke)	17/0.9	(±)	(+)	(+)	n.f	n.d	n.d	L939 (*NPHP4*, hetero)	(−)	(−)
11 years/F	Enuresis, polyuria	74/5.2	(1+)	(+)	(+)	SS(-2.5SD)	NPH	E677Q (hetero)	E642L (*NPHP4*, hetero)	(−)	(−)
18 years/F	Enuresis, polydipsia	82/8.1	(±)	(+)	(+)	SS(-1.8SD)	NPH	Gln547 (hetero)	S80L (*NPHP3*, hetero)	(−)	Protein uria (father)
8 years/M	Glycosuria (school urinalysis)	159/11.1	(2+)	(+)	(+)	n.f	Similar NPH	E677Q (hetero)	*NPHP4*(−)	(−)	(−)
14 years/M	Glycosuria (school urinalysis	48/5.0	(±)	(+)	(+)	RP	NPH	Large delation		(−)	NPH (younger sister)
13 years/F	Sibling with NPH	58/2.7	(1+)	(+)	(+)	RP	NPH	Large delation		(−)	NPH (elder brother)
20 years/F	Chance discovery of the RD (medical examination)	44.6/2.4	(1+)	(+)	(+)	n.f	n.d	(−)	L939Q (*NPHP4*, homo)	(−)	(−)
8 years/F	Chance discovery of the RD	32.2/1.4	(−)	(+)	(+)	n.f	NPH	Large delation		(−)	(−)
15 years/F	Protein uria (school urinalysis)	37/2.6	(−)	(+)	(+)	n.f	Tubular enlargement medullary cysts	Large delation		(−)	(−)
7 years/F	Chance discovery of the RD (urine tract infection)	40/3.0	(1+)	(+)	(+)	Joubert syndrome	n.d	(−)	AA/OO→AG/OT (exon 26/exon 20)	(−)	(−)
19 years/F	Chance discovery of the RD (bronchitis)	90.3/8.4	(1+)	(+)	(+)	n.f	n.d	(−)	A150V (*NPHP3*, hetero)	(−)	(−)

Table 1 continued

Age/gender	Motive of discovery	BUN/Orn (mg/dL)[a]	UP	Urinary LMP	Low gravity urine	Extrarenal symptom	Diagnosis at first biopsy	*NPHP*/mutation	The other *NPHP* mutation	Consenguineous marriage	Family history of renal disease
8 years/M	Visual impairment	46.5/1.9	(−)	(+)	(+)	RP	NPH	Large delation	D1980G (*NPHP4*, hetero)	(−)	(−)
16 years/F	Protein uria (school urinalysis)	43.3/2.6	(1+)	(+)	(+)	n.f	NPH	Large delation		(−)	(−)
13 years/F	Anemia, fatigue	39/2.2	(−)	(+)	(−)	n.f	TIN, tubular enlargement	Large delation		(−)	(−)

RD renal dysfunction, *n.f.* not found, *n.d* not done, *UP* urinary protein, *LMP* low molecule protein, *SS* short stature, *RP* retinitis pigmentosa, *TIN* tubulo interstitial nephritis

[a] Renal function at the time of the discovery

who were 5 years old or younger, the gene responsible for infantile NPHP (*NPHP2)* was analyzed first. In patients older than 5 years, *NPHP1* was analyzed first; if no mutation was detected, *NPHP4* was examined. *NPHP3* analysis was added when no mutation was detected in other genes in patients whose disease progressed to end-stage renal disease at an age of 16 years or older.

Clinical data

Data originally collected at our department as well as data provided by other institutions were surveyed using a questionnaire. Questionnaire consists of personal data including the patient's age, motive of discovery, urinary abnormality and renal dysfunction, detailed clinical data, extrarenal symptom, renal tissue diagnosis at the first biopsy, consanguineous marriage, and family history of renal disease.

Results

NPHP gene analysis

Among 35 patients, an *NPHP* gene mutation was identified in 19 patients. Although NPH was suspected clinicopathologically in the other 16 patients, no *NPHP* gene aberration was detected within the sequences analyzed (Fig. 2). Characteristics of patients with *NPHP1* gene mutations (Table 1) and without *NPHP* gene mutations (Table 2) were shown. A mutation was detected only in *NPHP1* in 13 patients; deletion was extensive in 10 (Fig. 3a) and partial in 1. Two other patients had a point mutation (E677Q and K334 N, both heterozygous). In all, these mutations accounted for 37.1 % (13/35) of patients. In another candidate gene responsible for the juvenile type, *NPHP4*, the mutation L939* was detected in 2 patients (Fig. 3b), while a D1980G mutation was detected in 1, accounting for 8.6 % (3/35) of all patients. Compound heterozygotes containing 1 mutation each in *NPHP1* G547* and *NPHP3* S80L (Fig. 4a), 1 mutation each in *NPHP1* E677Q and *NPHP4* E642L (Fig. 4b), and 1 mutation each in *NPHP3* A150 V and *NPHP4* D1089G (Fig. 4c) also were observed. The disease progressed to ESRD before 20 years of age in these patients, similar to the course of other patients with a single-gene mutation. No *NPHP2* mutation was detected in any patient.

Clinical and demographic features of patients

Patient background

Patients were reported from 46 prefectures without evident selection bias, and with no important regional

Table 2 Characteristics of patients without apparent NPHP gene mutations

Age/gender	Motive of discovery	BUN/Orn (mg/dL)[a]	UP	Urinary LMP	Low gravity urine	Extrarenal symptom	Diagnosis at first biopsy	NPHP1 mutation	NPHP3 mutation	NPHP4 mutation	Consanguineous marriage	Family history of renal disease
6 years/M	Lagging physical development	34/1.2	(−)	(−)	(−)	SS (−1.3SD)	NPH	(−)	n.d	(−)	(−)	(−)
12 years/M	SS, fatigue	48/1.3	(−)	(+)	(−)	Sensory deafness	Chronic interstitial nephritis, glomerulosclerosis	(−)	n.d	(−)	(−)	(−)
26 years/M	Chance discovery of the RD (medical examination)	21/1.6	(−)	(+)	(−)	n.f	Interstitial nephritis	(−)	(−)	(−)	(−)	Renal dysfunction (father, young sister)
11 years/M	Pallor, anemia	27.4/1.5	(−)	(+)	(+)	SS (−2.2SD)	n.d	(−)	n.d	(−)	(−)	(−)
17 years/M	SS	34/1.5	(±)	(+)	(+)	SS (−3.8SD)	n.d	(−)	n.d	(−)	(−)	(−)
22 years/M	Hypertention	32.5/1.5	(1+)	(+)	(−)	RP	TIN	(−)	(−)	(−)	(−)	(−)
11 years/F	polydipsia, polyuria	15.4/0.7	(−)	(+)	(+)	n.f	n.d	(−)	n.d	(−)	(−)	(−)
12 years/F	Chance discovery of the RD (protein uria at 3 years old)	32/1.6	(2+)	(+)	(+)	n.f	TIN, tubular enlargement	(−)	(−)	(−)	(−)	(−)
14 years/M	Protein uria (school urinalysis)	58/4.2	(1+)	(+)	(+)	n.f	TIN, tubular enlargement	(−)	(−)	(−)	(−)	(−)
26 years/M	Hypertention (medical examination)	38.7/1.5	(−)	(+)	(+)	n.f	TIN, glomerulosclerosis	(−)	(−)	(−)	(−)	(−)
10 years/M	Pallor, anemia	53.6/1.0	(1+)	(+)	(+)	n.f	NPH	(−)	n.d	(−)	(−)	(−)
28 years/F	Chance discovery of the RD anemia	47.5/2.9	(1+)	n.d	(+)	n.f	TIN, similar NPH	(−)	(−)	(−)	(−)	(−)
11 years/F	Pallor, polydipsia, polyuria	27.4/1.5	(−)	(+)	(+)	SS(-2.2SD)	n.d	(−)	n.d	(−)	(−)	(−)
18 years/M	Crud, fatigability	49.6/4	(±)	(+)	(+)	Specific complexion	Similar NPH	(−)	(−)	(−)	(−)	NPH (young sister)
16 years/F	Sibling with NPH	38.3/1.8	(−)	(+)	(−)	Specific complexion	Similar NPH	(−)	(−)	(−)	(−)	NPH (elder brother)
46 years/F	Protein uria, hematuria (at 30 years old)	33/1.8	(1+)	(+)	(−)	Sensory deafness	Chronic interstitial nephritis, glomerulosclerosis	(−)	(−)	(−)	(−)	NPH (elder brother)

RD renal dysfunction, *n.f* not found, *n.d* not done, *UP* urinary protein, *LMP* low molecule protein, *SS* short stature, *RP* retinitis pigmentosa, *TIN* tubular interstitial nephritis

[a] Renal function at the time of the discovery

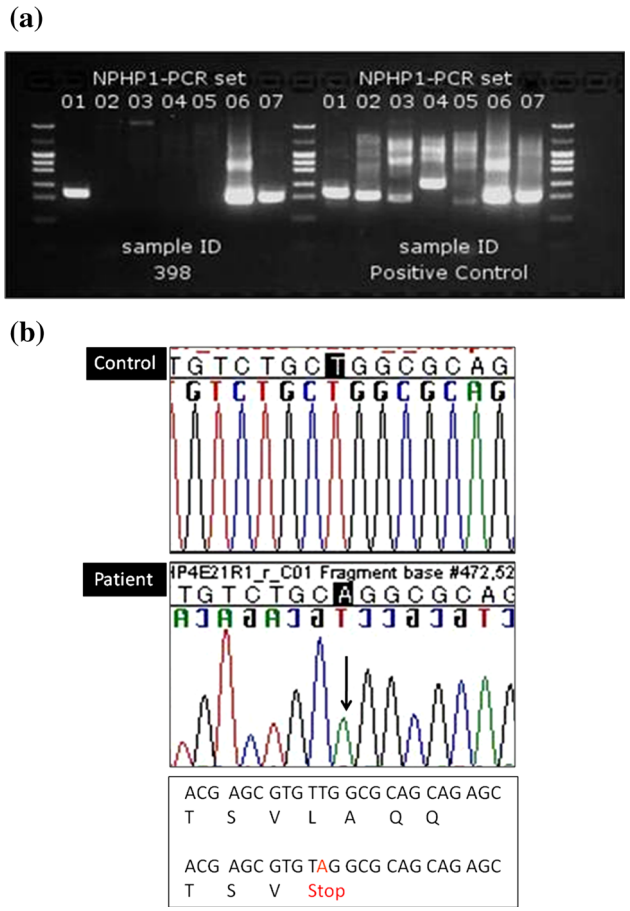

Fig. 3 Analysis of deletion in *NPHP1* (**a**) and analysis of *NPHP4* (**b**). In **a** *lane 1* and *lanes 6 and 7*, contain PCR products of regions within and outside *NPHP1*, respectively; *Lane 2* contains PCR products from the junction between *NPHP1* and the adjacent *MALL* gene. *Lanes 3–5* show the PCR products of *NPHP1* obtained with primers amplifying fragments of approximately 300 bp. *NPHP1* was nearly completely deleted (1.2 kbp deletion). In **b**, substitution of TAG for TTG formed a stop codon, prematurely terminating peptide synthesis

differences (Fig. 5). The male:female ratio was 16:19, with evident gender difference. Ages of patients ranged from 2 to 38 years (median; 12.5). Familial occurrence was noted in 3 families. Other occurrences were solitary, with no family member showing a urinary abnormality, a diagnosis of NPH, or any renal dysfunction of unknown cause.

Initial abnormality deletion

NPH sometimes was discovered following an abnormal urinary finding by mass screening, such as proteinuria detected in a urine test at school (18 %), or renal dysfunction discovered incidentally in working up other medical symptoms, or during medical check-ups (23 %). Approximately 20 % of cases were discovered because of urinary tract symptoms such as polyuria with or without polydipsia, enuresis (often nocturnal), or mellituria. Some 38 % were discovered because of either extrarenal manifestations such as lagging physical development, dwarfism, anemia, pallor, hypertension, or visual disturbance arising from pigmentary retinal degeneration; a prior diagnosis of NPH in a sibling; or both (Fig. 6).

Urinary findings

Urine specific gravity frequently was low (not greater than 1.010); approximately 75 % of cases. Low molecular weight proteinuria, such as β2-microgloburinuria, also was common (85 %), even though inclusion of renal function shown such as between blood urea nitrogen and serum creatinine was relatively mild at that time.

Renal histologic findings

Renal biopsy was performed in 25 patients (71 %). These included 13 patients demonstrated to have an *NPHP* gene mutation and in 12 with no *NPHP* gene mutation identified (suspected cases). Histologic findings included suspected NPH; interstitial nephritis, renal tubular dilation, and glomerulosclerosis. Cystic dilation of renal tubules and irregular contours of tubular basement membranes were observed in most patients, mainly in the renal medulla (Fig. 7a). Sclerotic glomeruli, inflammatory cell infiltration in the renal tubules and interstitium, and fibrosis were frequent, although not seen in all patients (Fig. 7b).

Discussion

Renal tubular epithelial cells are attached to the basement membrane through integrin cross-linking, which transmits extracellular signals to the cell nucleus [2]. Nephrocystin acts importantly in signal transmission between tubular epithelial cells and between these epithelial cells and the extracellular matrix functioning as a docking protein. Nephrocystin also is involved in cell adhesion, together with *N*-cadherin, catenin, and β-catenin [2, 8]. Furthermore, nephrocystin influences actin cytoskeleton structure together with β-tubulin, contributing to maintenance of the cytoskeleton and determination of cell polarity. Nephrocystin forms a complex with Crk-associated substrate, which promotes phosphorylation of Pyk2 and transmits intracellular information through a Pyk2-dependent pathway [2]. Furthermore, nephrocystin is present on primary cilia, where it functions in cooperation with α-tubulin; nephrocystin also is involved in signal transmission in organelles [9]. Accordingly, abnormalities in the nephrocystin molecule disrupt signal transmission between cells

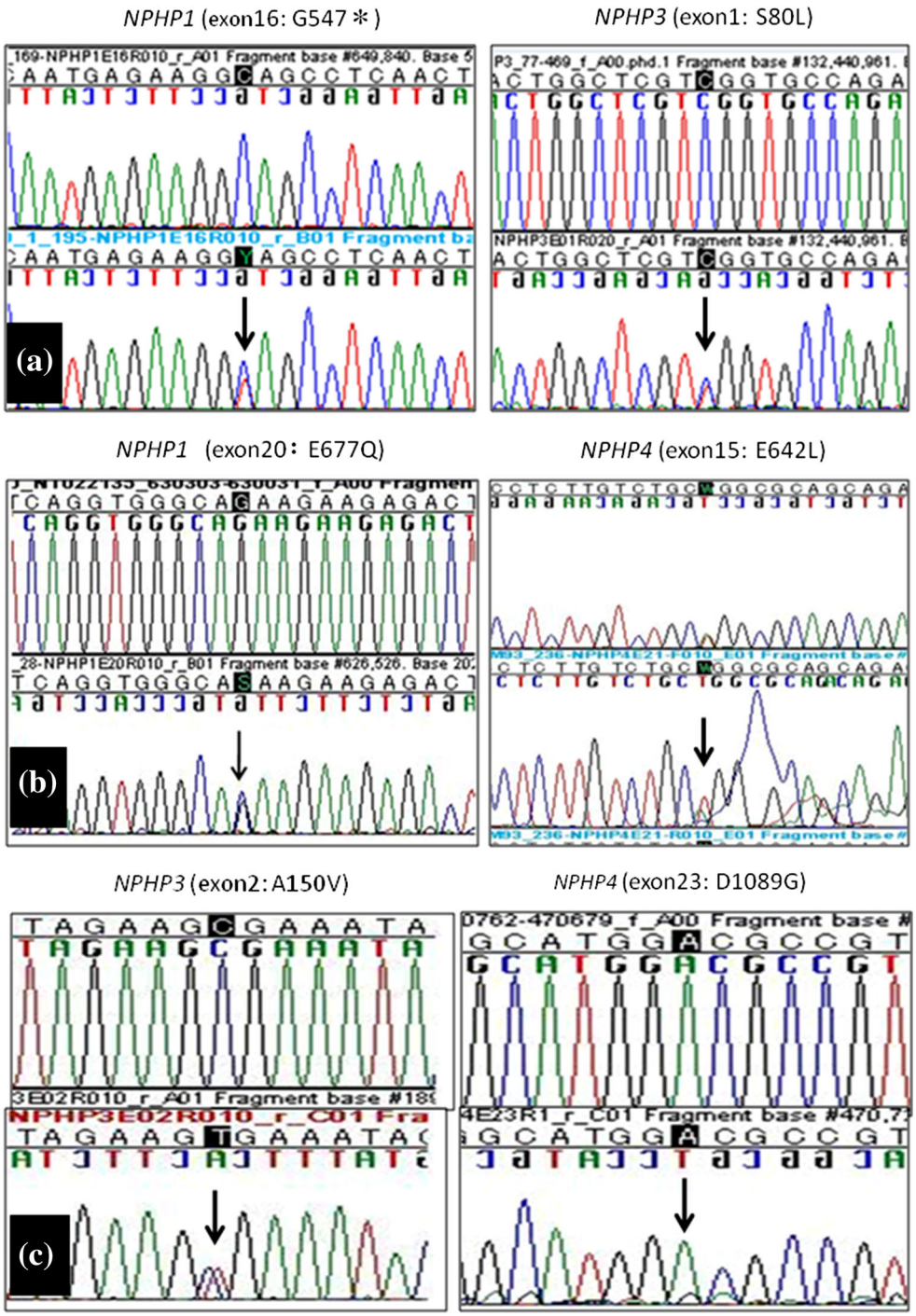

Fig. 4 Compound heterozygotes with heterozygous mutations in different *NPHP* genes. In **a**, a compound heterozygote has one heterozygous mutation involving each of *NPHP1* (G547*) and *NPHP3* (S80L). In **b**, a compound heterozygote has one heterozygous mutation involving each of *NPHP1* (E677Q) and *NPHP4* (E642L). In **c**, a compound heterozygote has one heterozygous mutation involving each of *NPHP3* (A150 V) and *NPHP4* (D1089G)

and the extracellular matrix, intercellular adhesion, cytoskeletal integrity, cell polarity, primary cilia function, and intracellular signal transmission to the nucleus. Structural and functional disorders involving the renal tubular epithelium result.

An *NPHP* gene mutation was detected in about 54 % of all patients, but no mutation was noted within the sequences analyzed in the other 46 %. However, nephronophthisis was suspected clinically and histologically, suggesting possible mutation in some other *NPHP* gene. An *NPHP1* mutation was most frequent among our Japanese patients, most often representing a large deletion rather than a point mutation. Frequency of an *NPHP1* mutation was similar to that reported in Western populations [10].

On the other hand, mutation in the gene responsible for the infantile type, *NPHP2*, a patient in a compound heterozygous stable with another abnormal *NPHP* gene such as that responsible for NPH3 recently has been

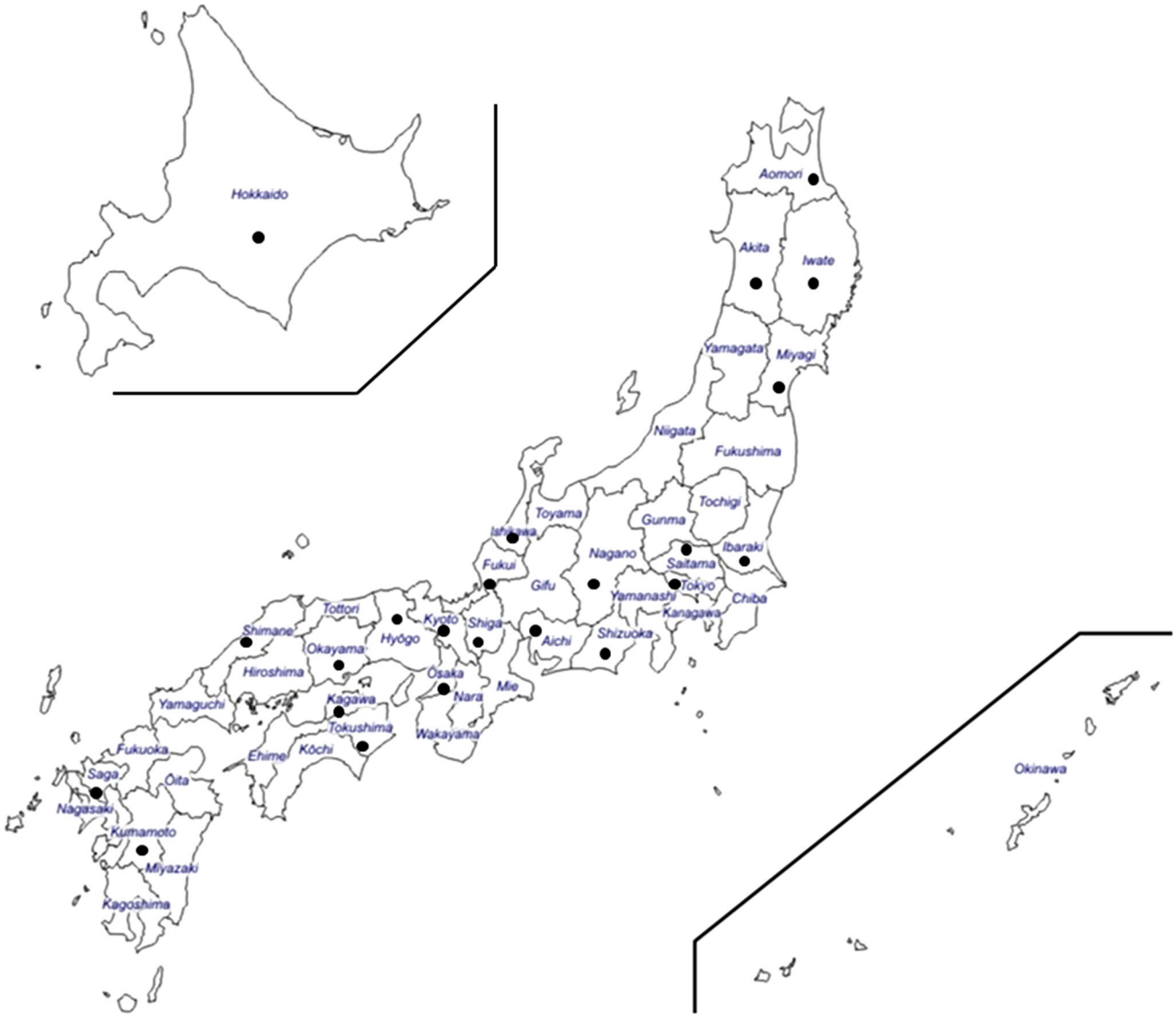

Fig. 5 Demographic features of patients in Japan. Regional distribution of study subjects within Japan, show as a *dot* for each patient

reported [11, 12]. We also found compound heterozygosity across multiple *NPHP* genes in some of our Japanese nephronophthisis patients. In *NPHP4*, L939* (IVS-20T > A) was detected in two geographically distant patients who were not consanguineous. The mutation formed a stop codon by substituting TAG for TTG in exon 21, terminating peptide synthesis. This might prove to be a 'hot spot' among Japanese patients.

We detected in three patients with two mutations in either *NPHP1*, *NPHP3*, or *NPHP4* in this study. As similar to the results of the other studies [13, 14], the age of the initial discovery of this disease and the course of progression to end-stage renal disease were not significantly different from those of the patients having mutation in single *NPHP* gene. An analysis of patient backgrounds revealed that NPH was distributed fairly evenly Japan, including the suspected cases where no causative mutation was identified. Heterozygotes carrying NPHP gene mutations also were rather evenly distributed nationwide. No gender difference was evident from our analysis. Although the median age at time of disease discovery was 12.5 years, individual presentation ranged from infantry to adulthood.

Frequency of disease discovery in mass screening programs, such as school urine tests, was low, as previously reported [15]. Incidental discovery of renal dysfunction during diagnostic workup of possibly unrelated symptoms, or during routine check-ups, accounted for less than 50 % of cases. Often symptoms that led to the discovery of NPH represented extrarenal manifestations such as incomplete physical development reported previously [15]. In particular, currently used urine test strips, intended mainly to detect albuminuria, are insensitive to this disease.

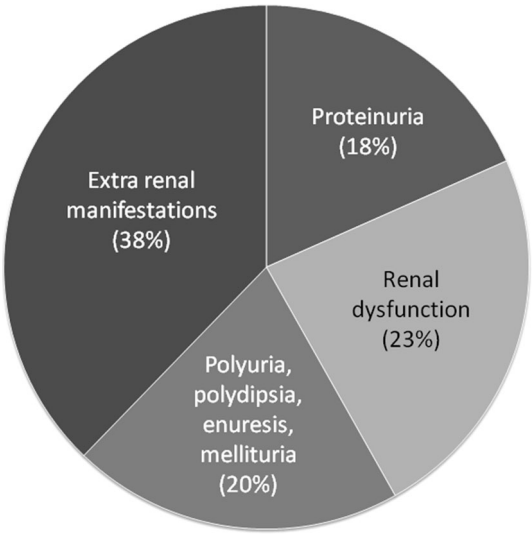

Fig. 6 Clinical suspicion and motivation to discover for NPH. Proteinuria is detected in a urine test at school (18 %), renal dysfunction discovered incidentally (23 %), urinary tract symptoms such as polyuria with or without polydipsia, enuresis, or melliturıa (approximately 20 %). Some 38 % were discovered because of either extrarenal manifestations such as lagging physical development, dwarfism, anemia, pallor, hypertension, or visual disturbance arising from pigmentary retinal degeneration

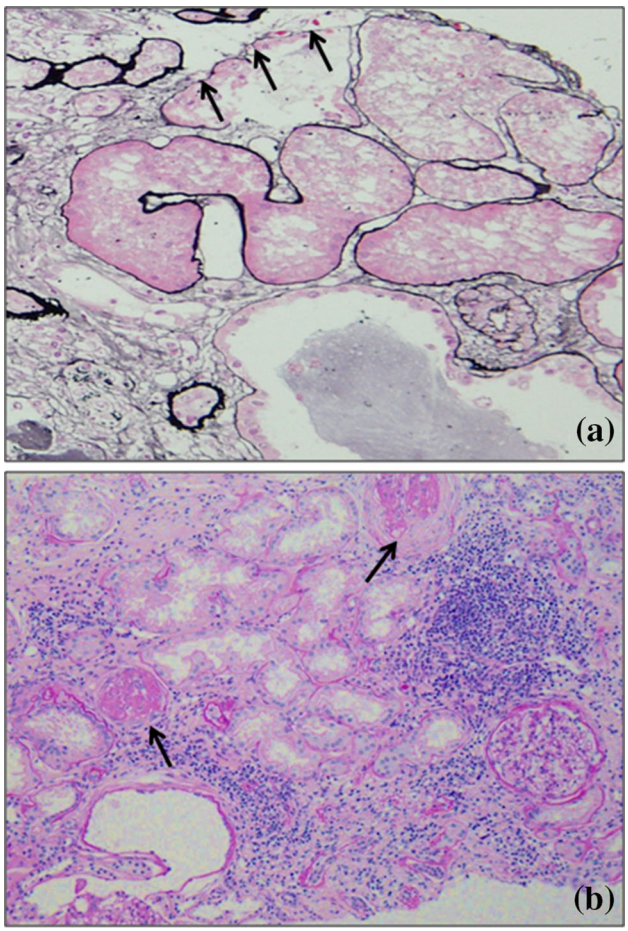

Fig. 7 Pathologic findings in the kidney in nephronophthisis patients. In **a** irregularity (*arrow*) of the renal tubular basement membrane was evident (methenamine silver stain, ×200). In **b**, Inflammatory cell infiltration involved the renal tubular interstitium, and sclerotic glomeruli (*arrow*) were present (periodic acid-Schiff stain, ×100)

Development in siblings was noted in three families, suggesting autosomal recessive inheritance. However, many cases appear to be sporadic. Familial genetic analysis centering on patients, parents is needed.

In contract to albuminuria, urinary findings such as low specific gravity and low-molecular-weight proteinuria are relatively helpful in early discovery. According to the results of this study, we suggest that the findings of the low-molecular weight proteinuria and hypotonic urine reflecting renal tubular disorder coupled with the histologic abnormalities involving cystic dilation of renal tubules and the irregularity of tubular basement membrane could be a convincing diagnostic criterion of this disease. Extrarenal manifestations, such as short stature, delayed physical development, and anemia also were frequent. Unfortunately, these tended to coincide with were progression of renal dysfunction rather than early NPH. Nonetheless, NPH needs to be considered in children with such presentations. Some patients have been reported to show somewhat distinctive extrarenal manifestations [13] such as pigmentary retinal degeneration (Senior-Loken syndrome), ocular dysmetria (Cogan's syndrome), cerebral ataxia, hepatic fibrosis, and skeletal and facial abnormalities [13, 16, 17]. Even the most frequent of these extrarenal manifestations, pigmentary retinal degeneration, was present only in some patients and not in others, even among children showing the same *NPHP1* deletion. Similar lesions also have been reported in Jeune, Joubert, oro-facial-digital (OFD1), and Meckel syndromes [13, 18, 19]. *NPHP1* mRNA is expressed predominantly in a wide range of extrarenal tissues including pituitary gland, spine, testis, lymph nodes, and thyroid [14]. Expression also is high in the central nervous system, which could account for associated cerebellar ataxia. However, associated symptoms may develop in organs with low *NPHP1* expression, such as hepatic fibrosis. The role of nephrocystin in extrarenal manifestations remains poorly understood. The 11 kb interval between the 3′ end of *NPHP1* and an inverted repeat containing the distal deletion breakpoint was found to contain the first exon of a second gene, *MALL* [20]. Although the detail of the *MALL* gene function has not been clarified, recent report suggested the involvement of the age-related macular degeneration (AMD) [21]. Interestingly, associations have also been reported between AMD and chronic kidney disease [22]. Since pigmentary retinal degeneration is the most common extrarenal

manifestation of NPH, similar to AMD, *MALL* gene may involve the pathogenesis of this eye disorder found in NPH patients as the contiguous gene syndrome.

No truly effective treatment currently is available for NPH. Dietary therapy and administration of ion exchange resins and bicarbonate are carried out to manage hyponatremia, hyperkalemia, or metabolic acidosis. Studies possibly relevant to drug therapy have been conducted in various animals, even protozoa [23, 24]. Previous studies reported that renal cyst expression was inhibited by stimulating the G-protein-coupled calcium sensing receptor and elevating Ca^{2+} and cAMP in the renal tubular epithelial cells of pcy mice. Morphology and function of cilia in zebrafish with ciliopathy may be improved by the administration of rapamycin and rescovitine [25, 26]; however, applicability to human NPHP is unknown. Living-donor kidney transplantation was found to have favorable outcome in many reports including the North American Pediatric Renal Trials and Collaborative Studies (NAPRTCS) [27].

Acknowledgments This study was performed after approval by the Ethics Committee of Kinki University Faculty of Medicine. Written informed consent was obtained from the patient's guardian for genetic examination. We thank Ai Itoh for technical support in tissue staining and manuscript preparation.

Compliance with ethical standards

Conflicts of interest This study was partly supported by a Grant-in-Aid for Scientific Research from Morinaga Hoshikai to Tsukasa Takemura (2013–2014) and from Ministry of Health, Labour and Welfare Japan (grant number: 26070201, Representative investigator: Kazumoto Iijima, Pediatrics, Kobe University School of Medicine). The authors declare that they have no competing interests involving this work.

References

1. Hildebrandt F, Otto E. Molecular genetics of the nephronophthisis-medullary cystic disease complex. J Am Soc Nephrol. 2000;11:1753–61.
2. Donaldson JC, Dise RS, Ritchie MD, Hanks SK. Nephrocystin-converted domains involved in targeting to epithelial cell-cell functions, interaction with filaments, and establishing cell polarity. J Biol Chem. 2002;277:29028–35.
3. Mollet G, Salomon R, Gribouval O, Silbermann F, Bacq D, Landthaler G, Milford D, Nayir A, Rizzoni G, Antignac C, Saunier S. The gene mutated in juvenile nephronophthisis type 4 encodes a novel protein that interacts with nephrocystin. Nat Genet. 2002;32:300–5.
4. Otto EA, Schermer B, Obara T, O'Toole JF, Hiller KS, Mueller AM, Ruf RG, Hoefele J, Beekmann F, Landau D, Foreman JW, Goodship JA, Strachan T, Kispert A, Wolf MT, Gagnadoux MF, Nivet H, Antignac C, Walz G, Drummond IA, Benzing T, Hildebrandt F. Mutations in INVS encoding inversin cause nephronophthisis type 2, linking renal cystic disease to the function of primary cilia and left-right axis determination. Nat Genet. 2003;34:413–20.
5. Omran H, Fernandez C, Jung M, Häffner K, Fargier B, Villaquiran A, Waldherr R, Gretz N, Brandis M, Rüschendorf F, Reis A, Hildebrandt F. Identification of a new gene locus for adolescent nephronophthisis, on chromosome 3q22 in a large Venezuelan pedigree. Am J Hum Genet. 2000;66:118–27.
6. Broyer M, Kleinknecht C. Structural tubulointerstitial disease: nephronophthisis. In: Morgan SH, Grunfeld JP, editors. Inherited disorders of the kidney. Investigation and management. Oxford: Oxford University Press; 1998. p. 340–8.
7. Hildebrandt F, Rensing C, Betz R, Sommer U, Birnbaum S, Imm A, Omran H, Leioldt M, Otto E. Arbeitsgemeinschaft für Paediatrische Nephrologie (APN) Study Group. Establishing an algorithm for molecular genetic diagnostics in 127 families with juvenile nephronophthisis. Kidney Int. 2001;59:434–45.
8. Salomon R, Saunier S, Niaudet P. Nephronopthisis. Pediatr Nephrol. 2009;24:2333–44.
9. Hurd TW, Hildebrandt F. Mechanisms of nephronophthisis and related ciliopathies. Nephron Exp Nephrol. 2011;118:e9–14.
10. Wolf MT. Nephronophthisis and related syndromes. Curr Opin Pediatr. 2015;27:201–11.
11. Tory K, Rousset-Rouvière C, Gubler MC, Morinière V, Pawtowski A, Becker C, Guyot C, Gié S, Frishberg Y, Nivet H, Deschênes G, Cochat P, Gagnadoux MF, Saunier S, Antignac C, Salomon R. Mutations of NPHP2 and NPHP3 in infantile nephronophthisis. Kidney Int. 2009;75:839–47.
12. Hoefele J, Wolf MT, O'Toole JF, Otto EA, Schultheiss U, Dêschenes G, Attanasio M, Utsch B, Antignac C, Hildebrandt F. Evidence of oligogenic inheritance in nephronophthisis. J Am Soc Nephrol. 2008;18:2789–95.
13. Benzing T, Schermer B. Clinical spectrum and pathogenesis of nephronophthisis. Curr Opin Nephrol Hypertens. 2012;21:272–8.
14. Hildebrandt F, Zhou W. Nephronophthisis-associated ciliopathies. J Am Soc Nephrol. 2007;18:1855–71.
15. Hirano D, Fujinaga S, Ohtomo Y, Nishizaki N, Hara S, Murakami H, Yamaguchi Y, Hattori M, Ida H. Nephronophthisis cannot be detected by urinary screening program. Clin Pediatr (Phila). 2013;52:759–61.
16. Ronquillo CC, Bernstein PS, Baehr W. Senior-Løken syndrome: a syndromic form of retinal dystrophy associated with nephronophthisis. Vision Res. 2012;75:88–97.
17. Deacon BS, Lowery RS, Phillips PH, Schaefer GB. Congenital ocular motor apraxia, the NPHP1 gene, and surveillance for nephronophthisis. J AAPOS. 2013;17:332–3.
18. Valente EM, Dallapiccola B, Bertini E. Joubert syndrome and related disorders. Handb Clin Neurol. 2013;113:1879–88.
19. Bredrup C, Saunier S, Oud MM, Fiskerstrand T, Hoischen A, Brackman D, Leh SM, Midtbø M, Filhol E, Bole-Feysot C, Nitschké P, Gilissen C, Haugen OH, Sanders JS, Stolte-Dijkstra I, Mans DA, Steenbergen EJ, Hamel BC, Matignon M, Pfundt R, Jeanpierre C, Boman H, Rødahl E, Veltman JA, Knappskog PM, Knoers NV, Roepman R, Arts HH. Ciliopathies with skeletal anomalies and renal insufficiency due to mutations in the IFT-A gene WDR19. Am J Hum Gene. 2011;89:634–43.
20. Hildebrandt F, Otto E, Rensing C, Nothwang HG, Vollmer M, Adolphs J, Hanusch H, Brandis M. A novel gene encoding an SH3 domain protein is mutated in nephronophthisis type 1. Nat Genet. 1997;17:149–53.
21. Meyer KJ, Davis LK, Schindler EI, Beck JS, Rudd DS, Grundstad AJ, Scheetz TE, Braun TA, Fingert JH, Alward WL, Kwon YH, Folk JC, Russell SR, Wassink TH, Stone EM, Sheffield VC. Genome-wide analysis of copy number variants in AMD. Hum Genet. 2011;129:91–100.
22. Cheung CM, Wong TY. Is age-related macular degeneration a manifestation of systemic disease? New prospects for early intervention and treatment. J Intern Med. 2014;276:140–53.

23. Sugiyama N, Kohno M, Yokoyama T. Inhibition of the p38 MAPK pathway ameliorates renal fibrosis in an NPHP2 mouse model. Nephrol Dial Transplant. 2012;27:1351–8.
24. Gattone VH 2nd, Sinders RM, Hornberger TA, Robling AG. Late progression of renal pathology and cyst enlargement is reduced by rapamycin in a mouse model of nephronophthisis. Kidney Int. 2009;76:178–82.
25. Chen NX, Moe SM, Eggleston-Gulyas T, Chen X, Hoffmeyer WD, Bacallao RL, Herbert BS, Gattone VH 2nd. Calcimimetics inhibit renal pathology in rodent nephronophthisis. Kidney Int. 2011;80:612–9.
26. Wang S, Dong Z. Primary cilia and kidney injury: current research status and future perspectives. Am J Physiol Renal Physiol. 2013;305:F1085–98.
27. Hamiwka LA, Midgley JP, Wade AW, Martz KL, Grisaru S. Outcomes of kidney transplantation in children with nephronophthisis: an analysis of the North American Pediatric Renal Trials and Collaborative Studies (NAPRTCS) Registry. Pediatr Transplant. 2008;12:878–82.

Please cite this article in press as: Miyake et al., Biallelic Mutations in Nuclear Pore Complex Subunit *NUP107* Cause Early-Childhood-Onset Steroid-Resistant Nephrotic Syndrome, The American Journal of Human Genetics (2015), http://dx.doi.org/10.1016/j.ajhg.2015.08.013

ARTICLE

Biallelic Mutations in Nuclear Pore Complex Subunit *NUP107* Cause Early-Childhood-Onset Steroid-Resistant Nephrotic Syndrome

Noriko Miyake,[1,17] Hiroyasu Tsukaguchi,[2,17,*] Eriko Koshimizu,[1] Akemi Shono,[3] Satoko Matsunaga,[4] Masaaki Shiina,[5] Yasuhiro Mimura,[6] Shintaro Imamura,[7] Tomonori Hirose,[8] Koji Okudela,[9] Kandai Nozu,[3] Yuko Akioka,[10] Motoshi Hattori,[10] Norishige Yoshikawa,[11] Akiko Kitamura,[12] Hae Il Cheong,[13,14,15] Shoji Kagami,[16] Michiaki Yamashita,[7] Atsushi Fujita,[1] Satoko Miyatake,[1] Yoshinori Tsurusaki,[1] Mitsuko Nakashima,[1] Hirotomo Saitsu,[1] Kenichi Ohashi,[9] Naoko Imamoto,[6] Akihide Ryo,[4] Kazuhiro Ogata,[5] Kazumoto Iijima,[3] and Naomichi Matsumoto[1,*]

The nuclear pore complex (NPC) is a huge protein complex embedded in the nuclear envelope. It has central functions in nucleocytoplasmic transport, nuclear framework, and gene regulation. Nucleoporin 107 kDa (NUP107) is a component of the NPC central scaffold and is an essential protein in all eukaryotic cells. Here, we report on biallelic *NUP107* mutations in nine affected individuals who are from five unrelated families and show early-onset steroid-resistant nephrotic syndrome (SRNS). These individuals have pathologically focal segmental glomerulosclerosis, a condition that leads to end-stage renal disease with high frequency. *NUP107* is ubiquitously expressed, including in glomerular podocytes. Three of four *NUP107* mutations detected in the affected individuals hamper NUP107 binding to NUP133 (nucleoporin 133 kDa) and NUP107 incorporation into NPCs in vitro. Zebrafish with *nup107* knockdown generated by morpholino oligonucleotides displayed hypoplastic glomerulus structures and abnormal podocyte foot processes, thereby mimicking the pathological changes seen in the kidneys of the SRNS individuals with *NUP107* mutations. Considering the unique properties of the podocyte (highly differentiated foot-process architecture and slit membrane and the inability to regenerate), we propose a "podocyte-injury model" as the pathomechanism for SRNS due to biallelic *NUP107* mutations.

Introduction

Nephrotic syndrome (NS) is a renal disease caused by disruption of the glomerular filtration barrier, which results in massive proteinuria, hypoalbuminemia, and dyslipidemia. Idiopathic NS occurs in 16/100,000 children.[1] Most children with idiopathic NS respond well to steroids, but 10%–20% of affected children are categorized as having steroid-resistant NS (SRNS).[2–6] SRNS is a clinically and genetically heterogeneous renal disorder that might have an immunological, structural, or functional etiology.[2,5,7–9] Higher rates of genetic delineation are expected in early-onset SRNS.[7] Clinical differences in SRNS have been suggested to depend on its age of onset.[7] Current medical management and prognosis in NS are based largely on the histological diagnosis. Effective SRNS treatments are not well established, and renal transplantation is eventually required. Importantly, 63%–73% of those with childhood-onset SRNS show pathologically focal segmental glomerulosclerosis (FSGS),which carries a great risk of progression to end-stage renal disease (ESRD).[1,6,8,10] To date, at least 27 genes are associated with SRNS, thereby expanding our knowledge of the pathomechanisms involved in SRNS and podocyte development and function.[11] Although SRNS is the leading cause of ESRD in children worldwide, approximately 70% of those with childhood-onset SRNS are genetically uncharacterized.[7,11] We describe here an additional genetic cause of early-onset SRNS and propose its possible pathomechanism.

Material and Methods

Human Subjects

A total of 18 families (10 with affected siblings and 8 with a single affected individual) who lack any known genetic causes of SRNS (in 27 known genes) were recruited to this study. They presented with non-syndromic early-onset SRNS with onset ages between 1 and 11 years. The clinical aspects of 7 of the 18 families have

[1]Department of Human Genetics, Yokohama City University Graduate School of Medicine, Yokohama 236-0004, Japan; [2]Second Department of Internal Medicine, Kansai Medical University, Osaka 570-8507, Japan; [3]Department of Pediatrics, Kobe University Graduate School of Medicine, Kobe 650-0017, Japan; [4]Department of Microbiology, Yokohama City University Graduate School of Medicine, Yokohama 236-0004, Japan; [5]Department of Biochemistry, Yokohama City University Graduate School of Medicine, Yokohama 236-0004, Japan; [6]Cellular Dynamics Laboratory, RIKEN, Wako 351-0198, Japan; [7]National Research Institute of Fisheries Science, Yokohama 236-8648, Japan; [8]Department of Molecular Biology, Yokohama City University Graduate School of Medicine, Yokohama 236-0004, Japan; [9]Department of Pathology, Yokohama City University Graduate School of Medicine, Yokohama 236-0004, Japan; [10]Department of Pediatric Nephrology, Tokyo Women's Medical University, Tokyo 162-8666, Japan; [11]Center for Clinical Research and Development, National Center for Child Health and Development, Tokyo 157-8535, Japan; [12]Department of Immunology & Parasitology, Institute of Biomedical Sciences, Tokushima University Graduate School, Tokushima 770-8503, Japan; [13]Department of Pediatrics, Seoul National University Children's Hospital, Seoul 03080, Korea; [14]Research Coordination Center for Rare Diseases, Seoul National University Hospital, Seoul 03080, Korea; [15]Kidney Research Institute, Medical Research Center, Seoul National University College of Medicine, Seoul 03080, Korea; [16]Department of Pediatrics, University of Tokushima Graduate School, Tokushima 770-8503, Japan
[17]These authors contributed equally to this work
*Correspondence: tsukaguh@hirakata.kmu.ac.jp (H.T.), naomat@yokohama-cu.ac.jp (N.M.)
http://dx.doi.org/10.1016/j.ajhg.2015.08.013.

been described previously.[12] Affected individuals were resistant to standard steroid therapy but were partially responsive to immunosuppressive drugs. At least ten affected individuals in eight families underwent renal transplants and have had no recurrence of SRNS to date. All samples were collected after written informed consent was obtained. The study protocol was approved by the institutional review boards of Yokohama City University School of Medicine, Kansai Medical University, RIKEN, Tokyo Women's Hospital, and Kobe University.

DNA Extraction

Peripheral-blood leukocytes or saliva from affected individuals and their families was collected. Genomic DNA was extracted with a QIAamp DNA Blood Max Kit (QIAGEN) or Oragene DNA (DNA Genoteck) according to the instructions of each manufacturer.

Whole-Exome Sequencing and Informatics Analyses

Whole-exome sequencing (WES) was performed on affected individuals (one individual from each family) and their parents when the samples were available, as reported previously.[13] In brief, 3-μg samples of genomic DNA were sheared with the Covaris S2 system (Covaris); genome partitioning was performed with SureSelect Human All Exon V5 (Agilent Technology) according to the manufacturer's instructions. Prepared samples were run on a HiSeq 2000 instrument (Illumina) with 101-bp paired-end reads and 7-bp index reads. The sequence reads were mapped to the human reference sequence (GRCh37) by Novoalign 3.00. Next, PCR duplication and variant calls were processed by Picard and the Genome Analysis Toolkit. Ten of the 18 families have multiple affected children, suggesting the autosomal-recessive model, in which homozygous or compound-heterozygous variants are focused in each affected individual. Genetic variants in exons and canonical splice sites (±2 bp) with a minor allele frequency (MAF) of >0.005 in the NHLBI Exome Sequencing Project Exome Variant Server (EVS), Exome Aggregation Consortium (ExAC) Browser, Human Genetic Variation Database (HGVD, which is a public exome database for the Japanese population), or in-house Japanese exome data (n = 575) were removed from the candidates. Genes that harbor recessive variants detected commonly in two or more probands were selected. Candidate recessive variants were checked in each family by Sanger sequencing for confirmation that such variants co-segregated with the disease.

Haplotype Analysis

To determine the haplotype associated with c.2492A>C (p.Asp831Ala), which was found commonly in the five families, we amplified samples of genomic DNA or whole-genome-amplified DNA with 13 microsatellite markers (*D12S364*, *S12S310*, *D12S1617*, *D12S345*, *D12S85*, *D12S368*, *D12S83*, *D12S326*, *D12S351*, *D12S346*, *D12S78*, *D12S79*, and *D12S86*) from the ABI PRISM Linkage Mapping Set (Life Technologies).The PCR products were run on a 3500xl Genetic Analyzer (Life Technologies) and analyzed with GeneMapper 5 software (Life Technologies). Additionally, informative SNPs were chosen from the WES data for each affected individual and used thereafter for constructing haplotype blocks.

Expression of Human *NUP107*

NUP107 (nucleoporin 107 kDa; GenBank: NM_020401.2; MIM: 607617) expression in human embryos and adults was checked by a TaqMan Gene Expression Assay with two probe sets (Hs00914854_g1 and Hs00220703_m1 from Life Technologies) internally standardized by beta actin (Life Technologies). cDNA from human fetal and adult tissues was purchased from Clontech. qPCR was performed by a Rotor-Gene Q instrument (QIAGEN), the data from which was analyzed by the ΔΔCt method with Rotor-Gene 6000 Series software (QIAGEN). The experiments were done in duplicate. The expression level of each tissue represents the mean value of the duplicates.

Histopathology and Transmission Electron Microscopy on Samples from Individuals with Early-Onset SRNS

We stained 3-μm-thick sections cut from paraffin-embedded biopsied kidney tissues with H&E, periodic acid-Schiff stain, and periodic acid methenamine silver stain according to standard methods. For transmission electron microscopy, 1-mm renal-biopsy specimen cubes were fixed in 2% phosphate-buffered glutaraldehyde (pH 7.3) at room temperature, dehydrated in an alcohol gradient, and embedded in Epon-Araldite resin. Sections of 1-μm thickness were cut with an ultra-microtome (Ultracut UCT, Leica), stained with toluidine blue, and examined with a light microscope. Ultrathin sections (60–90 nm) stained by lead citrate were examined with a JEM1011 transmission electron microscope (JEOL). The TUNEL method was used to detect apoptotic cells on tissue sections with an in situ apoptosis detection kit (Takara) according to the manufacturer's instruction.

Immunofluorescence Microscopy

We deparaffinized and rehydrated 3-μm-thick paraffin sections of a necropsy specimen and then autoclaved them in target retrieval solution (S1700, Dako) for 15 min at 105°C. The sections were subjected to immunofluorescence labeling with primary antibodies including rabbit anti-NUP107 mAb (1.5 μg/ml, EPR12241, ab182559, Abcam), mouse anti-WT1 mAb (1:100, WT49, NCL-L-WT1-562, Leica), and mouse anti-Ezrin mAb (1:500, 3C12, E8897, lot 102K4824, Sigma-Aldrich). Normal rabbit and mouse immunoglobulins (IgGs) (sc-2027 [lot L1212] and sc-2025 [lot H1512], respectively, Santa Cruz) were used for negative controls. The CSAII kit (K1497, DAKO) was used for signal amplification of WT1, and other primary antibodies were visualized with Alexa555-conjugated anti-rabbit (1 μg/ml) or Alexa647-conjugated anti-mouse IgG (2 μg/ml) secondary antibodies (A21429 or A21236, respectively, Life Technologies), and then samples were mounted with ProLong Gold antifade reagent (P36930, Life Technologies). Single optical sections were acquired at 16-bit data depth with a confocal microscope system (AxioImager.Z1 microscope with LSM 700 laser scanner, Carl Zeiss) equipped with a C-Apochromat water immersion objective (40×, 1.2 numerical aperture [NA], Carl Zeiss); images were arranged with Photoshop CS5 (Adobe Systems).

Expression Vectors

Mammalian expression vectors were prepared with the Gateway system (Life Technologies). The *NUP107* open reading frame was amplified by PCR with human cDNA derived from a human lymphoblastoid cell line. The PCR product was introduced into the Gateway pDONR221 vector (Life Technologies), and its sequence was confirmed by Sanger sequencing. For mutagenesis, a QuickChange II XL Site-Directed Mutagenesis Kit (Agilent Technologies) was used. After confirming appropriate mutagenesis, we performed LR recombination to create a mammalian expression

vector (pcDNA-DEST53, Life Technologies) to produce N-terminally GFP-fused NUP107 proteins. Among four *NUP107* mutations observed in this cohort, c.969+1G>A was mimicked by c.969_970insTAG, which created the nonsense codon just after the mutation (p.Asp324*). Whereas two truncating mutations (c.969+1G>A and c.1079_1083delAAGAG [p.Glu360Glyfs*6]) are thought unlikely to be present in vivo because of nonsense-mediated decay, these constructs were used as controls for the binding loss, given that C-terminally truncated proteins reportedly lose the NUP107-NUP133 interaction.[14]

Cell-free Protein Synthesis and In Vitro Pull-Down Assays

In vitro transcription and cell-free protein synthesis were performed as described previously.[15,16] In vitro transcription templates for wild-type or mutant *NUP107* were amplified by slit-primer PCR. For generation of transcription templates, the first PCR was performed with 50 ng/μl of each plasmid, 100 nM of the S1 common primer (5′-CCACCCACCACCACCAACAAAAAAG CAGGCTATG-3′), and 100 nM of the vector-specific reverse primer (5′-ATCTTTTCTACGGGGTCTGA-3′). The second PCR was performed with the first PCR product as a template with 100 μM of the SPu primer (5′-GCGTAGCATTTAGGTGACACT-3′), 100 μM of the vector-specific reverse primer (5′-ACGTTAAGGGATTTTGGT CA-3′), and 1 μM of either the deSP6-E02-FLAG-tagged primer or the biotin-ligation site (bls) primer for the addition of the nucleotide sequences of the FLAG tag or the bls tag, respectively (FLAG tagged: 5′-GGTGACACTATAGAACTCACCTATCTCTCTACACAAA ACATTTCCCTACATACAACTTTCAACTTCCTATTATGGACTACAA GGATGACGATGACAAGCTCCACCCACCACCACCAATG-3′; bls tagged: 5′-GGTGACACTATAGAACTCACCTATCTCTCTACACAAA ACATTTCCCTACATACAACTTTCAACTTCCTATTATGGGCCTGA ACGACATCTTCGAGGCCCAGAAGATCGAGTGGCACGAACTCC ACCCACCACCACCAATG-3′).

An ENDEXT Wheat Germ Expression Kit (CellFree Sciences) was used for cell-free protein synthesis according to the manufacturer's instructions for the bilayer translation method. Biotinylated proteins were produced as described previously.[17]

Biotinylated wild-type or altered NUP107 was mixed with FLAG-NUP133 (nucleoporin 133 kDa; GenBank: NM_018230.2; MIM: 607613) in lysis buffer containing 25 mM Tris-HCl (pH 7.5), 100 mM NaCl, 1 mM EDTA, 2% Triton X-100, 1 mM DTT, and 10 mg/ml BSA. After incubation for 1 hr at 26°C, streptavidin MagneSphere beads (Promega) were added, and the mixture was incubated for 30 min at room temperature. After three washes with lysis buffer, bound proteins were eluted from the beads with 20 μl of 2× SDS sample buffer. Bound proteins were separated by SDS-PAGE followed by immunoblotting with an anti-FLAG antibody (Sigma-Aldrich) or a Streptavidin-HRP conjugate (GE Healthcare). Proteins on the blot were detected with Immobilon Western Chemiluminescent HRP Substrate (Millipore) and FluorChem FC2 (Alpha Innotech) in accordance with the protocol from each manufacturer.

Immunoprecipitation

The cell lysate used for immunoprecipitation was prepared according to a method reported previously[18,19] with a slight modification. In brief, HeLa cells were transfected with the wild-type or altered N-terminally GFP-fused NUP107 construct by Viafect (Promega) according to the manufacturer's instructions. The cells were lysed with lysis buffer containing 10 mM Tris-HCl (pH 7.4), 400 mM NaCl, 1% Triton X-100, 2 mM EDTA, 1 mM DTT supplemented with complete proteinase inhibitor cocktail (Roche Diagnostics GmbH), and PhosSTOP (Roche Diagnostics); sonicated; and then incubated for 30 min at 4°C. For debris removal, the crude lysate was centrifuged at 20,630 × *g* for 20 min at 4°C. After collection, the supernatant was diluted 3.75× in dilution buffer (10 mM Tris-HCl [pH 7.4], 2 mM EDTA, 1 mM DTT, complete proteinase inhibitor cocktail, and PhosSTOP). For immunoprecipitation of the GFP-fused NUP107, mouse anti-GFP antibody (11-814-460-001, Roche Diagnostics) and Protein G Sepharose beads (17-0618-01, GE Healthcare) were added. After incubation for 2 hr at 4°C, the beads were washed with wash buffer (lysis buffer diluted 3.75× in dilution buffer). After the protein-bound beads were boiled, they were run on an SDS-PAGE gel and transferred to a polyvinylidene fluoride membrane (Millipore). Membranes prepared in this manner were incubated in 0.2% Casein in Tris-buffered saline containing 0.1% Tween 20 (TBS-T) for blocking. The membrane was probed with rabbit anti-GFP primary antibody (598, MBL) diluted at 1:1,000 and mouse anti-NUP133 (M00055746-M01, Abnova) diluted at 1:500 followed by secondary antibodies HRP-rabbit anti-rat IgG (A5795, Sigma-Aldrich) and HRP-goat anti-mouse IgG (170-6516, Bio-Rad) both diluted at 1:3,000 with 0.2% Casein in TBS-T. For obtaining protein signals, Immobilon Western Chemiluminescent HRP Substrate (Millipore) was used as a chemiluminescence substrate.

Subcellular Localization of NUP107

HeLa cells cultured in DMEM (Life Technologies) containing 10% fetal bovine serum (Sigma-Aldrich) at 37°C in an atmosphere of 5% CO_2 on poly-L-lysine-coated coverslips (Wako) were transfected with the wild-type or altered N-terminally GFP-fused NUP107 vector with the use of Viafect (Promega). After incubation for 48 hr, the cells were washed with pre-warmed PBS at 37°C and then fixed with pre-warmed 2% paraformaldehyde (Wako) in PBS at 37°C for 10 min. The cells were treated with 0.5% Triton X-100 in PBS for 2.5 min and then incubated with 5% normal goat serum (NGS, Merck Millipore) in PBS for 1 hr. After blocking, the cells were reacted with the primary antibody (MAb414 [mouse anti-nuclear pore complex (NPC) proteins], MMS-120P, Covance) diluted at 1:3,000 in 1% NGS in PBS for 2 hr, washed with PBS, and then reacted with the secondary antibody (Alexa Fluor 594 goat anti-mouse IgG, A11032, Life Technologies) in 1% NGS in PBS for 2 hr. After staining, the cells were mounted in paraphenylenediamine solution (80% glycerol in PBS and 1 mg/ml paraphenylenediamine, 11873580001, Roche Diagnostics). Images were captured with a DeltaVision microscope (Applied Precision) equipped with a Plan Apo objective lens (100×, 1.35 NA, Olympus) and a Cool Snap HQ2 CCD camera (Photometrics).

Zebrafish Knockdown by Microinjection of Morpholino Oligonucleotides

The antisense morpholino oligonucleotides (MOs) for *nup107* translation blocking (TB) (5′-AAGTCTGACTCCATTCCATATT GTC-3′)[20] and for *nup107* splice blocking (SB) (5′-ATACATTTA AGCTCACCTCTCTGAC-3′) and a standard MO control (5′-CCT CTTACCTCAGTTACAATTTATA-3′) obtained from Gene Tools were injected into 1- to 2-cell-stage embryos, each at a final concentration of 0.25 mM. The experiment was authorized by the Institutional Committee for Fish Experiments at the National Research Institute of Fisheries Science.

RNA Isolation and RT-PCR Analysis

Total RNA was extracted from embryos at 24 hr post-fertilization (hpf) with TRIzol reagent according to the manufacturer's (Life Technologies) protocol. Double-stranded cDNA was synthesized with M-MLV reverse transcriptase (Promega) and then amplified by PCR with ExTaq (Takara). For detecting the splicing mutation (caused by the MO injections) in *nup107* exon 24, the following primers were used: 5′-TGAACTGTCCTCCGGTGAAG-3′ (forward) and 5′-TGCGATGATGTCAGCAAGAC-3′ (reverse). For the PCR amplifications, the initial denaturing step at 94°C for 5 min was followed by 29 cycles of 30 s at 94°C, 30 s at 61°C, 30 s at 72°C, and a final extension of 7 min at 72°C. PCR products were separated on 3% agarose gels.

Histopathology and Transmission Electron Microscopy of Zebrafish

Larvae injected with control MO, *nup107*-TB MO, and *nup107*-SB MO at 5.5 days after fertilization were fixed with 2% paraformaldehyde and 2% glutaraldehyde in 0.1 M cacodylate buffer (pH 7.4) at 4°C overnight. After fixation, the samples were washed three times with 0.1 M cacodylate buffer for 30 min each and then postfixed with 2% osmium tetroxide in 0.1 M cacodylate buffer at 4°C for 3 hr. The samples were dehydrated in graded ethanol solution (50%, 70%, 90%, and 100%), infiltrated with propylene oxide (PO) two times for 30 min each, immersed in a 70:30 mixture of PO and resin (Quetol-812, Nisshin EM) for 1 hr, and then kept in an open-capped tube so that volatile PO would evaporate overnight. The samples were transferred to fresh 100% resin and polymerized at 60°C for 48 hr. The polymerized resins were cut into semi-thin (1.5-μm) sections with an Ultracut UCT (Leica) and then stained with 0.5% toluidine blue. Ultra-thin (70-nm) sections were cut on an Ultracut UCT (Leica) ultramicrotome and mounted on copper grids. The sections were stained with 2% uranyl acetate at room temperature for 15 min, washed with distilled water, and stained with lead stain solution (Sigma-Aldrich) at room temperature for 3 min. The grids were observed with a transmission electron microscope (JEM-1400Plus, JEOL) at 80 kV.

Molecular-Dynamics Simulation of the p.Asp831Ala Substitution in NUP107

Molecular-dynamics (MD) simulations of the wild-type and p.Asp831Ala Nup107 were carried out with the program package GROMACS (Groningen Machine for Chemical Simulation) version 5.0 with the Optimized Potentials for Liquid Simulations all-atom force field based on the local Møller-Plesset perturbation theory (OPLS-AA/L).[21] The starting structure of NUP107 was extracted from the crystal structure of the NUP107-NUP133 complex (PDB: 3CQC). The missing regions in NUP107 were modeled with the Phyre2 modeling server,[22] and the p.Asp831Ala substitution was introduced with FoldX software.[23] The wild-type and altered NUP107 molecules were solvated with simple-point-charge water molecules in a cubic box extending at least 1.0 nm from the protein surface. Sodium ions were added to neutralize the systems, which were then subjected to energy minimization for 50,000 steps by steepest descent. The minimized systems were then equilibrated by position-restrained MD simulation for soaking the water molecules in the macromolecules in two steps as follows: an NVT ensemble (constant number of particles, volume, and temperature) for 100 ps and an NPT ensemble (constant number of particles, pressure, and temperature) for 4,000 ps each at 310 K. The well-equilibrated systems were then subjected to MD simulations for 30 ns each at 310 K without any restrictions. In all simulations, for maintaining a constant temperature of 310 K, temperature coupling using velocity rescaling with a stochastic term[24] was employed with a coupling constant τ of 0.1 ps. Van der Waals interactions were modeled with 6–12 Lennard-Jones potentials with a 1.4-nm cutoff. Long-range electrostatic interactions were calculated with the particle-mesh Ewald method[25] with a 1.4-nm cutoff for the real-space term. Covalent bonds were constrained with the LINCS algorithm.[26]

Results

Pathogenic Mutations Detected by WES

To identify the genetic cause of early-onset SRNS, we performed WES on 18 probands. Because we found multiple affected siblings in ten families, we speculated on an autosomal-recessive inheritance pattern for SRNS and focused on the recessive variants shared by two or more families with well-performed WES data (Tables S1–S3, S4, and S5). Biallelic mutations in *NUP107*, which encodes NUP107, were common in five families, and the mutation co-segregated perfectly with the affected state in all five families (Figure 1A, Table 1, and Figure S1). None of the other families in our cohort had any pathological variants in *NUP107* or any other known genes associated with SRNS, as listed in Table S6.

We identified a total of four *NUP107* mutations, including two missense mutations (c.469G>T [p.Asp157Tyr] and c.2492A>C [p.Asp831Ala]), one 5-bp deletion (c.1079_1083delAAGAG [p.Glu360Glyfs*6]), and one splice-donor-site mutation (c.969+1G>A) (Table 2). Heterozygous c.2492A>C was common in all five families. The two missense mutations altered evolutionally conserved amino acids (Figure S2) and were predicted to be pathogenic by web-based programs PolyPhen-2 and MutationTaster (Table 2). Furthermore, p.Asp831Ala resides within the Nup84-Nup100 domain (Figure S3). The 5-bp deletion was subjected to nonsense-mediated mRNA decay and probably led to a lack of protein synthesis (Figure S4). The splicing mutation (c.969+1G>A) causes a loss of the intrinsic splicing donor site (Figure S5). All four variants were examined in the EVS, ExAC Browser, HGVD, and in-house Japanese exome database (n = 575). The c.1079_1083delAAGAG variant was observed at frequencies of 0.0000083 in the ExAC Browser and 0.0008696 in the in-house Japanese exome data. Another variant, c.2492A>C, was observed at a frequency of 0.0013587 only in HGVD, but not in the EVS, ExAC Browser, or in-house Japanese exome data (Table 2). The other mutations (c.469G>T and c.969+1G>A) were never observed in any of four variant databases. Among 881 *NUP107* variants registered in the ExAC Browser, a total of 31 variants with a MAF $\geq$ 0.005 were in non-coding regions (intronic but not in canonical acceptor or donor sites or UTRs) or were synonymous variants (Table S7). Furthermore, 36 loss-of-function variants in *NUP107* are not homozygous (all heterozygous; Table S8). Therefore, this genetic

Please cite this article in press as: Miyake et al., Biallelic Mutations in Nuclear Pore Complex Subunit *NUP107* Cause Early-Childhood-Onset Steroid-Resistant Nephrotic Syndrome, The American Journal of Human Genetics (2015), http://dx.doi.org/10.1016/j.ajhg.2015.08.013

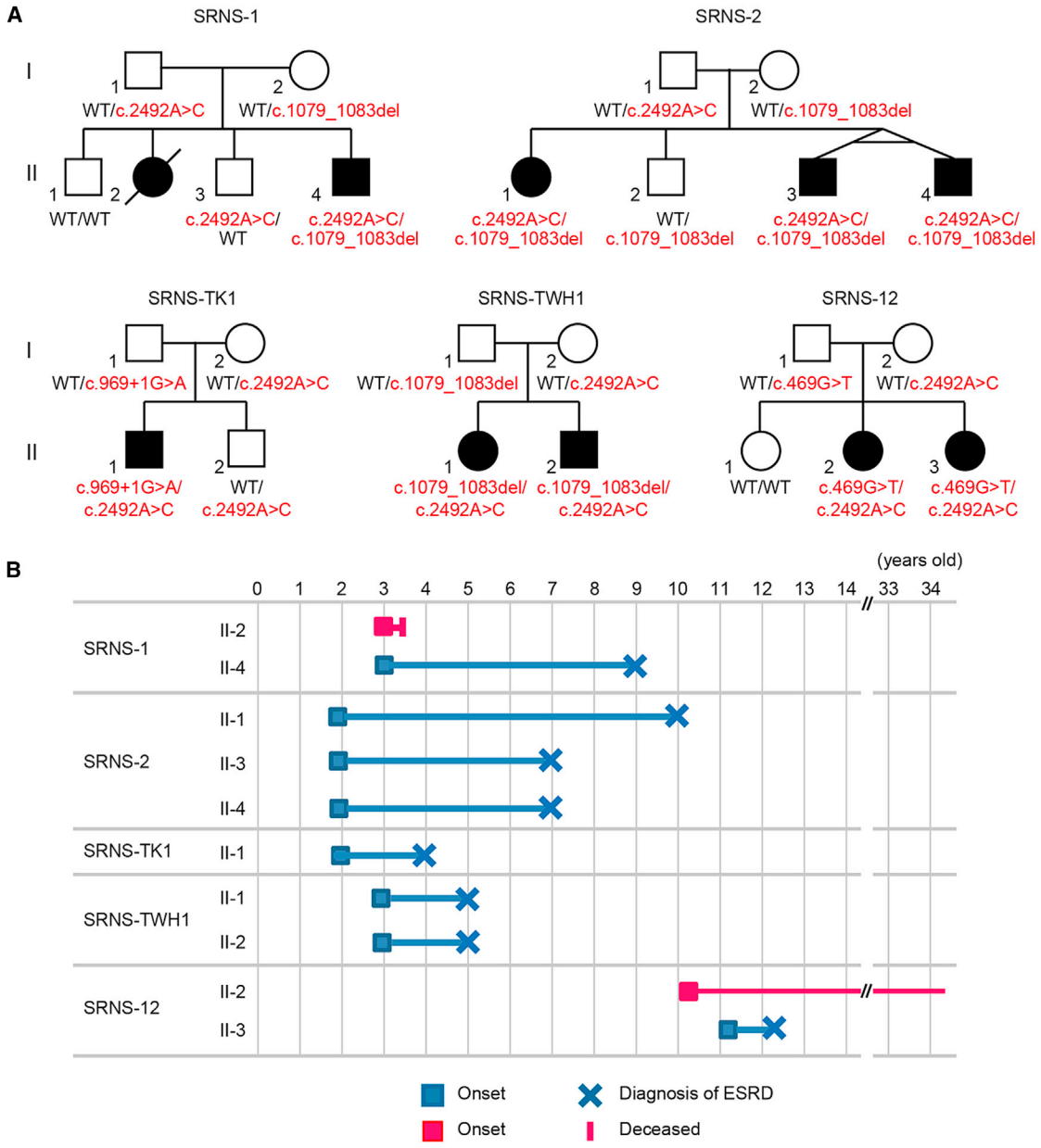

Figure 1. Genetic Analysis and Clinical Course of Early-Onset SRNS in Affected Individuals with *NUP107* Mutations
(A) Familial pedigrees and *NUP107* mutations. Mutant alleles are colored in red. WT indicates the wild-type allele. Filled and unfilled symbols represent affected and unaffected members, respectively.
(B) Clinical course of the affected individuals. The onset of renal symptoms and diagnosis of ESRD are represented by squares and crosses, respectively. Blue and red horizontal bars indicate the period leading to ESRD and the period before completed ESRD, respectively. SRNS-1 II-2 died from a viral infection before the advent of ESRD.

evidence strongly suggests that biallelic *NUP107* mutations could lead to autosomal-recessive SRNS.

A Common Haplotype Harboring c.2492A>C

Interestingly, all affected individuals carry c.2492A>C heterozygously. To determine whether c.2492A>C was derived from an ancestral chromosome, we constructed the haplotype in all families by using informative microsatellite markers and SNPs. We confirmed that a 412-kb haplotype was shared by all five families (Figure S6). Considering the extreme rarity of c.2492A>C in different whole-exome databases, c.2492A>C is likely to be specific to East Asians.

Clinical Characterization of NUP107-Related SRNS

Noticeably, the clinical course of affected individuals with *NUP107* mutations was similar (Figure 1B and the supplemental note). In brief, the four families consistently showed early-onset SRNS whereby NS first manifested itself at age 2–3 years and ESRD became evident before age 10

Please cite this article in press as: Miyake et al., Biallelic Mutations in Nuclear Pore Complex Subunit *NUP107* Cause Early-Childhood-Onset Steroid-Resistant Nephrotic Syndrome, The American Journal of Human Genetics (2015), http://dx.doi.org/10.1016/j.ajhg.2015.08.013

Table 1. Clinical and Genetic Summary of SRNS-Affected Families Harboring *NUP107* Mutations

Family	Individual	Mutation	Age at Onset (Years)	Age at Diagnosis of ESRD (Years)	Treatment	Histology (Subtype, Age in Years)
SRNS-1[a]	II-2[b]	ND	3	NA	Pred	FSGS (NOS, 3)
	II-4	c.[1079_1083del];[2492A>C]	3	9	Pred, CyA, CPA	FSGS (NOS, 3)
SRNS-2[a]	II-1	c.[1079_1083del];[2492A>C]	2	10	Pred, CPA	MCNS (NOS, 2), FSGS (NOS, 4)
	II-3	c.[1079_1083del];[2492A>C]	2	7	Pred	MCNS (2)
	II-4	c.[1079_1083del];[2492A>C]	2	7	Pred	FSGS (NOS, 2)
SRNS-TK1	II-1	c.[969+1G>A];[2492A>C]	2	4	Pred, CyA, CPA	FSGS (NOS, 2)
SRNS-TWH1	II-1	c.[1079_1083del];[2492A>C]	3	5	Pred, ARB, PP	FSGS (collapsing, 3)
	II-2	c.[1079_1083del];[2492A>C]	3	5	Pred, CyA, ARB	FSGS (collapsing, 3)
SRNS-12[a]	II-2	c.[469G>T];[2492A>C]	10	NA	ARB	ND
	II-3	c.[469G>T];[2492A>C]	11	12	Pred, ARB	FSGS (NOS, 11)

Abbreviations are as follows: ARB, AT II receptor blocker; collapsing, collapsing variants; CPA, cyclophosphamide; CyA, cyclosporine A; ESRD, end-stage renal disease; FSGS, focal segmental glomerulosclerosis; MCNS, minimal-change nephrotic syndrome; NA, not applicable; ND, not determined; NOS, non-specific type; PP, plasmapheresis; Pred, prednisone.
[a]These families appear in a previous report by Kitamura et al.[12]
[b]This individual died from a viral infection at the age of 3 years.

years. One family (SRNS-12) showed an exceptionally late onset of NS, which appeared after 10 years of age, and renal function has been relatively preserved at the current 34 years of age. Renal biopsies revealed histopathological FSGS in all affected individuals (Figure 2, Table 1, and Figure S7). Depletion of NUP107 was shown to lead to apoptosis in eukaryotes,[20,27] and we observed apoptotic changes in the renal biopsy samples from SRNS individuals (SRNS-TWH1 II-1 and II-2) with *NUP107* mutations. Cells with the characteristic morphological features, such as nuclear shrinkage and fragmentation, were occasionally found in the glomeruli and renal tubules (Figure S8). Some of these cells could be TUNEL positive (apoptotic), although we failed to recognize TUNEL-positive cells in the glomeruli of the few biopsied specimens, given that only ten glomeruli were observed (data not shown). Among them, five individuals underwent renal transplants and have experienced no recurrence of SRNS to date. Additionally, none of them showed neurological phenotypes.

NUP107 Function and *NUP107* Expression in Humans

NUP107 is an essential component of the NPC, which is one of the largest protein complexes (~125 MDa in vertebrates) in eukaryotes and comprises ~30 nucleoporins embedded in the nuclear envelope.[28,29] It facilitates the efficient transfer of macromolecules between the nucleus and cytoplasm in a highly selective manner and plays pivotal roles in the nuclear framework and gene expression.[28,30–33] Although some nucleoporins have tissue specificity,[34] *NUP107* and NUP107 are ubiquitously expressed as the core gene and the essential scaffold protein, respectively, of the NPC.[29,35–37] As the results of the TaqMan expression assay show, *NUP107* is expressed ubiquitously in most human fetal and adult tissues, including the kidney (Figure S9). To evaluate the physiological relevance of NUP107 in human podocytes, we examined the intracellular localization of NUP107, along with WT1 (a podocyte-specific transcription factor[38]) and Ezrin (a marker protein for apical domains of epithelial cells[39]), in human podocytes. Confocal microscopy demonstrated that NUP107 co-localized with WT1 and was distributed in a speckle-like pattern in the nuclei of human podocytes surrounding the glomerular capillary tufts (Figure S10). In addition to podocytes, most other cell types showed a similar staining pattern for NUP107. These data suggest that NUP107 has an important function for renal filtration in human podocytes. A direct link between NUP107 and renal disease has never been shown, but *NUP107* knockdown in HeLa cells altered the localization of ELYS, and this affected the proper localization of lamin A/C,[19] an alteration in which caused FSGS.[40]

Effect of the Common NUP107 p.Asp831Ala Substitution on the Structure of the Protein and Its Binding to NUP133

To evaluate the effect of p.Asp157Tyr and p.Asp831Ala substitutions from a structural viewpoint, we mapped the variant positions on the crystal structure of the yeast Sec13-Nup145C-Nup84 complex (PDB: 3IKO),[41] which is analogous to the human SEC13-NUP96-NUP107 complex (NUP96 is the C-terminal half product of *NUP98* [GenBank: NM_016320.4; MIM: 601021], processed after translation[42,43]) and the human NUP107-NUP133 complex (PDB: 3CQC).[14] Asp157 is predicted to reside on the surface of the protein, suggesting that the p.Asp157Tyr substitution does not affect the folded structure of NUP107 (Figure S11). However, because this protein interacts with many other proteins,[44] the possibility that the p.Asp157Tyr substitution might impair these interactions cannot be excluded, although no such changed

Please cite this article in press as: Miyake et al., Biallelic Mutations in Nuclear Pore Complex Subunit *NUP107* Cause Early-Childhood-Onset Steroid-Resistant Nephrotic Syndrome, The American Journal of Human Genetics (2015), http://dx.doi.org/10.1016/j.ajhg.2015.08.013

Table 2. *NUP107* Mutations in Affected Individuals with Early-Onset SRNS

Mutation	Amino Acid Change	PolyPhen-2	PyloP	MutationTaster	Grantham	EVS	ExAC	HGVD	In-House Exomes[a] (n = 575)
c.469G>T	p.Asp157Tyr	0.712	2.84	0.998403	160	0	0	0	0
c.969+1G>A	splice site	NA	NA	NA	NA	0	0	0	0
c.1079_1083delAAGAG	p.Glu360Glyfs*6	NA	NA	NA	NA	0	0.0000083	0	0.0008696
c.2492A>C	p.Asp831Ala	1.000	1.952	0.99995	126	0	0	0.0013587	0

Mutations were annotated according to *NUP107* cDNA (GenBank: NM_020401.2). Abbreviations are as follows: EVS, NHLBI Exome Sequencing Project Exome Variant Server; HGVD, Human Genetics Variation Database (the public exome database of the Japanese population).
[a]In-house exome database of Japanese control individuals.

interaction for this particular variant site has been reported. Because the Asp831 side chain forms hydrogen bonds with the Arg842 side chain, the p.Asp831Ala substitution is considered to disrupt these hydrogen bonds. To evaluate the effects of this variant on the structure of NUP107, we performed MD simulations for wild-type and altered NUP107 in solution. In this substitution, a region around the variant site and a region involved in interactions with NUP133 (amino acid residues 881–890) both showed more fluctuations than did those same regions in the wild-type protein (Figure S12). This NUP133-interacting region is considered to be structurally correlated with the variant site through van der Waals contacts (Figure S12B). The results from the MD simulations suggest that the p.Asp831Ala substitution impairs the molecular interaction between NUP107 and NUP133.

Impaired Function of the Altered NUP107

Because NUP107 interacts with NUP133 via its C-terminal tail,[14] we investigated the mutational effects on the protein-protein interaction between NUP107 and NUP133 in vitro. We used an in vitro pull-down assay with recombinant proteins produced in a wheat germ cell-free system to determine the contribution of the C-terminal region of NUP107. Consistent with a previous report,[14] the altered NUP107 that lacked a third of the C-terminal region (amino acids 645–925) did not bind to NUP133 as tightly as wild-type NUP107 under equilibrium conditions (Figure S13). Likewise, two truncated NUP107 proteins with extensively shorter C termini (p.Asp324* and p.Glu360Glyfs*6) also showed weaker binding to NUP133. Notably, a p.Asp831Ala protein with an altered C terminus exhibited significantly reduced binding to NUP133, whereas a p.Asp157Tyr protein with an altered N terminus retained full binding activity (Figure 3A). Wild-type GFP-fused NUP107, which was transiently produced by a mammalian expression vector, was bound to endogenous NUP133 in HeLa cells, and the p.Asp831Ala protein was also bound to NUP133 but weakly in comparison to the wild-type (Figure 3B). Observation of the intracellular localization of altered GFP-NUP107 indicated that the two truncated proteins were distributed mainly in the cytoplasm, whereas the wild-type protein was clearly localized in the nuclear envelope (Figure 3C). The p.Asp831Ala altered protein was localized in the nuclear envelope and cytoplasm (Figure 3C). These results are consistent with the impaired interaction observed between the altered NUP107 and NUP133.

Zebrafish with *nup107* Knockdown Have Glomerular Abnormalities Mimicking SRNS

Reportedly, zebrafish with homozygous *nup107* mutations and morphants with *nup107* knockdown produced with anti-sense MOs each similarly showed a thin pharyngeal skeleton, unfolded intestine, and loss of swim bladder and died on days 5 and 6.[20] However, the specific renal phenotype was not investigated. Therefore, we injected the *nup107*-TB MO or *nup107*-SB MO to create an in-frame (15-bp) deletion at exon 24 to mimic the commonly shared missense mutation (c.2492A>C [p.Asp831Ala]) and then carefully observed the renal phenotype in vivo (Figures S14 and S15). As reported previously,[20] neither of the zebrafish morphants developed edema until they died at around days 5 and 6 (Figure S14A). Furthermore, we sought to identify the glomerular filtration impairment in knockdown zebrafish (*nup107*-TB MO) but did not observe any traces of recognizable protein leakage in glomeruli at 96 hpf (data not shown). Although zebrafish might not be the best animal model for generating renal phenotypes, in a microscopic section of the *nup107*-SB morphant, we were able to find supportive findings in that the glomeruli were generally underdeveloped and showed hypoplastic or poorly organized capillary vessels and mesangial regions (Figures S14C–S14E). Electron microscopy revealed abnormally shaped foot processes and collapse of the capillary lumen in both morphants (Figures S14F–S14K and S16). Because these observations are similar to those from humans with FSGS, the zebrafish morphants might reflect the renal changes caused by the *NUP107* mutation.

Unchanged NPC Localization in Lymphoblastoid Cells from Affected Individuals with *NUP107* Mutations

Reportedly, NUP107 depletion results in decreased or absent NPCs.[29,36] However, a lymphoblastoid cell line derived from affected individuals showed no apparent NPC loss or abnormality by immunohistochemistry analysis (data not shown), which indicates that some residual

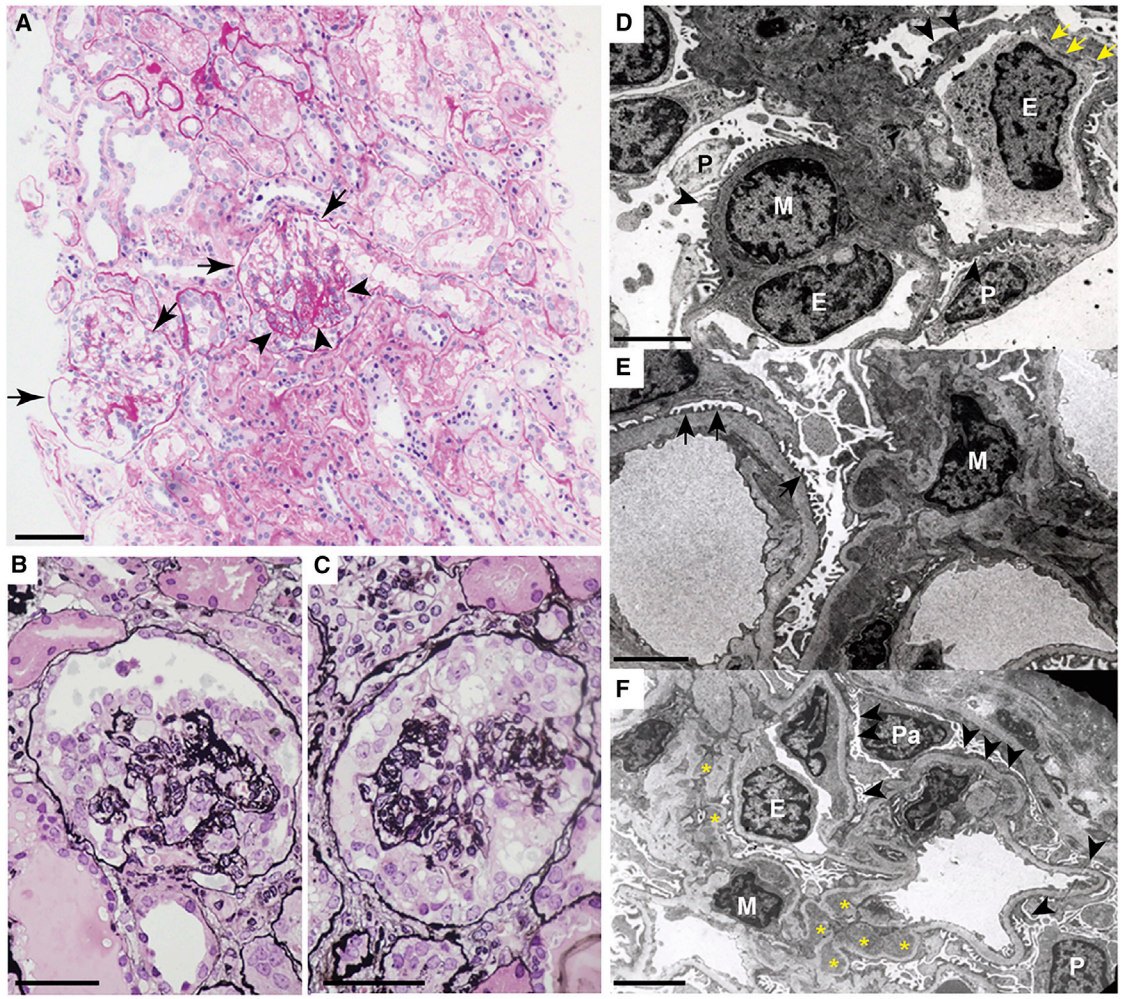

Figure 2. Kidney Histopathology of Affected Individuals with Biallelic *NUP107* Mutations
(A–C) Light micrographs of kidney biopsy specimens from SRNS-TWH II-1. (A) A low-power view (periodic acid-Schiff stain, 100× magnification) of two representative abnormal glomeruli (arrows). Half of the glomerulus is sclerosed (arrowheads). (B and C) Enlarged images (periodic acid methenamine silver stain, 400× magnification) show the collapse of glomerular tufts with hypertrophy and hyperplasia of the glomerular epithelial cells that fill the urinary space. Tubular injury accompanying atrophy of epithelia and interstitial fibrosis is noted.
(D–F) Electron micrographs of biopsy specimens from SRNS-2 II-1 (D), SRNS-2 II-3 (E), and SRNS-2 II-4 (F). Effacement of podocyte foot processes and some mesangial expansion with sub-endothelial electron-dense deposits are apparent. The thickness of the glomerular basement membrane appears normal and shows no evidence of splitting, lamellation, or fragmentation, thereby excluding the possibility of a primary basement-membrane defect. Accumulation of storage materials and dysmorphic mitochondria were not found in the podocyte cytoplasm. Abbreviations are as follows: E, endothelial cell; M, mesangial cell; P, podocyte; Pa, papillary epithelia. Arrowheads indicate effacement of podocyte foot processes, yellow arrows represent electron dense deposits, black arrows show flattened podocyte foot processes, and yellow asterisks show paramesangial deposits.
Scale bars represent100 μm (A), 40 μm (B and C), 2 μm (D and E), and 5 μm (F).

functions of altered NUP107 might persist in the cells of affected individuals, at least under non-stressful conditions. NUP107 is an essential scaffold protein in the NPC, a structure that is evolutionary conserved from yeast to vertebrates.[29,36] Therefore, in the null state, *NUP107* mutants might be lethal in humans.

Discussion

In this study, we have shown that biallelic *NUP107* mutations cause early-onset SRNS in humans. Affected individuals with *NUP107* mutations usually developed SRNS at 2–3 years of age and progressed to ESRD before 10 years of age but experienced no recurrence of the disease after renal transplantation. How do *NUP107* mutations cause a glomerular phenotype in humans? This might be partly explained by the specific properties of podocytes, which are highly differentiated with a unique architecture (foot processes and slit membranes).[45,46] In affected individuals with *NUP107* mutations, insufficient NUP107 function could cause immature and/or hypoplastic podocytes, or at least functionally impaired podocytes that are progressively destroyed by

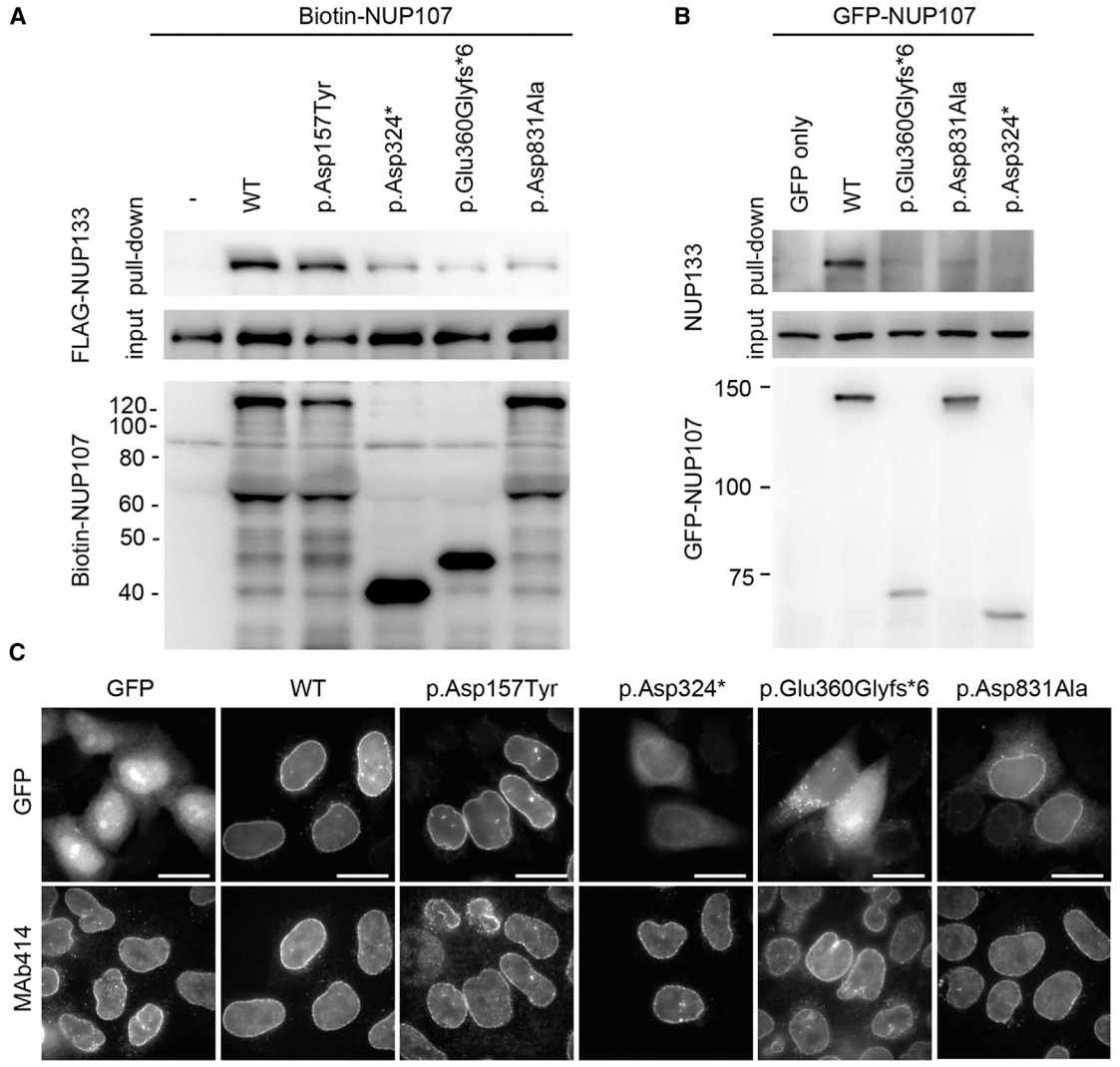

Figure 3. Decreased Intermolecular Interactions between NUP107 and NUP133
(A) In vitro protein-protein binding assay of altered NUP107 with NUP133. The FLAG-tagged NUP133 mixed with biotinylated altered NUP107 proteins was subjected to a pull-down assay with streptavidin magnetic beads. The bound proteins were separated by SDS-PAGE and then detected with an anti-FLAG antibody or with streptavidin-horseradish peroxidase. The corresponding protein inputs are shown in the middle and bottom panels.
(B) Evaluation of the interaction between NUP107 and NUP133 with the use of wild-type NUP107 and its alterations. Wild-type GFP-NUP107 or its alterations were transiently produced in HeLa cells and precipitated with an anti-GFP antibody. The NUP107-NUP133 interaction was analyzed via immunoblotting using the antibodies indicated.
(C) Subcellular localization of NUP107 or its alterations. For visualizing localization of altered or wild-type GFP-NUP107 in HeLa cells, the cells were fixed and stained with a MAb414 antibody recognizing the NPC on the nuclear envelopes. Scale bars represent 20 μm.
The following abbreviation is used: WT, wild-type.

increased filtration pressure after birth. Interestingly, nuclear-envelope proteins, including NPCs, are closely associated with mechanotransduction signaling,[47,48] and mechanical stretching decreases podocyte proliferation and cell-body size by reorganizing the actin cytoskeleton in vitro.[49,50] Thus, increased post-natal capillary pressure leading to mechanical stretching of vulnerable podocytes might accelerate glomerulus damage. Furthermore, mature podocytes do not regenerate.[51,52] Thus, the core pathological condition of SRNS caused by *NUP107* mutations is a structural abnormality, which correlates well with the early SRNS onset in childhood, its steroid resistance, and its lack of post-transplant relapse (Figure S17).

Recently, a homozygous missense mutation (c.303G>A [p.Met101Ile]) was reported in an affected individual who is from a consanguineous family and presents with global developmental delay and early-onset FSGS.[53] However, none of our affected individuals with *NUP107* recessive mutations show neurological impairment. Additional genetic factors might be involved in the neurological symptoms of the consanguineous family. Alternatively, different mutations could cause an additional neurological phenotype. This mutation has been suggested to lead to

abnormal splicing (and possibly a nearly null function), although no direct evidence has been shown.[53] As for p.Asp157Tyr, we could not find direct evidence of its functional impairment experimentally. However, it could be a hypomorphic variant; if so, this might explain the milder phenotype in the SRNS-12 family, who carries both missense mutations (c.469G>T [p.Asp157Tyr] and c.2492A>C [p.Asp831Ala]). Thus, it is possible that the residual NUP107 function left by missense mutations (including c.469G>T [p.Asp157Tyr]) is related to the late onset age and/or milder severity of the disease. It is intriguing that mutations in *NUP107*, which encodes an essential nucleoporin of the NPC, lead to a kidney-specific disease in humans.

In summary, biallelic *NUP107* mutations cause early-onset SRNS for which renal transplantation is the only effective treatment. Access to genetic information is useful for proper clinical management of NS. Therefore, screening *NUP107* mutations in SRNS individuals with broad ranges of clinical severity is strongly encouraged. Furthermore, we did not identify the genetic cause in six pairs of affected siblings and seven single affected individuals in our cohort, which implies a heterogenetic etiology for early-onset SRNS. Further research is necessary to uncover the whole picture of this type of SRNS.

Supplemental Data

Supplemental Data include a supplemental note, 17 figures, and 8 tables and can be found with this article online at http://dx.doi.org/10.1016/j.ajhg.2015.08.013.

Acknowledgments

We are grateful to all the affected individuals and their families who participated in this study. We also thank our clinical colleagues who supported the participating families: Dr. Makoto Endo (Laboratory of Fish Health Management, Tokyo University of Marine Science and Technology) for morphological evaluation of zebrafish and Ms. Sugimoto, Ms. Takabe, and Mr. Mitsui for technical assistance. This work was supported in part by a grant for Research on Measures for Intractable Diseases, a grant for Comprehensive Research on Disability Health and Welfare, and the Strategic Research Program for Brain Science from the Japan Agency for Medical Research and Development; a Grant-in-Aid for Scientific Research on Innovative Areas (Transcription Cycle) (24118007) from the Ministry of Education, Culture, Sports, Science, and Technology of Japan; Grants-in-Aid for Scientific Research (A, B, and C) and for Challenging Exploratory Research from the Japan Society for the Promotion of Science; the fund for Creation of Innovation Centers for Advanced Interdisciplinary Research Areas Program of the Project for Developing Innovation Systems from the Japan Science and Technology Agency; the Takeda Science Foundation; the Osaka Kidney Foundation; and grant HI12C0014 from the Korean Health Technology R&D Project, Ministry of Health & Welfare. K.I. also received grants from Pfizer Japan, Daiichi Sankyo, the Japan Blood Product Organization, Miyarisan Pharmaceutical, AbbVie, CSL Behring, JCR Pharmaceuticals, and Teijin Pharma; and consulting fees from Chugai Pharmaceutical and Astellas Pharma. N.Y. received grants from Novartis Pharma KK and Asahi Kasei Pharma.

Received: June 6, 2015
Accepted: August 28, 2015
Published: September 24, 2015

Web Resources

The URLs for data presented herein are as follows:

1000 Genomes FTP site, ftp://ftp.1000genomes.ebi.ac.uk/vol1/ftp/technical/reference/README.human_g1k_v37.fasta.txt
ExAC Browser, http://exac.broadinstitute.org/
Genome Analysis Toolkit, http://www.broadinstitute.org/gatk
HGVD, http://www.genome.med.kyoto-u.ac.jp/SnpDB/
NHLBI Exome Sequencing Project Exome Variant Server, http://evs.gs.washington.edu/EVS/
Novoalign, http://www.novocraft.com
OMIM, http://www.omim.org
PDB, http://www.rcsb.org/pdb/home/home.do
Picard, http://picard.sourceforge.net
RefSeq, http://www.ncbi.nlm.nih.gov/refseq/
UCSC Genome Browser, https://genome.ucsc.edu/

References

1. Gipson, D.S., Massengill, S.F., Yao, L., Nagaraj, S., Smoyer, W.E., Mahan, J.D., Wigfall, D., Miles, P., Powell, L., Lin, J.J., et al. (2009). Management of childhood onset nephrotic syndrome. Pediatrics *124*, 747–757.
2. Bullich, G., Trujillano, D., Santín, S., Ossowski, S., Mendizábal, S., Fraga, G., Madrid, Á., Ariceta, G., Ballarín, J., Torra, R., et al. (2015). Targeted next-generation sequencing in steroid-resistant nephrotic syndrome: mutations in multiple glomerular genes may influence disease severity. Eur. J. Hum. Genet. *23*, 1192–1199.
3. McKinney, P.A., Feltbower, R.G., Brocklebank, J.T., and Fitzpatrick, M.M. (2001). Time trends and ethnic patterns of childhood nephrotic syndrome in Yorkshire, UK. Pediatr. Nephrol. *16*, 1040–1044.
4. Kim, J.S., Bellew, C.A., Silverstein, D.M., Aviles, D.H., Boineau, F.G., and Vehaskari, V.M. (2005). High incidence of initial and late steroid resistance in childhood nephrotic syndrome. Kidney Int. *68*, 1275–1281.
5. Saleem, M.A. (2013). New developments in steroid-resistant nephrotic syndrome. Pediatr. Nephrol. *28*, 699–709.
6. Zagury, A., Oliveira, A.L., Montalvão, J.A., Novaes, R.H., Sá, V.M., Moraes, C.A., and Tavares, Mde.S. (2013). Steroid-resistant idiopathic nephrotic syndrome in children: long-term follow-up and risk factors for end-stage renal disease. J. Bras. Nefrol. *35*, 191–199.
7. Trautmann, A., Bodria, M., Ozaltin, F., Gheisari, A., Melk, A., Azocar, M., Anarat, A., Caliskan, S., Emma, F., Gellermann, J., et al.; PodoNet Consortium (2015). Spectrum of steroid-resistant and congenital nephrotic syndrome in children: the PodoNet registry cohort. Clin. J. Am. Soc. Nephrol. *10*, 592–600.
8. Lovric, S., Fang, H., Vega-Warner, V., Sadowski, C.E., Gee, H.Y., Halbritter, J., Ashraf, S., Saisawat, P., Soliman, N.A., Kari, J.A., et al.; Nephrotic Syndrome Study Group (2014). Rapid detection of monogenic causes of childhood-onset steroid-resistant nephrotic syndrome. Clin. J. Am. Soc. Nephrol. *9*, 1109–1116.

9. Machuca, E., Benoit, G., and Antignac, C. (2009). Genetics of nephrotic syndrome: connecting molecular genetics to podocyte physiology. Hum. Mol. Genet. *18* (R2), R185–R194.
10. Mekahli, D., Liutkus, A., Ranchin, B., Yu, A., Bessenay, L., Girardin, E., Van Damme-Lombaerts, R., Palcoux, J.B., Cachat, F., Lavocat, M.P., et al. (2009). Long-term outcome of idiopathic steroid-resistant nephrotic syndrome: a multicenter study. Pediatr. Nephrol. *24*, 1525–1532.
11. Sadowski, C.E., Lovric, S., Ashraf, S., Pabst, W.L., Gee, H.Y., Kohl, S., Engelmann, S., Vega-Warner, V., Fang, H., Halbritter, J., et al.; SRNS Study Group (2015). A single-gene cause in 29.5% of cases of steroid-resistant nephrotic syndrome. J. Am. Soc. Nephrol. *26*, 1279–1289.
12. Kitamura, A., Tsukaguchi, H., Iijima, K., Araki, J., Hattori, M., Ikeda, M., Honda, M., Nozu, K., Nakazato, H., Yoshikawa, N., et al. (2006). Genetics and clinical features of 15 Asian families with steroid-resistant nephrotic syndrome. Nephrol. Dial. Transplant. *21*, 3133–3138.
13. Tsurusaki, Y., Koshimizu, E., Ohashi, H., Phadke, S., Kou, I., Shiina, M., Suzuki, T., Okamoto, N., Imamura, S., Yamashita, M., et al. (2014). De novo SOX11 mutations cause Coffin-Siris syndrome. Nat. Commun. *5*, 4011.
14. Boehmer, T., Jeudy, S., Berke, I.C., and Schwartz, T.U. (2008). Structural and functional studies of Nup107/Nup133 interaction and its implications for the architecture of the nuclear pore complex. Mol. Cell *30*, 721–731.
15. Takai, K., Sawasaki, T., and Endo, Y. (2010). Practical cell-free protein synthesis system using purified wheat embryos. Nat. Protoc. *5*, 227–238.
16. Sawasaki, T., Morishita, R., Gouda, M.D., and Endo, Y. (2007). Methods for high-throughput materialization of genetic information based on wheat germ cell-free expression system. Methods Mol. Biol. *375*, 95–106.
17. Sawasaki, T., Kamura, N., Matsunaga, S., Saeki, M., Tsuchimochi, M., Morishita, R., and Endo, Y. (2008). Arabidopsis HY5 protein functions as a DNA-binding tag for purification and functional immobilization of proteins on agarose/DNA microplate. FEBS Lett. *582*, 221–228.
18. Hawryluk-Gara, L.A., Shibuya, E.K., and Wozniak, R.W. (2005). Vertebrate Nup53 interacts with the nuclear lamina and is required for the assembly of a Nup93-containing complex. Mol. Biol. Cell *16*, 2382–2394.
19. Clever, M., Funakoshi, T., Mimura, Y., Takagi, M., and Imamoto, N. (2012). The nucleoporin ELYS/Mel28 regulates nuclear envelope subdomain formation in HeLa cells. Nucleus *3*, 187–199.
20. Zheng, X., Yang, S., Han, Y., Zhao, X., Zhao, L., Tian, T., Tong, J., Xu, P., Xiong, C., and Meng, A. (2012). Loss of zygotic NUP107 protein causes missing of pharyngeal skeleton and other tissue defects with impaired nuclear pore function in zebrafish embryos. J. Biol. Chem. *287*, 38254–38264.
21. Van Der Spoel, D., Lindahl, E., Hess, B., Groenhof, G., Mark, A.E., and Berendsen, H.J. (2005). GROMACS: fast, flexible, and free. J. Comput. Chem. *26*, 1701–1718.
22. Kelley, L.A., and Sternberg, M.J. (2009). Protein structure prediction on the Web: a case study using the Phyre server. Nat. Protoc. *4*, 363–371.
23. Guerois, R., Nielsen, J.E., and Serrano, L. (2002). Predicting changes in the stability of proteins and protein complexes: a study of more than 1000 mutations. J. Mol. Biol. *320*, 369–387.
24. Bussi, G., Donadio, D., and Parrinello, M. (2007). Canonical sampling through velocity rescaling. J. Chem. Phys. *126*, 014101.
25. Darden, T., York, D., and Pedersen, L. (1993). Particle mesh Ewald: An N·log(N) method for Ewald sums in large systems. J. Chem. Phys. *98*, 10089–10092. http://dx.doi.org/10.1063/1.464397.
26. Hess, B., Bekker, H., Berendsen, H.J.C., and Fraaije, J.G.E.M. (1998). LINCS: A linear constraint solver for molecular simulations. J. Comput. Chem. *18*, 1463–1472, 10.1002/(SICI)1096-987X(199709)18:12<1463:AID-JCC4>3.0.CO;2-H.
27. Banerjee, H.N., Gibbs, J., Jordan, T., and Blackshear, M. (2010). Depletion of a single nucleoporin, Nup107, induces apoptosis in eukaryotic cells. Mol. Cell. Biochem. *343*, 21–25.
28. Antonin, W., Ellenberg, J., and Dultz, E. (2008). Nuclear pore complex assembly through the cell cycle: regulation and membrane organization. FEBS Lett. *582*, 2004–2016.
29. Boehmer, T., Enninga, J., Dales, S., Blobel, G., and Zhong, H. (2003). Depletion of a single nucleoporin, Nup107, prevents the assembly of a subset of nucleoporins into the nuclear pore complex. Proc. Natl. Acad. Sci. USA *100*, 981–985.
30. Hoelz, A., Debler, E.W., and Blobel, G. (2011). The structure of the nuclear pore complex. Annu. Rev. Biochem. *80*, 613–643.
31. Weis, K. (2003). Regulating access to the genome: nucleocytoplasmic transport throughout the cell cycle. Cell *112*, 441–451.
32. Fried, H., and Kutay, U. (2003). Nucleocytoplasmic transport: taking an inventory. Cell. Mol. Life Sci. *60*, 1659–1688.
33. Strambio-De-Castillia, C., Niepel, M., and Rout, M.P. (2010). The nuclear pore complex: bridging nuclear transport and gene regulation. Nat. Rev. Mol. Cell Biol. *11*, 490–501.
34. Ori, A., Banterle, N., Iskar, M., Andrés-Pons, A., Escher, C., Khanh Bui, H., Sparks, L., Solis-Mezarino, V., Rinner, O., Bork, P., et al. (2013). Cell type-specific nuclear pores: a case in point for context-dependent stoichiometry of molecular machines. Mol. Syst. Biol. *9*, 648.
35. Bui, K.H., von Appen, A., DiGuilio, A.L., Ori, A., Sparks, L., Mackmull, M.T., Bock, T., Hagen, W., Andrés-Pons, A., Glavy, J.S., and Beck, M. (2013). Integrated structural analysis of the human nuclear pore complex scaffold. Cell *155*, 1233–1243.
36. Walther, T.C., Alves, A., Pickersgill, H., Loïodice, I., Hetzer, M., Galy, V., Hülsmann, B.B., Köcher, T., Wilm, M., Allen, T., et al. (2003). The conserved Nup107-160 complex is critical for nuclear pore complex assembly. Cell *113*, 195–206.
37. González-Aguilera, C., and Askjaer, P. (2012). Dissecting the NUP107 complex: multiple components and even more functions. Nucleus *3*, 340–348.
38. Mundlos, S., Pelletier, J., Darveau, A., Bachmann, M., Winterpacht, A., and Zabel, B. (1993). Nuclear localization of the protein encoded by the Wilms' tumor gene WT1 in embryonic and adult tissues. Development *119*, 1329–1341.
39. Saotome, I., Curto, M., and McClatchey, A.I. (2004). Ezrin is essential for epithelial organization and villus morphogenesis in the developing intestine. Dev. Cell *6*, 855–864.
40. Thong, K.M., Xu, Y., Cook, J., Takou, A., Wagner, B., Kawar, B., and Ong, A.C. (2013). Cosegregation of focal segmental glomerulosclerosis in a family with familial partial lipodystrophy due to a mutation in LMNA. Nephron Clin. Pract. *124*, 31–37.
41. Nagy, V., Hsia, K.C., Debler, E.W., Kampmann, M., Davenport, A.M., Blobel, G., and Hoelz, A. (2009). Structure of a trimeric

nucleoporin complex reveals alternate oligomerization states. Proc. Natl. Acad. Sci. USA *106*, 17693–17698.

42. Fontoura, B.M., Blobel, G., and Matunis, M.J. (1999). A conserved biogenesis pathway for nucleoporins: proteolytic processing of a 186-kilodalton precursor generates Nup98 and the novel nucleoporin, Nup96. J. Cell Biol. *144*, 1097–1112.
43. Loïodice, I., Alves, A., Rabut, G., Van Overbeek, M., Ellenberg, J., Sibarita, J.B., and Doye, V. (2004). The entire Nup107-160 complex, including three new members, is targeted as one entity to kinetochores in mitosis. Mol. Biol. Cell *15*, 3333–3344.
44. Alber, F., Dokudovskaya, S., Veenhoff, L.M., Zhang, W., Kipper, J., Devos, D., Suprapto, A., Karni-Schmidt, O., Williams, R., Chait, B.T., et al. (2007). Determining the architectures of macromolecular assemblies. Nature *450*, 683–694.
45. Pavenstädt, H., Kriz, W., and Kretzler, M. (2003). Cell biology of the glomerular podocyte. Physiol. Rev. *83*, 253–307.
46. Quaggin, S.E., and Kreidberg, J.A. (2008). Development of the renal glomerulus: good neighbors and good fences. Development *135*, 609–620.
47. Swift, J., and Discher, D.E. (2014). The nuclear lamina is mechano-responsive to ECM elasticity in mature tissue. J. Cell Sci. *127*, 3005–3015.
48. Fedorchak, G.R., Kaminski, A., and Lammerding, J. (2014). Cellular mechanosensing: getting to the nucleus of it all. Prog. Biophys. Mol. Biol. *115*, 76–92.
49. Endlich, N., Kress, K.R., Reiser, J., Uttenweiler, D., Kriz, W., Mundel, P., and Endlich, K. (2001). Podocytes respond to mechanical stress in vitro. J. Am. Soc. Nephrol. *12*, 413–422.
50. Petermann, A.T., Hiromura, K., Blonski, M., Pippin, J., Monkawa, T., Durvasula, R., Couser, W.G., and Shankland, S.J. (2002). Mechanical stress reduces podocyte proliferation in vitro. Kidney Int. *61*, 40–50.
51. Kriz, W. (1996). Progressive renal failure–inability of podocytes to replicate and the consequences for development of glomerulosclerosis. Nephrol. Dial. Transplant. *11*, 1738–1742.
52. Nagata, M., Nakayama, K., Terada, Y., Hoshi, S., and Watanabe, T. (1998). Cell cycle regulation and differentiation in the human podocyte lineage. Am. J. Pathol. *153*, 1511–1520.
53. Alazami, A.M., Patel, N., Shamseldin, H.E., Anazi, S., Al-Dosari, M.S., Alzahrani, F., Hijazi, H., Alshammari, M., Aldahmesh, M.A., Salih, M.A., et al. (2015). Accelerating novel candidate gene discovery in neurogenetic disorders via whole-exome sequencing of prescreened multiplex consanguineous families. Cell Rep. *10*, 148–161.

Pediatr Nephrol (2016) 31:105–112
DOI 10.1007/s00467-015-3196-1

ORIGINAL ARTICLE

Insignificant impact of VUR on the progression of CKD in children with CAKUT

Kenji Ishikura[1,2] · Osamu Uemura[3,13] · Yuko Hamasaki[4] · Hideo Nakai[5] · Shuichi Ito[6] · Ryoko Harada[2] · Motoshi Hattori[7] · Yasuo Ohashi[8] · Ryojiro Tanaka[9] · Koichi Nakanishi[10] · Tetsuji Kaneko[11] · Kazumoto Iijima[12] · Masataka Honda[2] · on behalf of the Pediatric CKD Study Group in Japan in conjunction with the Committee of Measures for Pediatric CKD of the Japanese Society for Pediatric Nephrology

Received: 7 February 2015 / Revised: 13 August 2015 / Accepted: 14 August 2015 / Published online: 24 September 2015

Abstract
Background Vesicoureteral reflux (VUR) is associated with an increased risk of kidney disorders. It is unclear whether VUR is associated with progression from chronic kidney disease (CKD) to end-stage kidney disease (ESKD) in children with congenital anomalies of the kidney and urinary tract (CAKUT).
Methods We conducted a 3-year follow-up survey of a cohort of 447 children with CKD (stage 3–5). Rates of and risk factors for progression to ESKD were determined using the Kaplan–Meier method and Cox regression respectively.
Results Congenital anomaly of the kidney and urinary tract was the primary etiology in 278 out of 447 children; 118 (42.4 %) had a history of VUR at the start of the cohort study. There were significantly more boys than girls with VUR, whereas the proportions were similar in children without VUR. The types of urinary anomalies/complications of the two groups were significantly different. Three-year renal survival rates of the groups were not significantly different, irrespective of CKD stage. Age <2 years and age after puberty, stage 4 or 5 CKD, and heavy proteinuria, but not history of VUR, were significantly associated with progression to ESKD.
Conclusions History of VUR at the start of follow-up was not associated with the progression of stage 3–5 CKD in children with CAKUT.

Keywords Chronic kidney disease · Cohort study · Congenital anomalies of the kidney and urinary tract · End-stage kidney disease · Vesicoureteral reflux

Electronic supplementary material The online version of this article (doi:10.1007/s00467-015-3196-1) contains supplementary material that is available to authorized users

✉ Kenji Ishikura
kenzo@ii.e-mansion.com

[1] Department of Nephrology and Rheumatology, National Center for Child Health and Development, 2-10-1 Okura, Setagaya-ku, Tokyo 157-8535, Japan

[2] Department of Nephrology, Tokyo Metropolitan Children's Medical Center, Tokyo, Japan

[3] Department of Pediatric Nephrology, Aichi Children's Health and Medical Center, Aichi, Japan

[4] Department of Pediatric Nephrology, Toho University Faculty of Medicine, Tokyo, Japan

[5] Department of Pediatric Urology, Jichi Medical University, Children's Medical Center, Tochigi, Japan

[6] Department of Pediatrics, Yokohama City University Graduate School of Medicine, Kanagawa, Japan

[7] Department of Pediatric Nephrology, Tokyo Women's Medical University, Tokyo, Japan

[8] Department of Integrated Science and Engineering for Sustainable Society, Faculty of Science and Engineering, Chuo University, Tokyo, Japan

[9] Department of Nephrology, Hyogo Prefectural Kobe Children's Hospital, Hyogo, Japan

[10] Department of Pediatrics, Wakayama Medical University, Wakayama, Japan

[11] Division of Clinical Research Support Center, Tokyo Metropolitan Children's Medical Center, Tokyo, Japan

[12] Department of Nephrology, Tokyo Metropolitan Children's Medical Center, Tokyo, Japan

[13] Department of Clinical Medicine, Japanese Red Cross Toyota College of Nursing, Aichi, Japan

Introduction

Congenital anomalies of the kidney and urinary tract (CAKUT), particularly hypoplastic and dysplastic kidneys, are the most common causes of advanced chronic kidney disease (CKD) in children. Children with hypoplastic and dysplastic kidneys often display other structural and physiological abnormalities in the urinary tract system, such as vesicoureteral reflux (VUR). It is probable that VUR predisposes children to urinary tract infections (UTIs) [1–4], although in children with normal kidneys, it was noted that childhood UTIs were unlikely to be associated with the development of CKD [3]. In some studies, VUR was reported to be associated with an increased risk of pyelonephritis, renal scarring, and end-stage kidney disease (ESKD) [5–7], while other studies have reported conflicting results [8–10]. Currently, however, the impact of VUR on the progression of CKD to ESKD in children remains controversial, and it is debated whether VUR is a benign or nonbenign condition [8, 9]. Indeed, some researchers have proposed that VUR is not a risk factor for renal scarring after UTI [10], while another report showed that children with higher-grade VUR (grade III or higher) were more likely to develop renal scarring than children with lower-grade VUR [5]. This controversy extends to the management and treatment of VUR and associated conditions/UTIs, and whether to administer prophylactic antibiotics to prevent recurrent UTIs or consider surgical correction of the ureterovesical junction responsible for VUR [11–13].

In 2010, we started a prospective study of a cohort of 447 Japanese children (aged 3 months to 15 years) with stage 3–5 CKD and reported that 62 % (n=278) of the children had CAKUT [14]. In a subsequent follow-up study, the 1-year renal survival rates, defined as cases that did not progress to ESKD or CKD-related death, were 98.3, 80.0, and 40.9 % for stage 3, 4, and 5 CKD respectively, and risk factors for ESKD were advanced CKD stage, age (<2 years and after the start of puberty), and severe proteinuria [15].

As part of the cohort study, we sent questionnaires to participating institutions to document the clinical characteristics of CKD patients, including history of VUR and its management, history of other urinary tract anomalies and subsequent complications, and history of UTIs. Therefore, the data obtained in this questionnaire provided a valuable opportunity to examine the association, if any, between congenital anomalies of the kidney and VUR. Because we have now accumulated 3 years of follow-up data for our initial cohort of 447 children with stage 3–5 CKD, we also assessed the outcomes of children with a history of VUR at 1 April 2010, namely at the start of the cohort study, in terms of the 3-year renal survival rate. Additionally, we evaluated whether VUR is associated with progression to ESKD. Our objective in this study was to examine the association between a history of VUR at the start of the follow-up and the progression of CKD to ESKD in children with congenital anomalies of the kidney.

Materials and methods

Study design and subjects

The study design and patient population are described in more detail in our previous reports [14, 15]. In August 2010, we sent surveys to 1,190 Japanese institutions asking them to report on their cases of pediatric CKD managed as of 1 April 2010. The first survey documented the number of children with stage 3–5 CKD at each institution. The respondents were asked to review their medical records to determine the numbers of patients with a confirmed diagnosis of CKD, or patients with abnormal serum creatinine values. A total of 925 out of 1,190 institutions (77.7 %) responded to the first questionnaire. In the second survey, questionnaires were sent to 130 institutions treating children with stage 3–5 CKD, as the remaining 795 institutions reported that they did not treat children with stage 3–5 CKD. Respondents were asked to record the clinical characteristics of their patients. In the second survey, 119 out of 130 institutions provided data for 479 children treated within 6 months of 1 April 2010. Of these, 447 children at 113 institutions were eligible, and 278 had a primary etiology of CAKUT [14, 15]. In the other 169 children, CAKUT was not the primary etiology. These children are referred to as children without CAKUT in this study. To determine pubertal stage, the patients were divided into three age groups for boys (<2, ≥2 to <10.8, and ≥10.8 years) and girls (<2, ≥2 to <10.0, and ≥10.0 years), where 10.8 and 10.0 years correspond to the mean age of Japanese boys and girls, respectively, at the start of puberty [16].

Survey on the etiology of chronic kidney disease

The second survey inquired about the factors that led to the discovery of CKD, the presence and type of CAKUT, what led to the detection of CAKUT, and the history/severity of VUR. Among 73 institutions that provided data on VUR assessments, 55 adopted the conventional bottom–up method, and 11 adopted the so-called top–down method (in which 99mTc-dimercaptosuccinic acid renal scans are performed before voiding cystourethrography) [17]. At the other 7 institutions, the method was selected based on the patient's situation. VUR was graded according to the International Classification of Vesicoureteral Reflux [4, 18], into unilateral VUR, low-grade bilateral VUR (with at least one side classified as mild, i.e., grades I and II), and high-grade bilateral VUR (with both sides classified as severe). For the purposes of the present study, we identified all patients with CAKUT and divided them according to the history of VUR, as documented in the second survey.

Survey on patient outcomes at 3 years

To assess the outcomes of patients at 3 years, another survey was sent to the participating institutions (n=113) in July 2013, with a deadline of September 2013. The survey recorded similar information to that recorded in our 1-year follow-up survey [15], and included patient characteristics, cardiac function, blood/urine parameters, renal outcomes, and CKD complications. The present survey also recorded urological complications and bladder dysfunction. As before, all surveys were to be returned using the envelopes provided and data entry was conducted by an independent data center (Japan Clinical Research Support Unit, Tokyo). In the third survey, 91 out of 113 institutions provided data for 384 of the 447 children covered by the second survey.

As previously described, stages 3, 4, and 5 CKD were defined as serum creatinine levels (measured enzymatically) more than twice, four times, and eight times respectively the median normal levels in age- and sex-matched Japanese children [14, 15, 19]. Using the Schwartz equation [20], we verified the accuracy of the classification, yielding a weighted κ-value of 0.71 (95 % confidence interval [CI] 0.65–0.77).

Statistical analyses

The characteristics of children with or without VUR were compared using unpaired t tests for continuous variables and Chi-squared tests for categorical variables. The 3-year renal survival rates were assessed using the Kaplan–Meier method, where death was also considered as an event. The date of measurement of serum creatinine closest to 1 April 2010 represented the starting point (i.e., t=0 years). The log-rank test was used to compare survival rates in patients with and those without VUR at each stage. Cox's proportional hazard regression model was used to identify possible predictors of CKD progression by calculating hazard ratios with 95 % confidence intervals. Values of P<0.05 were considered statistically significant. All statistical analyses were carried out using SAS system version 9 (SAS Institute, Cary, NC, USA).

Results

Characteristics of the children with CAKUT

Of 278 children with CAKUT and stage 3–5 CKD, 60 children (21.6 %) had obstructive urological malformations, which included the posterior urethral valve, stricture of the urethra, hydronephrosis, hydroureter, and cloacal anomalies [14]. The characteristics of 278 children with CAKUT according to history of VUR are presented in Table 1. A history of VUR at 1 April 2010 was present in 118 children (42.4 %), and was absent in 115 children (41.4 %), or unknown/not evaluated in 45 children (16.2 %); data were not provided for 9 children (3.2 %). Among 118 children with VUR, 39 (33.3 %) were previously diagnosed with unilateral VUR, 10 (8.8 %) with low-grade bilateral VUR, and 59 (50.4 %) with high-grade bilateral VUR. The other 10 children were reported by the physician to have been diagnosed with VUR, but the classification was not stated. Among 169 children without a primary etiology of CAKUT, 6 had a history of VUR, of whom 3 had neurogenic bladder, 2 had nephronophthisis, and 1 had polycystic kidney disease. The mean ages at April 2010 were comparable in children with/without VUR. Furthermore, the distributions of stage 3–5 CKD were comparable in the two groups, as were the distributions of proteinuria, the use of antihypertensive drugs, and hypertension. However, there were significantly more boys than girls with VUR, whereas the proportions of boys and girls were approximately equal in children without VUR. Sixty children underwent surgical treatment for the correction of VUR. A large proportion of children with VUR had a history of UTI (66.9 %), and about half of the children with VUR had a history of≥2 episodes of UTIs. These percentages were significantly greater than those in children without VUR or in whom voiding cystourethrography was not performed. In addition, there were significant differences in the distribution of the types of urinary anomalies/complications between the groups, with hydronephrosis, megaureter, bladder dysfunction, and posterior urethral valve anomalies being significantly more frequent in children with VUR. Surgical treatment was performed in 58 children with VUR; the characteristics of children who did or did not undergo surgical treatment are presented in Supplementary Table 1.

The factors that led to the detection of CKD are listed in Table 1. Fetal/neonatal ultrasonography was the most common reason that led to the detection of CKD in both groups. However, the history of a UTI led to the detection of CKD in a significantly greater proportion of children with VUR than children without VUR (23.7 % vs 7.0 %, P<0.001). The rates of other factors that led to the detection CKD (e.g., incidental finding, failure to thrive, and blood analysis in the neonatal period) were comparable in the two groups.

Renal survival rates

The 3-year renal survival rates in children with CAKUT according to CKD stage are shown in Fig. 1a. As expected, renal survival rates declined with increasing CKD stage at the start of the survey. Figure 1b shows the renal survival rates according to CKD stage and history of VUR at 1 April 2010. The renal survival rates were not significantly different in children with VUR and children without VUR at each CKD stage. The renal survival rate was unaffected by the laterality or severity of VUR (Fig. 1c).

Table 1 Characteristics of children with congenital anomalies of the kidney and urinary tract (CAKUT) according to history of vesicoureteral reflux (VUR)

Variable	History of VUR		*P* value	Unknown VUR status
	Yes	No		
n	118	115		45
Sex, *n* (%)				
Male	91 (77.1)	58 (50.4)	<0.001*	26 (57.8)
Female	27 (22.9)	57 (49.6)		19 (42.2)
Age in April 2010, years	8.04±4.63	8.73±4.60	0.251**	7.23±4.27
Age at diagnosis, years	1.48±2.76	3.01±3.99	0.001**	2.08±3.25
CKD stage 3/4/5, *n* (%)				
Stage 3	77 (65.3)	79 (68.7)	0.432*	33 (73.3)
Stage 4	36 (30.5)	28 (24.4)		10 (22.2)
Stage 5	5 (4.2)	8 (7.0)		2 (4.4)
SCr (mg/dL)	1.66±1.13	1.66±1.24	0.960**	1.40±0.92
eGFR abbreviated (mL/min/1.73 m^2)[a]	38.30±16.98	39.79±16.69	0.513**	38.30±16.98
eGFR complete (mL/min/1.73 m^2)[b]	41.81±12.69	38.98±13.32	0.238**	41.81±12.69
History of UTI, *n* (%)	79 (66.9)	15 (13.0)	<0.001*	5 (11.1)
History of ≥2 UTIs, *n* (%)	56 (47.5)	9 (7.8)	<0.001*	2 (4.4)
Proteinuria (g/g creatinine)	1.23±2.66	0.94±1.01	0.376**	1.23±2.66
Heavy proteinuria, *n* (%)[c]	9 (7.6)	12 (10.4)	0.662*	4 (8.9)
Hypertension, *n* (%)[d]	21 (17.8)	20 (17.4)	0.916*	7 (15.6)
Use of antihypertensive drugs, *n* (%)	24 (20.3)	16 (13.9)	0.171*	1 (2.2)
Urinary anomalies/complications, *n* (%)				
Single kidney	18 (15.3)	19 (16.5)	0.791*	2 (4.4)
MCDK	3 (2.5)	9 (7.8)	0.068	2 (4.4)
Hydronephrosis	40 (33.9)	12 (10.4)	<0.001*	5 (11.1)
Megaureter	19 (16.1)	0 (0.0)	<0.001*	0 (0.0)
Bladder dysfunction	19 (16.1)	2 (1.7)	<0.001*	1 (2.2)
Posterior urethral valve	17 (14.4)	3 (2.6)	<0.001*	0 (0.0)
Duplication of pelvis and ureter	4 (3.4)	2 (1.7)	<0.426*	0 (0.0)
Factors leading to the detection of CKD, *n* (%)				
Fetal/neonatal ultrasonography	31 (26.3)	37 (32.2)	0.678*	11 (24.4)
UTI	28 (23.7)	8 (7.0)	<0.001*	3 (6.7)
Incidental finding	13 (11.0)	18 (15.7)	0.298*	8 (17.8)
Failure to thrive, weight loss, or general fatigue	9 (7.6)	13 (11.3)	0.337*	3 (6.7)
Blood analysis in the neonatal period, asphyxia, neonatal shock, or another event	9 (7.6)	9 (7.8)	0.955*	7 (15.6)

Values are *n* (%) or means±standard deviation

VUR vesicoureteral reflux, *CKD* chronic kidney disease, *SCr* serum creatinine, *eGFR* estimated glomerular filtration rate, *UTI* urinary tract infection, *MCDK* multicystic dysplastic kidney, *BUN* blood urea nitrogen

*Chi-squared test

***t* test

[a] Abbreviated Schwartz equation [20], eGFR=41.3 [height (m)/SCr (mg/dL)]

[b] Complete Schwartz equation [20], eGFR=39.1 [height (m)/SCr (mg/dL)]$^{0.516}$ ×[1.8/cystatin C (mg/L)]$^{0.294}$ ×[30/BUN (mg/dL)]$^{0.169}$ ×[1.099 if male]×[height (m)/1.4]$^{0.188}$

[c] Urine protein/creatinine ratio >2.0 g/g urine creatinine

[d] Systolic blood pressure >95th percentile

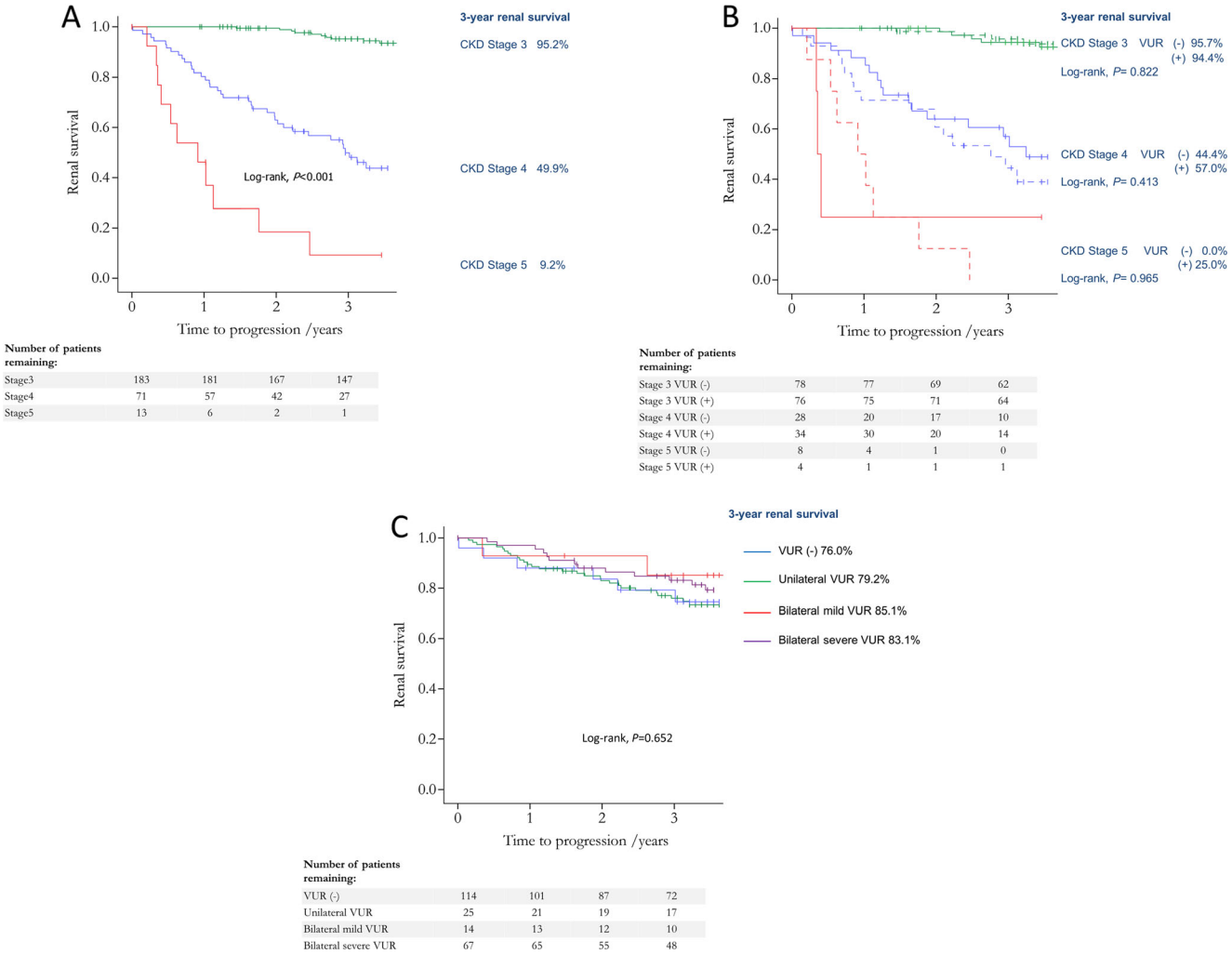

Fig. 1 Renal survival rates at 3 years according to the stage of chronic kidney disease (*CKD*) in patients with congenital anomalies of the kidney and urinary tract (CAKUT). **a** Renal survival rates according to CKD stage (n=267). **b** Renal survival rates according to the presence (n=114) or absence (n=114) of vesicoureteral reflux (*VUR*) for each CKD stage. *Solid lines* children with VUR [VUR (+)]; *dashed lines* children without VUR [VUR (−)]. **c** Renal survival rates according to the laterality and severity of VUR (n=220, those without information on VUR grade were excluded). Children were assessed for progression to end-stage kidney disease or death

Risk factors for progression to end-stage kidney disease

The risk factors for progression to ESKD at 3 years in 278 children with CAKUT, as determined by Cox regression, are shown in Table 2. Age <2 years and age after puberty (vs 2 years to the start of puberty), stage 4 or 5 CKD (vs stage 3 CKD), and heavy proteinuria (urine protein/creatinine ratio >2.0 g/g urine creatinine) were significant risk factors for progression to ESKD. Consistent with the Kaplan–Meier analysis of renal survival rates, the Cox regression model showed that the history of VUR was not associated with progression to ESKD (hazard ratio: 1.19; 95 % confidence interval: 0.53–2.64; P=0.675). Replacing history of VUR with the maximum severity of VUR (none, unilateral, bilateral mild, or bilateral severe) or latest VUR status at 1 April 2010 did not appreciably affect the associations observed (data not shown). When we repeated this analysis only in children with a history of VUR, the risk factors for progression to ESKD included age and CKD stage, but not sex, heavy proteinuria, or history of surgical treatment of VUR (Supplementary Table 2).

Discussion

This 3-year prospective cohort study of children with stage 3–5 CKD caused by CAKUT revealed that the history of VUR at the start of follow-up did not influence the progression to ESKD in these children. However, there were significant differences in the sex distribution and the frequencies of urinary anomalies/complications between children with VUR and those without VUR. These features suggest that the main cause of kidney dysfunction and its progression in these

Table 2 Risk factors for end-stage kidney disease at 3 years (Cox regression model; n=278)

Variable	HR	95 % CI	P value
Female (vs male)	1.75	0.70–4.37	0.232
Age			
Age <2 years (vs 2 years to the start of puberty)	5.31	0.89–28.83	0.053
Age after puberty (vs 2 years to the start of puberty)	6.25	2.53–15.44	<0.001
CKD stage			
Stage 4 (vs stage 3)	37.45	11.56–121.31	<0.001
Stage 5 (vs stage 3)	249.38	43.20–1439.70	<0.001
History of VUR[a]	1.19	0.53–2.64	0.675
Heavy proteinuria[b]	5.08	1.98–13.05	<0.001

HR hazard ratio, *CI* confidence interval, *CKD* chronic kidney disease, *VUR* vesicoureteral reflux

[a] The associations did not change appreciably when history of VUR was replaced with the severity of VUR (none, unilateral, bilateral mild, or bilateral severe) or the maximum grade of VUR

[b] Urine protein/creatinine ratio >2.0 g/g urine creatinine

children might be the presence of a hypoplastic/dysplastic kidney, not VUR.

Notably, a history of VUR at the start of follow-up did not influence the progression of stage 3–5 CKD to ESKD in our cohort. However, it was of interest that there were several statistically significant and clinically relevant differences in the characteristics of children with VUR versus children without VUR. First, although the two groups of children were of similar age, there were significantly more boys than girls with VUR, whereas the proportions of boys and girls were approximately equal in children without VUR. Second, children with VUR were also more likely to have urinary tract anomalies/complications, including hydronephrosis and posterior urethral valve, compared with children without VUR. These differences, in addition to the nonsignificant effect of VUR on the progression of CKD, suggest that it might be important to consider the background etiology other than VUR, such as hypoplastic/dysplastic kidneys.

It is interesting that the majority of children with VUR had a history of UTIs, and about half of the children had a history of multiple UTIs, consistent with the notion that VUR might be a major risk factor for UTI [21–24]. However, despite the evidence supporting an association between UTIs and VUR, there is no conclusive evidence that either contributes to the progression of CKD to end-stage kidney disease in children. In addition, there is currently a limited consensus on how to treat UTIs, primary VUR, and associated anomalies in children [21, 23].

In the present study, risk factors for progression to ESKD included age <2 years and age after puberty (vs 2 years to the start of puberty), stage 4 or 5 CKD (vs stage 3 CKD), and heavy proteinuria (urine protein/creatinine ratio >2.0). These factors are identical to those identified in our previous study [15], which analyzed data on children with CKD with a 1.49-year follow-up period, and were confirmed to be risk factors in those with CAKUT with a longer follow-up period. Importantly, however, the 3-year renal survival rate was not markedly affected by a history of VUR at the start of follow-up in children with stage 3–5 CKD. These findings were also supported by the results of Cox regression, which further revealed that history of VUR was not a risk factor for progression to ESKD in this cohort of children. Our results suggest that VUR itself might not markedly affect the prognosis of children with CAKUT and CKD, addressing the controversy surrounding whether VUR is a benign or nonbenign condition, and helping to clarify the relationship between VUR and progression to ESKD in children with stage 3–5 CKD.

Some potential limitations warrant a mention. First, we did not observe the course of these children during stage 1–2 CKD. It is conceivable that VUR influences the emergence of CKD or progression through the early stages (i.e., stages 1–2). We must also consider that we used "history of VUR" (i.e., the diagnosis of VUR at any time) in the analyses examining the influence of VUR on the progression of CKD. Although similar results were obtained using the "severity of VUR" and the latest VUR status at the start of follow-up, many cases of VUR spontaneously resolve in clinical practice. Indeed, the severity of VUR is changeable over time; thus, the grade at any one time is difficult to know, especially given the invasiveness of the examination for VUR. Additionally, many children with a history of VUR underwent surgical treatment, which may have attenuated the pathological effects of VUR. However, the surgical treatment of VUR was not associated with progression to ESKD (Supplementary Table 2, Supplementary Figure). A similar limitation also applies to the analysis of UTIs, which was assessed as the history of UTIs before 2010. Another limitation is the duration of the survey period; 3 years may be too short to detect progression of CKD to ESKD in some children, depending on the cause of CKD.

In conclusion, about 40 % of children with CAKUT, who account for approximately 60 % of pediatric patients with stage 3–5 CKD, also had a history of VUR. However, the

history or severity of VUR was not associated with increased risk of progression of CKD to ESKD during a follow-up of 3 years. We found marked differences in the general and clinical characteristics of children with VUR vs children without VUR in terms of sex distribution and the proportions of children with urinary tract anomalies. Therefore, while children with CKD caused by CAKUT may have diverse backgrounds, the presence or absence of VUR may enable different backgrounds to be distinguished. Nevertheless, we observed no association between a history of VUR at the start of follow-up and the progression of CKD to ESKD in these children, which may implicate some background etiological factor other than VUR, such as the hypoplastic/dysplastic kidney itself, as the main cause of CKD and its progression to ESKD.

Acknowledgements The authors would like to thank Drs Takuhito Nagai (Aichi), Kenichi Satomura (Osaka), Tomoo Kise (Okinawa), Takuji Yamada (Aichi), Midori Awazu (Tokyo), Hiroshi Asanuma (Tokyo), Toshiyuki Ohta (Hiroshima), Takeshi Matsuyama (Tokyo), Hidefumi Nakamura (Tokyo), Mayumi Sako (Tokyo), Tomoyuki Sakai (Shiga), Yusuke Okuda (Shiga), Shunsuke Shinozuka (Saitama), Yoshinobu Nagaoka (Hokkaido), Shuichiro Fujinaga (Saitama), Hiroshi Kitayama (Shizuoka), Naoya Fujita (Shizuoka), Masataka Hisano (Chiba), Daishi Hirano (Tokyo), Yuko Akioka (Tokyo), Naoaki Mikami (Tokyo), Hiroshi Hataya (Tokyo), Hiroyuki Satoh (Tokyo), Tae Omori (Tokyo), Takashi Sekine (Tokyo), Yoshimitsu Goto (Aichi), Yohei Ikezumi (Niigata), Takeshi Yamada (Niigata), and Akira Matsunaga (Yamagata) of The Pediatric CKD Study Group in Japan for their contributions to the study. The authors would also like to thank all the institutions that participated in the surveys listed in the Supplement, and Mr Masaaki Kurihara, Ms Chie Matsuda, Ms Naomi Miyamoto, and Ms Takako Arai of the Japan Clinical Research Support Unit (Tokyo) for their help with data management; Dr Naoaki Mikami and Ms Sachiko Kawabe of Tokyo Metropolitan Children's Medical Center for their contribution to manuscript preparation; and Nicholas Smith, PhD, of Edanz Group Ltd., for providing language editorial support in the preparation of the manuscript. The results presented in this paper have not been published previously in whole or part, except in abstract format.

Ethics The study was conducted in accordance with the principles of the Declaration of Helsinki and the ethical guidelines issued by the Ministry of Health, Labour, and Welfare, Japan. The study was approved by the ethics committee of the Tokyo Metropolitan Children's Medical Center (ID: 23–49). Because data were reported using patient medical records, informed consent was not obtained in accordance with the above guidelines.

Funding This work was supported by a Health and Labour Sciences Research Grant for Research on Rare and Intractable Diseases from the Ministry of Health, Labour, and Welfare, Japan (H25-nanchitou(nan)-ippan-017 and H26-nanchitou(nan)-ippan-036) and the 2013 Tokyo Metropolitan Hospitals' Clinical Research Fund (Special Research).

Conflict of interest Kenji Ishikura has received lecture fees from Novartis Pharma and Asahi Kasei Pharma. Osamu Uemura has received lecture fees from Asahi Kasei Pharma, Kyowa Hakko Kirin, Takeda Pharmaceutical, and Siemens Group in Japan. Yuko Hamasaki has received research grants from Novartis Pharma, and lecture fees from Novartis Pharma, Astellas Pharma, and Pfizer Japan. Hideo Nakai has received a research grant from Astellas Pharma. Ryojiro Yasuo Ohashi has received research grants from Kyowa Hakko Kirin and Chugai pharmaceutical. Tanaka has received lecture fees from Pfizer Japan and Asahi Kasei Pharma. Koichi Nakanishi has received lecture fees from Novartis Pharma, Asahi Kasei Pharma, and Astellas Pharma. Kazumoto Iijima has received research grants from Novartis and Pfizer Japan, and lecture fees from Novartis, Asahi Kasei Pharma, and Pfizer Japan. Masataka Honda has received lecture fees from Novartis Pharma, Asahi Kasei Pharma, Takeda Pharmaceutical, and Chugai Pharmaceutical. Drs Ito, Harada, Hattori, and Mr Kaneko have no conflicts of interest to declare.

References

1. Brandstrom P, Esbjorner E, Herthelius M, Swerkersson S, Jodal U, Hansson S (2010) The Swedish reflux trial in children: III. Urinary tract infection pattern. J Urol 184:286–291
2. Swerkersson S, Jodal U, Sixt R, Stokland E, Hansson S (2007) Relationship among vesicoureteral reflux, urinary tract infection and renal damage in children. J Urol 178:647–651
3. Salo J, Ikaheimo R, Tapiainen T, Uhari M (2011) Childhood urinary tract infections as a cause of chronic kidney disease. Pediatrics 128:840–847
4. Montini G, Tullus K, Hewitt I (2011) Febrile urinary tract infections in children. N Engl J Med 365:239–250
5. Shaikh N, Ewing AL, Bhatnagar S, Hoberman A (2010) Risk of renal scarring in children with a first urinary tract infection: a systematic review. Pediatrics 126:1084–1091
6. Chen MJ, Cheng HL, Chiou YY (2013) Risk factors for renal scarring and deterioration of renal function in primary vesicoureteral reflux children: a long-term follow-up retrospective cohort study. PLoS One 8:e57954
7. Sjostrom S, Jodal U, Sixt R, Bachelard M, Sillen U (2009) Longitudinal development of renal damage and renal function in infants with high grade vesicoureteral reflux. J Urol 181:2277–2283
8. Coulthard MG (2009) Vesicoureteric reflux is not a benign condition. Pediatr Nephrol 24:227–232
9. Venhola M, Uhari M (2009) Vesicoureteral reflux, a benign condition. Pediatr Nephrol 24:223–226
10. Moorthy I, Easty M, McHugh K, Ridout D, Biassoni L, Gordon I (2005) The presence of vesicoureteric reflux does not identify a population at risk for renal scarring following a first urinary tract infection. Arch Dis Child 90:733–736
11. Hewitt IK, Zucchetta P, Rigon L, Maschio F, Molinari PP, Tomasi L, Toffolo A, Pavanello L, Crivellaro C, Bellato S, Montini G (2008) Early treatment of acute pyelonephritis in children fails to reduce renal scarring: data from the Italian Renal Infection Study Trials. Pediatrics 122:486–490
12. Mathews R, Carpenter M, Chesney R, Hoberman A, Keren R, Mattoo T, Moxey-Mims M, Nyberg L, Greenfield S (2009) Controversies in the management of vesicoureteral reflux: the rationale for the RIVUR study. J Pediatr Urol 5:336–341
13. Sung J, Skoog S (2012) Surgical management of vesicoureteral reflux in children. Pediatr Nephrol 27:551–561
14. Ishikura K, Uemura O, Ito S, Wada N, Hattori M, Ohashi Y, Hamasaki Y, Tanaka R, Nakanishi K, Kaneko T, Honda M, Pediatric CKD Study Group (2013) Pre-dialysis chronic kidney disease in children: results of a nationwide survey in Japan. Nephrol Dial Transplant 28:2345–2355
15. Ishikura K, Uemura O, Hamasaki Y, Ito S, Wada N, Hattori M, Ohashi Y, Tanaka R, Nakanishi K, Kaneko T, Honda M, Pediatric CKD Study Group (2014) Progression to end-stage kidney disease in Japanese children with chronic kidney disease: results of a nationwide prospective cohort study. Nephrol Dial Transplant 29:878–884
16. Matsuo N (1993) Skeletal and sexual maturation in Japanese children. Clin Pediatr Endocrinol 2 [Suppl 1]:1–4

17. Shaikh N, Hoberman A, Rockette HE, Kurs-Lasky M (2012) Identifying children with vesicoureteral reflux: a comparison of 2 approaches. J Urol 188:1895–1899
18. International Reflux Study Committee (1981) Medical versus surgical treatment of primary vesicoureteral reflux: report of the International Reflux Study Committee. Pediatrics 67:392–400
19. Uemura O, Honda M, Matsuyama T, Ishikura K, Hataya H, Yata N, Nagai T, Ikezumi Y, Fujita N, Ito S, Iijima K, Kitagawa T (2011) Age, gender, and body length effects on reference serum creatinine levels determined by an enzymatic method in Japanese children: a multicenter study. Clin Exp Nephrol 15:694–699
20. Schwartz GJ, Munoz A, Schneider MF, Mak RH, Kaskel F, Warady BA, Furth SL (2009) New equations to estimate GFR in children with CKD. J Am Soc Nephrol 20:629–637
21. Japanese Society of Nephrology (2014) Evidence-based clinical practice guideline for CKD 2013. Clin Exp Nephrol 18:346–423
22. Elder JS, Peters CA, Arant BS Jr, Ewalt DH, Hawtrey CE, Hurwitz RS, Parrott TS, Snyder HM 3rd, Weiss RA, Woolf SH, Hasselblad V (1997) Pediatric Vesicoureteral Reflux Guidelines Panel summary report on the management of primary vesicoureteral reflux in children. J Urol 157:1846–1851
23. Peters CA, Skoog SJ, Arant BS Jr, Copp HL, Elder JS, Hudson RG, Khoury AE, Lorenzo AJ, Pohl HG, Shapiro E, Snodgrass WT, Diaz M (2010) Summary of the AUA guideline on management of primary vesicoureteral reflux in children. J Urol 184:1134–1144
24. Silva JM, Diniz JS, Silva AC, Azevedo MV, Pimenta MR, Oliveira EA (2006) Predictive factors of chronic kidney disease in severe vesicoureteral reflux. Pediatr Nephrol 21:1285–1292

Pediatr Nephrol (2016) 31:425–434
DOI 10.1007/s00467-015-3174-7

ORIGINAL ARTICLE

Long-term outcome of idiopathic steroid-resistant nephrotic syndrome in children

Aya Inaba[1] · Yuko Hamasaki[2] · Kenji Ishikura[3,7] · Riku Hamada[3] · Tomoyuki Sakai[4] · Hiroshi Hataya[3] · Fumiyo Komaki[5] · Tetsuji Kaneko[6,8] · Masaaki Mori[1] · Masataka Honda[3]

Received: 8 December 2014 / Revised: 13 July 2015 / Accepted: 15 July 2015 / Published online: 3 September 2015

Abstract
Background Several recent studies have shown improved short-term outcome of steroid-resistant nephrotic syndrome (SRNS) in children; however, only a few studies have evaluated the long-term outcome. The aims of our study were to obtain detailed data and analyze the long-term outcome of children with SRNS.
Methods Sixty-nine children with idiopathic SRNS were enrolled and divided into two groups based on initial histopathological patterns: focal segmental glomerulosclerosis (FSGS) and minimal change (MC)/diffuse mesangial proliferation (DMP). The effects of initial treatment with the immunosuppressant of choice (cyclosporine or cyclophosphamide) on renal survival, remission, and incidence of complications were analyzed in both groups (4 subgroups).
Results The renal survival rate was significantly different among the four different subgroups based on different combinations of initial histopathological pattern (FSGS vs. MC/DMP) and initial immunosuppressant used for treating SRNS (cyclosporine vs. cyclophosphamide) (P=0.013), with renal survival in the FSGS (cyclophosphamide) subgroup being especially low (54.6 %). Disease- and/or treatment-associated complications were relatively low; however, hypertension at last examination was observed in a considerable number of patients (31.9 %).
Conclusions Our results suggest that a recently developed therapeutic regimen with cyclosporine considerably improves both the initial remission rate and the long-term renal survival rate of children with idiopathic SRNS.

Keywords Children · Steroid-resistant nephrotic syndrome · Long-term outcome · Immunosuppressant · Minimal change · Diffuse mesangial proliferation · Focal segmental glomerulosclerosis

Electronic supplementary material The online version of this article (doi:10.1007/s00467-015-3174-7) contains supplementary material, which is available to authorized users.

✉ Yuko Hamasaki
yuhamasaki@med.toho-u.ac.jp

[1] Department of Pediatrics, Yokohama City University Medical Center, Kanagawa, Japan

[2] Department of Pediatric Nephrology, Toho University Faculty of Medicine, 6-11-1, Omori-Nishi, Ota-ku, Tokyo 143-8541, Japan

[3] Department of Nephrology, Tokyo Metropolitan Children's Medical Center, Tokyo, Japan

[4] Department of Pediatrics, Shiga University of Medical Science, Shiga, Japan

[5] Community Health Welfare Division, Kawasaki Saiwai Ward Office Health and Welfare Center, Kanagawa, Japan

[6] Department of Clinical Research, Tokyo Metropolitan Children's Medical Center, Tokyo, Japan

[7] Department of Nephrology and Rheumatology, National Center for Child Health and Development, Tokyo, Japan

[8] Teikyo Academic Research Center, Teikyo University, Tokyo, Japan

Introduction

In general, 10 % of children with idiopathic nephrotic syndrome (INS) show steroid resistance. Early studies reported that 30–40 % of children with steroid-resistant nephrotic syndrome (SRNS) progress to end stage-kidney disease (ESKD) during follow-up of 10 years [1, 2].

Methylprednisolone pulse therapy and/or immunosuppressant therapy, such as cyclophosphamide or cyclosporine, have been used for many years to treat children with SRNS. Cyclophosphamide has been used since the 1960s, and in the 1990s,

uncontrolled trials had found that up to 60 % of children treated with the combination of methylprednisolone pulse therapy and cyclophosphamide or chlorambucil achieved complete remission [3]. Cyclosporine was added to the battery of therapeutic strategies in 1987, and many recent studies have shown the efficacy of cyclosporine for SRNS [4–6]. Hamasaki et al. recently reported a high remission rate (88.6 %) and high renal survival rate (94.3 %) in a prospective 12-month protocol treatment trial using a combined cyclosporine/prednisolone therapeutic regimen for children with SRNS [7]. However, the long-term outcome of children with SRNS, including the renal survival rate, permanent remission rate, and incidence of treatment-related complications, as well as the impact of each therapeutic regimen on these rates have not yet been sufficiently evaluated.

The aims of this retrospective cohort study were to analyze the clinical and histopathological parameters of children with SRNS and to evaluate the remission rate of the initial SRNS episode, renal survival rate, permanent remission rate, and long-term complications. We also analyzed whether the remission rate of the initial SRNS episode and the long-term outcome differ according to the choice of initial immunosuppressant used to treat the SRNS, namely, cyclosporine or cyclophosphamide. The incidence of complications related to SRNS and treatment for SRNS was also evaluated.

Methods

Patients

This study was a retrospective analysis of children with SRNS who were followed in Tokyo Metropolitan Kiyose Children's Hospital (predecessor of Tokyo Metropolitan Children's Medical Center), a tertiary care center for children with kidney disease. Data were retrieved from the hospital's database on children with nephrotic syndrome who fulfilled the following criteria: (1) INS initially diagnosed between 1 January 1990 and 1 January 2005; (2) SRNS, either initial non-responder or late non-responder; (3) followed up for ≥4 years. Children were excluded if they (1) had underlying secondary causes [Henoch–Schönlein nephritis, systemic lupus erythematosus, immunoglobulin (Ig) A nephropathy, membranous nephropathy, membranoproliferative glomerulonephritis, among others]; (2) had congenital or inherited forms of nephrotic syndrome; (3) were younger than 1 year or older than 15 years when diagnosed with nephrotic syndrome; (4) had not undergone renal biopsy.

The database and medical records were reviewed to collect relevant data over the period from diagnosis of INS to last examination, including the date on which each child was diagnosed as having INS and SRNS, demographic characteristics (age, gender) at the time of diagnosis of SRNS, initial histopathological pattern [minimal change (MC), diffuse mesangial proliferation (DMP), or focal segmental glomerulosclerosis (FSGS)], steroid response (primary or late non-responder), therapeutic strategies of immunosuppressant, the date on which each child achieved complete remission of the initial SRNS episode, the date of diagnosis of ESKD, the date on which each child achieved complete remission after last relapse episode, clinical aspects (height, weight, and blood pressure), the usage of anti-hypertensive agents, renal function, the condition of nephrotic syndrome, the complications of nephrotic syndrome or treatment-related complications at the last examination, and the findings of chronic cyclosporine nephrotoxicity at the last renal biopsy.

Definitions

Nephrotic syndrome was diagnosed if the urinary protein/creatinine ratio was ≥1.8 mg/mg and the serum albumin level was ≤2.5 g/dl [7]. SRNS was diagnosed if complete remission was not achieved after treatment with 2 mg/kg prednisolone daily for 4 weeks [8]. Complete remission was defined as negative or trace proteinuria (by the dipstick method or a urinary protein/creatinine ratio of ≤0.20 mg/mg) on urinalysis and a serum albumin level of>2.5 g/dl. Partial remission was defined as a serum albumin level of >2.5 g/dl, but persisting proteinuria on urinalysis (dipstick method +1 or greater, or urinary protein/creatinine ratio of>0.2 mg/mg). The state of remission included both complete remission and partial remission. Non-remission was defined as persisting nephrotic syndrome. Relapse of nephrotic syndrome was defined as increased proteinuria and a serum albumin level of ≤2.5 g/dl. Permanent remission was defined as the relapse-free state without any immunosuppressant or steroid over the previous 2 years or more up to the last examination. Frequently relapsing nephrotic syndrome (FRNS) was defined as four or more relapses within any 12-month period or the condition in which any immunosuppressant was used to control relapse of steroid-sensitive nephrotic syndrome (SSNS). ESKD was defined as the requirement for dialysis or kidney transplantation. Late non-response to steroids was defined as an initial response to steroid therapy but none during a subsequent relapse.

The estimated glomerular filtration rate (eGFR) was calculated using the Schwartz formula for patients aged ≤17 years [9]: $194 \times SCr^{-1.094} \times Age^{-0.278}$ in male patients aged ≥18 years, and $194 \times SCr^{-1.094} \times Age^{-0.278} \times 0.739$ in female patients aged ≥18 years, where SCr is the serum creatinine level [10]. Hypertension was defined as the need for anti-hypertensive therapy, except when given for renoprotective purpose. The height measurements were expressed as the height standard deviation score (SDS) compared with normal stature values for age- and sex-matched healthy Japanese children. Short stature was defined as a height of less than −2.0 SDS.

Histopathology

Renal biopsy was performed after the diagnosis of SRNS. Repeat biopsy was performed for the patients who were treated with cyclosporine to evaluate cyclosporine-related nephrotoxicity. Renal pathologists at our institution evaluated the initial histopathological findings and the development of chronic cyclosporine nephrotoxicity, defined as cyclosporine-associated arteriolopathy and/or cyclosporine-induced tubulointerstitial lesions showing characteristic striped tubulointerstitial lesions.

Treatment

All patients were treated initially with prednisolone at a dose of 2 mg/kg per day administered in three separate doses for 4 weeks (maximum 80 mg/day) and diagnosed with SRNS if they did not achieve complete remission during this period.

Up until the 1990s, following a diagnosis of SRNS, oral cyclophosphamide, methylprednisolone pulse therapy, or a combination of these therapies were administered. Cyclophosphamide was used at a dose 2.5 mg/kg per day (maximum 100 mg per day) orally for 12 weeks (with a total cumulative dose of 210 mg/kg). The basic protocol of methylprednisolone pulse therapy consisted of the administration of methylprednisolone 30 mg/kg per day (2-h infusion, maximum 1000 mg) every day for 3 days—considered to be one course; one course per week was given in weeks 1 and 2, then one course per month was given from week 4 to month 6, followed by one course per 3 months from month 7 to year 2 [11]. Beginning in the mid-1990s, the main immunosuppressant used to treat SRNS was changed to cyclosporine combined with prednisolone, the dose of which was adjusted to maintain a whole-blood trough level of 120–150 ng/ml for the initial 3 months, followed by 80–100 ng/ml for months 4–12, and 60–80 ng/ml for months 13–24, with subsequent tapering of the cyclosporine dose after 2 years of therapy. Among those patients treated with cyclosporine, some additionally received methylprednisolone pulse therapy consisting of methylprednisolone 30 mg/kg per day (2-h infusion, maximum 1000 mg) every day for 3 days—considered to be one course; one course per week was given in weeks 1, 2, 5, 9, and 13 [7]. Prednisolone was started at 1 mg/kg per day in three separate doses for 4 weeks and then was reduced to 1 mg/kg in a single dose every other day for generally 1 year in those patients diagnosed with SRNS.

If a therapeutic regimen failed to induce remission, another regimen or a combination of regimens was considered. That is, if the regimen with cyclosporine failed to induce remission, we switched to the regimen with cyclophosphamide, and if the cyclophosphamide regimen failed to induce remission, we switched to one with cyclosporine. We considered a therapeutic regimen as having failed to induce remission if remission was not induced within 4–6 months after commencement of administration.

Statistical analyses

Results were expressed in terms of median, range, and percentage. The endpoints were the incidences of complete remission of the initial SRNS episode, ESKD, and permanent remission. The duration from the date of diagnosis of SRNS to the date on which each respective endpoint was reached was measured and evaluated using Kaplan–Meier analysis according to subgroup analysis of the initial histopathological patterns (FSGS or MC/DMP) and initial immunosuppressant used for SRNS (cyclosporine or cyclophosphamide). Thus, there were four subgroups. Differences between subgroups were compared using the log-rank test. Regarding renal survival rate, variables, including gender, age at time of SRNS diagnosis, initial histopathological pattern (FSGS or MC/DMP), and initial immunosuppressant used for SRNS were assessed by multivariate analysis with Cox regression. A two-sided P-value of <0.05 was considered to be statistically significant. All statistical analyses were performed using the SAS software package for Windows (release 9.3; SAS Institute Inc., Cary, NC, USA).

Results

In total, 230 patients were diagnosed with INS between 1 January 1990 and 1 January 2005, of whom 147 showed SSNS. Among the remaining 83 SRNS patients, ten patients had been followed for <4 years and four patients had not undergone renal biopsy. Therefore, 69 children were ultimately enrolled in the analysis (Fig. 1). Basic characteristics of these children are shown in Table 1. The first renal biopsy showed MC in 39 children (57 %), FSGS in 22 (32 %), and DMP in eight (11 %). Among the eight patients who showed DMP, two showed mild IgM deposition on immunofluorescence staining, one showed mild C1q deposition, one showed intense C3 deposition and mild IgM and C1q deposition, two showed no deposition, and two had no data about immunofluorescence staining. The median age at diagnosis of SRNS was 3.2 (range 1.1–15.3) years. In children with FSGS diagnosed on the first renal biopsy, cyclophosphamide and cyclosporine were used as the initial immunosuppressant for the initial SRNS episodes in 11 and ten patients, respectively; one patient did not receive any immunosuppressant. In children with MC/DMP on the first renal biopsy, cyclophosphamide was used as the initial immunosuppressant for initial SRNS episodes in 13 patients, cyclosporine was used in 29 patients, and no immunosuppressant was used in five patients, two of whom underwent methylprednisolone pulse therapy. Therapeutic strategies from the time of the initial diagnosis of SRNS to achievement of first complete remission or

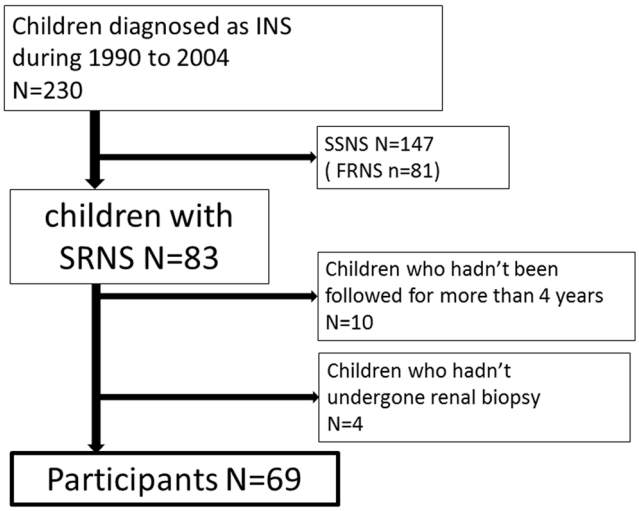

Fig. 1 Overview of idiopathic nephrotic syndrome (*INS*) patients in this study. Of the 230 children diagnosed with INS between 1 January 1990 and 1 January 2005, 69 patients with steroid-resistant nephritic syndrome (*SRNS*) met the entry criteria. *SSNS*, steroid-sensitive nephrotic syndrome; *FRNS*, frequently relapsing nephrotic syndrome

progression to ESKD are shown in Table 2. During the observation period of this study we did not use rituximab, mycophenolate mofetil, or tacrolimus. The overall median follow-up period was 10.1 (range 4.5–19.3) years.

No immunosuppressant was used in six patients (1 in FSGS, 5 in MC/DMP). Of these, three patients attained complete remission early and maintained that condition; one patient was diagnosed with SRNS and had been treated with prednisolone for 1 year only at another institution and did not require any immunosuppressant when she came to our hospital for the first time; one patient had relatively mild proteinuria and spontaneously attained complete remission after prednisolone was discontinued; one patient was treated with prednisolone only and achieved partial remission but not complete remission within 1 month of the start of prednisolone, prednisolone therapy was discontinued after 2 months, and complete remission was finally achieved 7 years after the initial diagnosis of SRNS and maintained to date. Because the above six patients achieved complete remission without any immunosuppressant, they were excluded from the analysis, and the analyses of remission rate, renal survival rate, and permanent remission rate were conducted using only the data of the remaining 63 patients.

Kaplan–Meier analysis revealed that the complete remission rate of the initial SRNS episode at 4 months in those patients whose initial histopathological pattern was FSGS and initial immunosuppressant was cyclosporine [FSGS (cyclosporine) subgroup] was 40 %. In comparison, that of the patients whose initial histopathological pattern was FSGS and initial immunosuppressant was cyclophosphamide [FSGS (cyclophosphamide) subgroup] was 0 %. The complete remission rate of those patients whose initial histopathological pattern was MC/DMP and initial immunosuppressant was cyclosporine [MC/DMP (cyclosporine) subgroup] was 69.0 %. In comparison, that of the patients whose initial histopathological pattern was MC/DMP and initial immunosuppressant was cyclophosphamide [MC/DMP (cyclophosphamide)

Table 1 Basic (background) characteristics of participants in the study

Basic (background) characteristics of participants							
First renal biopsy finding:	FSGS			MC/DMP			Total
First immunosuppressant used to treat SRNS:	CP	CSA	None	CP	CSA	None	
Number of patients	11	10	1	13	29	5	69
Gender (*n*)							
Male	6	7	0	8	21	3	45
Female	5	3	1	5	8	2	24
Age when diagnosed with SRNS (years)							
<3	4	5	0	5	15	1	30
≥3, <7	5	1	0	5	7	2	20
≥7, <11	2	1	0	2	4	2	11
≥11	0	3	1	1	3	0	8
Median age (years) at last follow-up (range)	19.7 (13.6–26.9)	12 (10.0–28.1)	23.3	17.7 (8.2–23.6)	12.1 (6.9–24.9)	16.8 (15.5–27.6)	13.9 (6.9–28.1)
Steroid response							
Late non-responder	0	2	1	3	9	0	15

SRNS, Steroid-resistant nephritic syndrome; MC, minimal change; DMP, diffuse mesangial proliferation; FSGS, focal segmental glomerulosclerosis; CP, cyclophosphamide; CSA, cyclosporine

Table 2 Therapeutic strategies in each initial treatment from the initial diagnosis of steroid-resistant nephrotic syndrome to the first complete remission or progression to end-stage kidney disease

Therapeutic strategies	FSGS			MC/DMP			All patients		
	Number of patients	CR	Progressing to ESKD	Number of patients	CR	Progressing to ESKD	Number of patients	CR	Progressing to ESKD
CSA (n=39)									
CSA alone	1	0	1	20	20	0	21	20	1
CSA+MPT	7	7	0	8[b]	7	0	15[b]	14	0
CSA+MPT→CP→CSA+MZB	0	0	0	1	0	1	1	0	1
CSA→CP+MPT→CSA+MPT→CSA+MZB→MPT→LDL apheresis→CSA	1	0	1	0	0	0	1	0	1
CSA→CP+MPT→MZB	1	1	0	0	0	0	1	1	0
Total	10	8	2	29[b]	27	1	39[b]	35	3
Median follow-up period (years) (range)	9.0 (6.3–16.1)			8.6 (4.5–16.4)			8.7 (4.5–16.4)		
Median duration (years) to CR (range)	0.4 (0.1–5.1)			0.2 (0.0–1.5)			0.2 (0.0–5.1)		
Median duration (years) to ESKD (range)	11.5 (10.1–12.8)			1.8 (–)			10.1 (1.8–12.8)		
CP (n=24)									
CP alone	2	2	0	7	7	0	9	9	0
CP→CSA	3	2	1	0	0	0	3	2	1
CP→CSA→MZB	1	0	1	0	0	0	1	0	1
CP→CSA→CP	1	0	1	0	0	0	1	0	1
CP→CSA→CP+MPT	1	1	0	0	0	0	1	1	0
CP→CSA→MPT	0	0	0	1	1	0	1	1	0
CP→CSA→MPT→CSA	0	0	0	1	1	0	1	1	0
CP→CSA→MPT→CSA→LDL apheresis	0	0	0	1	0	1	1	0	1
CP+MPT[a]	1	0	1	2	2	0	3	2	1
CP+MPT→CSA→CP[a]	1	0	1	0	0	0	1	0	1
CP+MPT→CSA→MPT[a]	1	1	0	1	1	0	2	2	0
Total	11	6	5	13	12	1	24	18	6
Median follow-up period (years) (range)	14.6 (10.4–19.0)			11.5 (5.3–16.3)			12.1(5.3–19.0)		
Median duration (years) to CR (range)	2.5 (0.7–8.6)			1.5 (0.1–3.8)			2.0 (0.1–8.6)		
Median duration (years) to ESKD (range)	2.2 (1.0–3.7)			8.5 (−)			2.3(1.0–8.5)		
Others (n=6)									
MPT[a]	0	0	0	2	2	0	2	2	0
PSL only	1	1	0	3	3	0	4	4	0
Total	1	1	0	5	5	0	6	6	0
Median follow-up period (years) (range)	19.3 (−)			12.8 (6.9–17.7)			15.1(6.9–19.3)		
Median duration (years) to CR (range)	2.4 (−)			1.4 (0.0–7.4)			1.2 (0.0–7.4)		
Median duration (years) to ESKD (range)	–			–			–		

Data are presented as numbers unless stated otherwise

MPT, methylprednisolone pulse therapy; MZB, mizoribine; PSL, prednisolone; CR, complete remission; ESKD, end-stage kidney disease; LDL apheresis, low-density lipoprotein apheresis

[a] The maximum number and median number of courses of methylprednisolone pulse therapy were 16 and 3.5, respectively

[b] Of those, one patient did not achieve CR and remained as partial remission until the last examination

subgroup] was 38.5 % (P=0.001) (Fig. 2). After exclusion of patients with DMP from the analysis, the complete remission rate of the initial SRNS of the MC (cyclosporine) subgroup was 75.0 % and that of the MC (cyclophosphamide) subgroup was 45.4 % (not shown).

The actual renal survival rate at 10 years in the FSGS (cyclosporine) subgroup was 100 %, as calculated by Kaplan–Meier analysis (P=0.013). However, actual renal survival rate in the FSGS (cyclophosphamide) subgroup, MC/DMP (cyclosporine) subgroup, and MC/DMP (cyclophosphamide) subgroup was 54.6, 96.6, and 90.9 %,

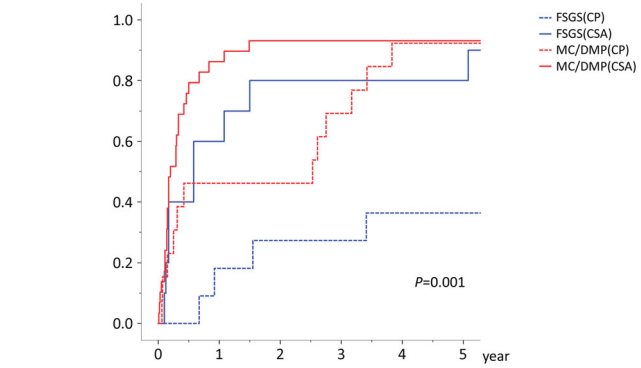

Number of patients remaining:						
FSGS(CP)	11	9	8	8	7	7
FSGS(CSA)	10	4	2	2	2	2
MC/DMP(CP)	13	7	7	4	1	1
MC/DMP(CSA)	29	4	2	2	2	2

Fig. 2 The complete remission rate of the initial SRNS episode, analyzed by Kaplan-Meier analysis according to subgroup {initial histopathological patterns [minimal change (*MC*)/diffuse mesangial proliferation (*DMP*) vs. focal segmental glomerulosclerosis (*FSGS*)] and initial immunosuppressive agents used to treat for SRNS [cyclosporine (*CSA*) vs. cyclophosphamide (*CP*)]}. Number of children at risk at each time point is shown *below the x-axis*

respectively (Fig. 3). The risk of ESKD was assessed by multivariate analysis, revealing that the initial immunosuppressant of cyclophosphamide [hazard rate (HR) 20.2; 95 % confidence interval (CI) 1.6–260.6; $P=0.021$], initial histopathogical pattern of FSGS (HR 10.7; 95 % CI 1.3–89.7; $P=0.029$), and age of >11 years when diagnosed with SRNS (HR 36.3; 95 % CI 2.2–604.6; $P=0.012$) were significant risk factors for progression to ESKD (Table 3). After exclusion of patients with DMP from the analysis, the renal survival rate at 10 years was 100 % in both the MC

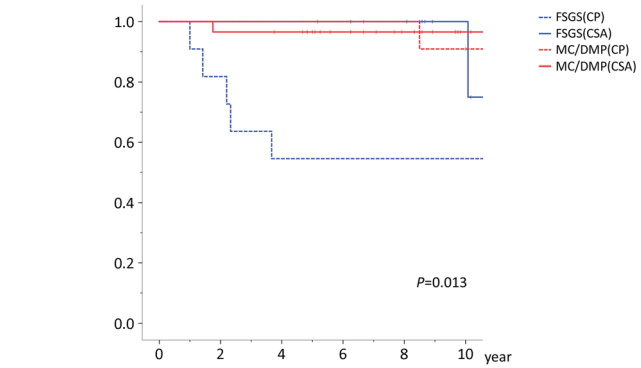

Number of patients remaining:						
FSGS(CP)	11	9	6	6	6	6
FSGS(CSA)	10	10	10	10	9	4
MC/DMP(CP)	13	13	13	12	11	9
MC/DMP(CSA)	29	28	27	20	14	4

Fig. 3 Renal survival rate in subgroups based on the initial histopathological patterns [minimal change (MC)/diffuse mesangial proliferation (DMP) vs. focal segmental glomerulosclerosis (FSGS)] and initial immunosuppressive agents [cyclosporine (CSA) vs. cyclophosphamide (CP)] used to treat SRNS. Number of children at risk at each time point is shown *below the x-axis*

(cyclosporine) group and MC (cyclophosphamide) subgroup (not shown).

As calculated by Kaplan–Meier analysis, the permanent remission rate at 10 years in the FSGS (cyclosporine) group, FSGS (cyclophosphamide) group, MC/DMP (cyclosporine) group, and MC/DMP (cyclophosphamide) group was 10.0, 27.3, 24.1, and 23.1 %, respectively (Fig. 4). Significant differences between groups were not found ($P=0.747$).

At the last follow-up examination, the disease was in remission in 57 (83 %) patients, was not in remission in three (4 %) patients, and had progressed to ESKD in nine (13 %; see Electronic Supplementary Material for the detailed clinical course of these 9 patients) patients (Fig. 5). Of those patients who achieved remission at the last follow-up examination ($n=57$), 48 (84 %) were in complete remission but only 18 (31 %) were in permanent remission.

Nephrotic syndrome- or treatment-related complications at the last examination are listed in Table 4. No patient died during the follow-up period. The median eGFR, excluding children with ESKD at the last examination, was 121.4 ml/min/1.73 m^2 (81.0–180.8 ml/min/1.73 m^2), that of FSGS group was 121.0 ml/min/1.73 m^2 (82.5–180.8 ml/min/1.73 m^2), and that of the MC/DMP group was 123.0 ml/min/1.73 m^2 (81.0–170.4 ml/min/1.73 m^2).

In total, 55 patients underwent repeat renal biopsy, and six of these patients (10.9 %) exhibited significant cyclosporine-related nephrotoxicity in the last renal biopsy (FSGS group, 3/19; MC/DMP group, 3/36). Of these six patients, three showed tubulointerstitial fibrosis only, one showed arteriolar hyalinosis only, and two showed both arteriolar hyalinosis and tubulointerstitial fibrosis. The median duration from the date of starting of cyclosporine therapy to the date on which cyclosporine toxicity was found was 4.8 (range 2.0–5.8) years.

Discussion

In this retrospective cohort study, we found that children with SRNS treated with cyclosporine had better outcome than those treated with cyclophosphamide, particularly those with FSGS, in terms of both induction of complete remission and long-term renal survival. On the other hand, most of the patients had been suffering frequent relapse for a long-term period, up to 10 years.

Among our study subjects, our analysis showed that the renal survival rates of those who received cyclosporine as the initial immunosuppressant were better than those of patients who received cyclophosphamide, regardless of the initial histopathological patterns. Those who received cyclosporine as initial immunosuppressant showed both higher short-term remission rate and higher long-term renal survival rate, suggesting that early induction of complete remission by cyclosporine might lead to better renal survival. SRNS has been recognized

Table 3 Risk factor for end-stage kidney disease by multivariate analysis

Variable	Hazard ratio	95 % Confidence interval	*P* value
Female gender (vs. male)	1.7	0.2–12.6	0.624
Age at time of SRNS diagnosis (years) (vs. <3 years)			
≧3, <7	0.8	0.1–6.6	0.834
≥7, <11	0.6	0.0–7.4	0.672
≥11	36.3	2.2–604.6	0.012
FSGS as the first renal biopsy finding (vs. MC/DMP)	10.7	1.3–89.7	0.029
CP as the first immnosuppressive agent for SRNS (vs. CSA)	20.2	1.6–260.6	0.021

The data are presented as numbers unless stated otherwise

SRNS, Steroid-resistant nephritic syndrome; MC, minimal change; DMP, diffuse mesangial proliferation; FSGS, focal segmental glomerulosclerosis; CP, cyclophosphamide; CSA, cyclosporine

as a disease associated with a high risk to progress to ESKD over the long term, although several recent studies have reported good short-term remission rate in patients with SRNS and, consequently, the effect of cyclosporine to induce remission in SRNS patients is beginning to be established [7, 12–14]. However, there have been only a few reports of children with SRNS in which the observation time was >10 years [15, 16]. In our study, we assessed long-term renal survival rate in children with SRNS mainly with respect to the initial immunosuppressant and showed for the first time the higher effectiveness of cyclosporine.

Our results show that the immunosuppressant used to treat SRNS, the initial histopathological pattern, and the age of patient diagnosis of SRNS were significant predictive factors of renal survival. Children who received cyclosporine had a significantly higher renal survival, even after adjustment for the other factors. In previous studies, FSGS as the initial histopathological pattern was found to be a predictive factor of progression to ESKD, particularly in those who could not attain remission [16–20]. In this regard, our results are compatible with those reported previously. Moreover, our results demonstrate that those children with FSGS treated with oral cyclophosphamide had a much lower renal survival rate (Fig. 3). Treatment regimens for patients with SRNS that include oral cyclophosphamide have been tentatively advocated by the authors of a number of reports (including patients with FSGS) [16, 21]; however, the results of our study suggest that the treatment regimen of oral cyclophosphamide can not be recommended—at least not to patients with SRNS with the FSGS histopathological pattern. Our institution has not adopted regimens with intravenous cyclophosphamide for the treatment of children with SRNS, but the results of other studies evaluating the efficacy of such therapeutic regimens are conflicting [12, 22, 23]. The older children in our study

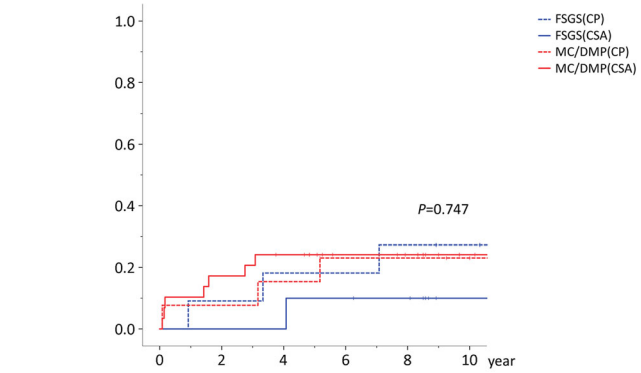

Fig. 4 The permanent remission rate in subgroups based on the initial histopathological patterns [minimal change (MC)/diffuse mesangial proliferation (DMP) vs. focal segmental glomerulosclerosis (FSGS)] and initial immunosuppressive agents [cyclosporine (CSA) vs. cyclophosphamide (CP)] used to treat SRNS. Number of children at risk at each time point is shown *below the x-axis*

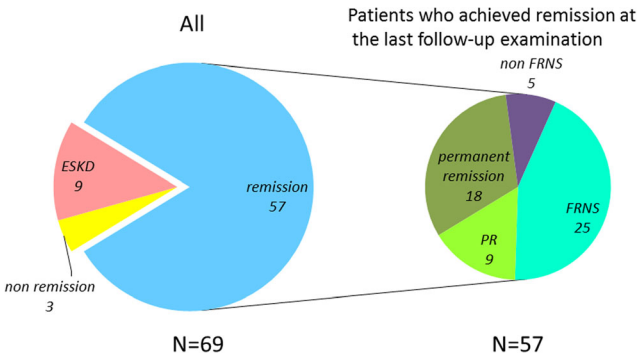

Fig. 5 Condition of patients at the last follow-up examination. Of 69 patients with SRNS, 57 patients had achieved remission by the last follow-up examination (*right pie chart*). *SRNS*, steroid-resistant nephritic syndrome; *ESKD*, end-stage kidney disease; *PR*, partial remission; *FRNS*, frequently relapsing nephrotic syndrome. The median duration of follow-up for patients with permanent remission was 10.3 (range, 5.2–15.9) years; with non-FRNS, 8.7 (5.5–12.5) years; with FRNS, 8.6 (4.9–15.8) years; with PR, 16.3 (4.5–19.3) years; with non-remission, 10.1 (6.3–16.4) years; with ESKD, 14.6 (9.2–19.0) years

Table 4 Nephrotic syndrome or treatment-related complications at the last examination

Variable	Total	Initial renal biopsy finding	
		FSGS	MC/DMP
Number of patients	69	22	47
Short stature	5 (7.2)	1 (4.5)	4 (8.5)
Excessive body weight[a]	9 (13.0)	3 (13.6)	6 (12.8)
Obesity[b]	4 (5.8)	1 (4.5)	3 (6.4)
Hypertension	22 (31.9)	11 (50.0)	11 (23.4)
Number of patients with ESKD	9	7	2
Hypertension among patients with ESKD	5 (55.6)	3 (42.8)	2 (100)
Number of patients undergoing repeat renal biopsy	55	19	36
CSA-related nephrotoxicity	6 (10.9)	3 (15.8)	3 (8.3)

The data are presented as numbers with the percentage in parenthesis

ESKD, end-stage kidney disease; FSGS, focal segmental glomerulosclerosis; MC, minimal change; DMP, diffuse mesangial proliferation; CSA, cyclosporine

[a] Defined as the body mass index (BMI): weight (kg)/square of height (m^2) of >25 in men and >24 in women

[b] Defined as a BMI of >30

cohort showed a significantly lower renal survival rate, which is a similar result to that reported previously [15]

On the other hand, the permanent remission rate among our study cohort was relatively low regardless of the initial immunosuppressant, and we found no evidence of any superiority of cyclosporine in achieving permanent remission. Moreover, many children in our study showed were in the state of FRNS at the last follow-up examination (Fig. 5). These results support those which we reported previously [24] and suggest that treatment strategies for children with SRNS to achieve long-term remission without immunosuppressant or steroid therapy still need to be improved.

Disease- and/or treatment-associated complications were relatively low among our study cohort and were comparable with those of the previous studies on long-term outcomes in patients with SSNS, except for hypertension [25, 26]. Excluding those who deteriorated to ESKD, only a few children showed mild kidney dysfunction. There were also only a few children who showed short stature or obesity, which might be attributable to the treatment, such as alternate-day administration of prednisolone. The rate of children who showed chronic cyclosporine nephrotoxicity in repeated biopsy was 10.9 %, which is lower than that reported in previous studies [27–31], possibly due to the advantage of trough control of cyclosporine. Close attention should be paid to cyclosporine nephrotoxicity. The rate of children who showed hypertension at last examination was relatively high, which might be attributed to the use of prednisolone or cyclosporine. However, the frequency of hypertension in our children with SRNS and in children with SRNS in previously reported studies was higher than that of children with FRNS [24, 32], which suggests that SRNS might itself be a significant risk factor for developing hypertension.

Our study has a number of strengths. First, a relatively large number of patients were included in the analysis, among whom 22 showed FSGS as the initial histopathological pattern. Second, we analyzed a rare refractory disease. Third, patient data for the analysis were collected over a relatively long term. These strengths should be balanced against this study's limitations. First, there was a diversity with the patient study groups, with the analysis including patients with MC and those with DMP in the same group. Second, the study cohort consisted of a homogeneous population. This study was confined to Japanese patients and did not include other races, such as Black Africans who typically show poorer long-term outcome. The homogeneity of our patient population might have contributed to the better outcome demonstrated in this study. Third, no genetic analyses were performed. Several recent papers have reported lack of efficacy of immunosuppression in SRNS secondary to genetic causes. We did not perform genetic analyses; however, none of our patients were indicated for this at the time of diagnosis. Fourth, the immunosuppression treatment course (including methylprednisolone pulse therapy) was quite complex, making the analysis of any given variable impossible. Patients who used cyclosporine only as the first immunosuppressive agent for SRNS and those who used cyclosporine plus methylprednisolone pulse therapy were not analyzed separately; as such, it is very difficult to compare the results of this study with those having other protocols. Finally, our assessment of the side effects in this study relied mainly on medical records, and thus some side effects might not have been identified and the assessment might be insufficient.

In conclusion, our results suggest that the recently reported therapeutic regimen with cyclosporine could

considerably improve both the initial remission rate and the long-term renal survival rate of children with idiopathic SRNS, regardless of initial histopathological pattern (i.e., FSGS or MC/DMP). However, further studies are required to resolve remaining problems, such as the management of SRNS in children who show frequent relapse after SRNS remission, and the establishment of a new therapeutic regimen for those who show resistance to the existing therapeutic regimens.

Acknowledgments The results presented in this paper have not been published previously in whole or part. The authors would like to thank Drs. Kentaro Ogata (Tokyo), Ryugo Hiramoto (Chiba), Takeshi Matsuyama (Tokyo), Hitoshi Wakaki (Tokyo), and Kaori Kikunaga (Tokyo) for their contributions to this study.

Financial declaration Kenji Ishikura has received lecture fees from Novartis Pharma and Asahi Kasei Pharma. Yuko Hamasaki has received research grants from Novartis Pharma and lecture fees from Novartis Pharma, Astellas Pharma, and Pfizer Japan. Hiroshi Hataya has received lecture fees from Asahi Kasei Pharma, Astellas Pharma, Baxter, JMS, and Meiji Seika Pharma Co. Ltd. Masataka Honda has received lecture fees from Novartis Pharma, Takeda Pharmaceutical Co. Ltd., Chugai Pharmaceutical Co. Ltd., Japan Blood Products Organization, JCR Pharmaceuticals Co. Ltd., and Asahi Kasei Pharma. Masaaki Mori has received lecture fees from Astellas Pharma, Pfizer Japan, Asahi Kasei Pharma, Meiji Seika Pharma Co. Ltd., and Chugai Pharmaceutical Co. Ltd.

Ethical approval The study was conducted in accordance with the ethical principles set out in the Declaration of Hesinki, and with the ethical guideline for epidemiological studies issued by the Minstry of Health, Labor and Welfare in Japan. The study was approved by the ethics committee of Tokyo Metropolitan Children's medical Center (H25-2).

Informed Consent Because data were reported retrospectively based on patient charts, informed consent was not obtained, in accordance with the above guidelines.

References

1. Mendoza SA, Reznik VM, Griswold WR, Krensky AM, Yorgin PD, Tune BM (1990) Treatment of steroid-resistant focal segmental glomerulosclerosis with pulse methylprednisolone and alkylating agents. Pediatr Nephrol 4:303–307
2. Cattran DC, Rao P (1998) Long-term outcome in children and adults with classic focal segmental glomerulosclerosis. Am J Kidney Dis 32:72–79
3. Tune BM, Kirpekar R, Sibley RK, Reznik VM, Griswold WR, Mendoza SA (1995) Intravenous methylprednisolone and oral alkylating agent therapy of prednisone-resistant pediatric focal segmental glomerulosclerosis: a long-term follow-up. Clin Nephrol 43: 84–88
4. Garin EH, Orak JK, Hiott KL, Sutherland SE (1988) Cyclosporine therapy for steroid-resistant nephrotic syndrome. A controlled study. Am J Dis Child 142:985–988
5. Ponticelli C, Rizzoni G, Edefonti A, Altieri P, Rivolta E, Rinaldi S, Ghio L, Lusvarghi E, Gusmano R, Locatelli F, Pasquali S, Castellani A, Casa-Alberighi OD (1993) A randomized trial of cyclosporine in steroid-resistant idiopathic nephrotic syndrome. Kidney Int 43:1377–1384
6. Lieberman KV, Tejani A (1996) A randomized double-blind placebo-controlled trial of cyclosporine in steroid-resistant idiopathic focal segmental glomerulosclerosis in children. J Am Soc Nephrol 7:56–63
7. Hamasaki Y, Yoshikawa N, Hattori S, Sasaki S, Iijima K, Nakanishi K, Matsuyama T, Ishikura K, Yata N, Kaneko T, Honda M (2009) Cyclosporine and steroid therapy in children with steroid-resistant nephrotic syndrome. Pediatr Nephrol 24:2177–2185
8. Ishikura K, Matsumoto S, Sako M, Tsuruga K, Nakanishi K, Kamei K, Saito H, Fujinaga S, Hamasaki Y, Chikamoto H, Ohtsuka Y, Komatsu Y, Ohta T, Nagai T, Kaito H, Kondo S, Ikezumi Y, Tanaka S, Kaku Y, Iijima K (2015) Clinical practice guideline for pediatric idiopathic nephrotic syndrome 2013: medical therapy. Clin Exp Nephrol 19:6–33
9. Schwartz GJ, Haycock GB, Edelmann CM Jr, Spitzer A (1976) A simple estimate of glomerular filtration rate in children derived from body length and plasma creatinine. Pediatrics 58:259–263
10. Matsuo S, Imai E, Horio M, Yasuda Y, Tomita K, Nitta K, Yamagata K, Tomino Y, Yokoyama H, Hishida A (2009) Revised equations for estimated GFR from serum creatinine in Japan. Am J Kidney Dis 53:982–992
11. Mori K, Honda M, Ikeda M (2004) Efficacy of methylprednisolone pulse therapy in steroid-resistant nephrotic syndrome. Pediatr Nephrol 19:1232–1236
12. Plank C, Kalb V, Hinkes B, Hildebrandt F, Gefeller O, Rascher W (2008) Cyclosporin A is superior to cyclophosphamide in children with steroid-resistant nephrotic syndrome-a randomized controlled multicentre trial by the Arbeitsgemeinschaft fur Padiatrische Nephrologie. Pediatr Nephrol 23:1483–1493
13. Ehrich JH, Geerlings C, Zivicnjak M, Franke D, Geerlings H, Gellermann J (2007) Steroid-resistant idiopathic childhood nephrosis: overdiagnosed and undertreated. Nephrol Dial Transplant 22: 2183–2193
14. Choudhry S, Bagga A, Hari P, Sharma S, Kalaivani M, Dinda A (2009) Efficacy and safety of tacrolimus versus cyclosporine in children with steroid-resistant nephrotic syndrome: a randomized controlled trial. Am J Kidney Dis 53:760–769
15. Mekahli D, Liutkus A, Ranchin B, Yu A, Bessenay L, Girardin E, Van Damme-Lombaerts R, Palcoux JB, Cachat F, Lavocat MP, Bourdat-Michel G, Nobili F, Cochat P (2009) Long-term outcome of idiopathic steroid-resistant nephrotic syndrome: a multicenter study. Pediatr Nephrol 24:1525–1532
16. Kirpekar R, Yorgin PD, Tune BM, Kim MK, Sibley RK (2002) Clinicopathologic correlates predict the outcome in children with steroid-resistant idiopathic nephrotic syndrome treated with pulse methylprednisolone therapy. Am J Kidney Dis 39:1143–1152
17. Abrantes MM, Cardoso LS, Lima EM, Penido Silva JM, Diniz JS, Bambirra EA, Oliveira EA (2006) Predictive factors of chronic kidney disease in primary focal segmental glomerulosclerosis. Pediatr Nephrol 21:1003–1012
18. Paik KH, Lee BH, Cho HY, Kang HG, Ha IS, Cheong HI, Jin DK, Moon KC, Choi Y (2007) Primary focal segmental glomerular sclerosis in children: clinical course and prognosis. Pediatr Nephrol 22:389–395
19. Gipson DS, Chin H, Presler TP, Jennette C, Ferris ME, Massengill S, Gibson K, Thomas DB (2006) Differential risk of remission and ESRD in childhood FSGS. Pediatr Nephrol 21:344–349
20. Martinelli R, Okumura AS, Pereira LJ, Rocha H (2001) Primary focal segmental glomerulosclerosis in children: prognostic factors. Pediatr Nephrol 16:658–661
21. Mantan M, Sriram CS, Hari P, Dinda A, Bagga A (2008) Efficacy of intravenous pulse cyclophosphamide treatment versus combination of intravenous dexamethasone and oral cyclophosphamide treatment in steroid-resistant nephrotic syndrome. Pediatr Nephrol 23:1495–1502

22. Hari P, Bagga A, Jindal N, Srivastava RN (2001) Treatment of focal glomerulosclerosis with pulse steroids and oral cyclophosphamide. Pediatr Nephrol 16:901–905
23. Bajpai A, Bagga A, Hari P, Dinda A, Srivastava RN (2003) Intravenous cyclophosphamide in steroid-resistant nephrotic syndrome. Pediatr Nephrol 18:351–356
24. Hamasaki Y, Yoshikawa N, Nakazato H, Sasaki S, Iijima K, Nakanishi K, Matsuyama T, Ishikura K, Ito S, Kaneko T, Honda M (2013) Prospective 5-year follow-up of cyclosporine treatment in children with steroid-resistant nephrosis. Pediatr Nephrol 28: 765–771
25. Fakhouri F, Bocquet N, Taupin P, Presne C, Gagnadoux MF, Landais P, Lesavre P, Chauveau D, Knebelmann B, Broyer M, Grunfeld JP, Niaudet P (2003) Steroid-sensitive nephrotic syndrome: from childhood to adulthood. Am J Kidney Dis 41:550–557
26. Ruth EM, Kemper MJ, Leumann EP, Laube GF, Neuhaus TJ (2005) Children with steroid-sensitive nephrotic syndrome come of age: long-term outcome. J Pediatr 147:202–207
27. Niaudet P, Fuchshuber A, Gagnadoux MF, Habib R, Broyer M (1997) Cyclosporine in the therapy of steroid-resistant idiopathic nephrotic syndrome. Kidney Int Suppl 58:S85–S90
28. Iijima K, Hamahira K, Tanaka R, Kobayashi A, Nozu K, Nakamura H, Yoshikawa N (2002) Risk factor for cyclosporine-induced tubulointerstitial lesions in children with minimal change nephrotic syndrome. Kidney Int 61: 1801–1805
29. Kengne-Wafo S, Massella L, Diomedi-Camassei F, Gianviti A, Vivarelli M, Greco M, Stringini GR, Emma F (2009) Risk factors for cyclosporin A nephrotoxicity in children with steroid-dependent nephrotic syndrome. Clin J Am Soc Nephrol 4:1409–1416
30. Sinha A, Sharma A, Mehta A, Gupta R, Gulati A, Hari P, Dinda AK, Bagga A (2013) Calcineurin inhibitor induced nephrotoxicity in steroid resistant nephrotic syndrome. Indian J Nephrol 23:41–46
31. Fujinaga S, Shimizu T (2013) Chronic cyclosporine-induced nephrotoxicity in children with steroid-resistant nephrotic syndrome. Pediatr Nephrol 28:2065–2066
32. Ishikura K, Yoshikawa N, Nakazato H, Sasaki S, Iijima K, Nakanishi K, Matsuyama T, Ito S, Yata N, Ando T, Honda M (2012) Two-year follow-up of a prospective clinical trial of cyclosporine for frequently relapsing nephrotic syndrome in children. Clin J Am Soc Nephrol 7:1576–1583

Clin Exp Nephrol
DOI 10.1007/s10157-015-1142-y

ORIGINAL ARTICLE

Efficacy and safety of eculizumab in childhood atypical hemolytic uremic syndrome in Japan

Naoko Ito[1] · Hiroshi Hataya[2] · Ken Saida[3] · Yoshiro Amano[4] · Yoshihiko Hidaka[5] · Yaeko Motoyoshi[6] · Toshiyuki Ohta[7] · Yasuhiro Yoshida[2] · Chikako Terano[2] · Tadashi Iwasa[8] · Wataru Kubota[2] · Hidetoshi Takada[1] · Toshiro Hara[1] · Yoshihiro Fujimura[9] · Shuichi Ito[3,10]

Received: 19 February 2015 / Accepted: 26 June 2015

Abstract

Background Atypical hemolytic uremic syndrome (aHUS) is a severe life-threatening disease with frequent progression to end-stage renal disease (ESRD). Eculizumab, a humanized anti-C5 monoclonal antibody targeting the activated complement pathway, has recently been introduced as a novel therapy against aHUS. We, therefore, investigated the efficacy and safety of eculizumab in Japanese pediatric patients.

Methods We retrospectively analyzed clinical course and laboratory data of the first ten children with aHUS treated with eculizumab nationwide.

Results Seven patients were resistant to plasma therapy and three were dependent on it. Causative gene mutations were found in five patients. Two patients had anti-complement factor H autoantibody. Three patients had a family history of thrombotic microangiopathy (TMA). After initiation of eculizumab, all patients immediately achieved hematological remission and could successfully discontinue plasma therapy. The median periods to normalization of platelet count, lactate dehydrogenase levels and disappearance of schistocytes were 5.5, 17 and 12 days, respectively. Nine patients recovered their renal function and the median period to terminate renal replacement therapy (RRT) was 3 days. However, two patients progressed to ESRD and required chronic RRT at the last observation. No patients had a relapse of TMA under regular eculizumab therapy. No serious adverse events occurred during the follow-up period.

Conclusions Eculizumab is efficacious and well-tolerated therapy for children with aHUS. Although pathogenic mutations could not be detected in five patients, all patients showed immediate normalization of hematological abnormalities, strongly suggesting complement-related aHUS. This prompt hematological amelioration can become an indicator for therapeutic efficacy of eculizumab. However, appropriate indications and optimal duration of the treatment remain unclear.

✉ Shuichi Ito
itoshu@yokohama-cu.ac.jp

[1] Department of Pediatrics, Graduate School of Medical Sciences, Kyushu University, 3-1-1 Maidashi, Higashi-ku, Fukuoka 812-8583, Japan

[2] Department of Pediatric Nephrology, Tokyo Metropolitan Children's Medical Center, 2-8-29 Musashidai, Fuchu, Tokyo 183-8561, Japan

[3] Division of Nephrology and Rheumatology, National Center for Child Health and Development, 2-10-1 Okura, Setagaya-ku, Tokyo 157-8535, Japan

[4] Department of Pediatrics, Nagano Red Cross Hospital, 5-22-1 Wakasato, Nagano 380-8582, Japan

[5] Department of Pediatrics, Shinshu University School of Medicine, 3-1-1 Asahi, Matsumoto, Nagano 390-8621, Japan

[6] Department of Pediatrics and Developmental Biology, Tokyo Medical and Dental University Graduate School of Medicine, 1-5-45 Yushima, Bunkyo-ku, Tokyo 113-8519, Japan

[7] Department of Pediatric Nephrology, Hiroshima Prefectural Hospital, 1-5-54 Ujina-Kanda, Minami-ku, Hiroshima 734-8530, Japan

[8] Department of Pediatrics, Mie University Graduate School of Medicine, 2-174 Edobashi, Tsu, Mie 514-8507, Japan

[9] Department of Blood Transfusion Medicine, Nara Medical University, 840 Shijo, Kashihara, Nara 634-8521, Japan

[10] Department of Pediatrics, Graduate School of Medicine, Yokohama City University, 3-9 Fukuura, Kanazawa-ku, Yokohama, Kanagawa 236-0004, Japan

Published online: 09 July 2015

Keywords Eculizumab · Atypical hemolytic uremic syndrome · Plasma therapy · Alternative complement pathway · Children

Introduction

Hemolytic uremic syndrome (HUS) is defined by microangiopathic hemolytic anemia, thrombocytopenia and acute kidney injury. In children, more than 90 % of cases with HUS are caused by Shiga toxin-producing *Escherichia coli* (STEC) infection. In contrast, atypical HUS (aHUS), accounting for less than 10 % of HUS, is rare and mainly caused by unregulated complement activation via the alternative pathway due to genetic abnormalities. aHUS is known as a severe life-threatening disease which often develops multiple organ damage, and has a very poor prognosis with high mortality rate, frequent progression to end-stage renal disease (ESRD) and high recurrence even after kidney transplantation [1, 2].

In approximately 50 % of patients with aHUS, genetic abnormalities in complement regulatory factors are identified, which include complement factor H (CFH), complement factor I (CFI), complement factor H-related proteins (CFHR), membrane cofactor protein (MCP), complement factor B (CFB), complement 3 (C3), and thrombomodulin (THBD) [1–6]. Unregulated complement activation is often triggered by infection, pregnancy, drugs and surgery in aHUS [1, 2]. For decades, plasma therapy (plasma infusion and exchange) has been the only, first-line and standard treatment against aHUS. In spite of plasma therapy, the disease frequently developed ESRD associated with a high fatality rate [7–9].

In recent years, eculizumab has been used as a successful treatment for both adult and pediatric aHUS patients [9–12]. Eculizumab is a recombinant, fully humanized hybrid IgG_2/IgG_4 monoclonal antibody directly blocking human complement component C5. This drug terminates the activated complement pathway by binding C5 and inhibiting the generation of pro-inflammatory C5a and the lytic C5b-9 membrane attack complex [9]. To date, some reports have demonstrated that eculizumab is effective in pediatric aHUS patients [9, 12–16]. However, the efficacy and safety of eculizumab for Japanese pediatric aHUS patients remain unclear.

In Japan, eculizumab received approval for the indication of aHUS in September 2013. Some Japanese pediatric aHUS patients had already been treated with eculizumab provided by Alexion Pharmaceuticals, Inc on compassionate grounds before the approval. In this nationwide study, we retrospectively investigated the indication, efficacy, adverse events and outcomes of this new therapy for the treated pediatric aHUS patients in Japan.

Materials and methods

Patients

Japanese pediatric aHUS patients less than 18 years of age treated with eculizumab (Alexion Pharmaceuticals, Chesire, CT, USA) between April 2011 and November 2013 were eligible for this study. We defined aHUS according to the diagnostic criteria proposed by the joint committee of the Japanese Society of Nephrology and the Japan Pediatric Society; microangiopathic hemolytic anemia (hemoglobin < 10 g/dL), thrombocytopenia (platelet count $<150{,}000/\mu L$) and acute kidney injury (increased serum creatinine to a level 1.5-fold higher than reference values) with the exclusion of STEC infection and thrombotic thrombocytopenic purpura (TTP) diagnosed with markedly reduced ADAMTS13 activity [17]. During the study period, eculizumab was administered to 13 pediatric aHUS patients in Japan. We excluded three patients from this study owing to bone marrow transplantation-associated aHUS, and analyzed ten patients at seven institutions based on medical records retrospectively. This study was conducted following the principles established in the Declaration of Helsinki and approved by the Institutional Review Board/Ethics Committee of Kyushu University (approval number 25-241).

Evaluation of eculizumab therapy

On the indications of eculizumab therapy, we defined as follows: "refractory to" as failing to achieve thrombotic microangiopathy (TMA) remission after two or more sessions of plasma therapy, and "dependent on" as having any episode of relapsing TMA after the pause or the cessation of plasma therapy. The clinical efficacy of eculizumab was evaluated by the achievement of hematological remission and of the withdrawal from plasma therapy and renal replacement therapy (RRT). Hematological remission of aHUS was defined as normalization of platelet count ($>150{,}000/\mu L$), normalization of lactate dehydrogenase (LDH) levels (under reference values at each institution) and disappearance of schistocytes. Estimated glomerular filtration rate (eGFR) was calculated using the polynomial formula in Japanese children for patients between the ages of 2 and 13 years [18], and the classical Schwartz formula for patients under the age of 2 years [19]. Adverse events associated with eculizumab, outcomes including relapse of TMA and renal injury at the last observation were also evaluated.

Statistical analysis

All data were analyzed with GraphPad Prism version 5.0 (GraphPad Software, Inc., San Diego, CA, USA). Paired analysis was performed using Wilcoxon test. *P* values <0.05 were considered to be statistically significant.

Results

Patient characteristics

Table 1 shows the characteristics of the ten patients (four males, six females) at aHUS onset. The median age at the onset was 0.95 (range 0.1–13.8) years. Three patients had a family history of HUS. No patients had a history of parental consanguinity. Four patients had episodes of probable triggers of aHUS including respiratory infection, gastroenteritis and vaccination. Serum C3 levels were low (<70 mg/dL) in three patients. The result of hemolytic assay for CFH activity evaluation by incubating patient plasma with sheep red blood cells [20] was enhanced in four patients and mildly enhanced in another three patients. In two patients, anti-CFH antibody was detected. In all patients, the genes responsible for aHUS, which include CFH, CFI, MCP, C3, CFB and THBD, were investigated [20]. Five patients carried potentially causative mutations: previously reported mutations in two (Patients 1, 8) and novel ones in three (Patients 5, 9, 10). Renal biopsy was performed in six patients and all biopsy specimens revealed evidence of TMA histologically.

Post-aHUS onset, prior to eculizumab administration

The baseline characteristics and parameters, and therapies of ten patients before the administration of eculizumab are shown in Table 2. During the course of disease before the administration of eculizumab, plasma therapy had been performed in all patients and eight patients had received RRT. The major indications for eculizumab were critically "refractory to ($n = 7$)" or "dependent on ($n = 3$)" plasma therapy for TMA remission. The median period from aHUS onset to administration of eculizumab was 22 days (range 3–1591 days). All patients received meningococcal vaccine before or after the administration of eculizumab according to the appended paper. When the patients were vaccinated after or less than two weeks before the initiation of eculizumab, they were given temporary antibiotic prophylaxis such as ampicillin [21].

Efficacy and outcomes of eculizumab therapy

The efficacy of eculizumab therapy in ten patients is summarized in Table 2. After the first infusion of eculizumab, the median periods to normalization of platelet count, LDH levels, and disappearance of schistocytes were 5.5 days (range 4–14), 17 days (range 1–93) and 12 days

Table 1 Patient characteristics at aHUS onset

Patient no.	Sex	Age at onset (years)	Probable trigger	Family history	Low C3 levels (<70 mg/dL)	Hemolytic assay[a]	Anti-CFH antibody	Mutation of candidate genes[b]	Renal biopsy
1	F	1.4	URI, flu vaccination	HUS	(−)	(+)	nd	CFH	TMA
2	F	7.6	(−)	CKD	(+)	(+)	(+)	(−)	TMA
3	M	0.4	(−)	Cerebral infarction	(+)	(−)	(−)	(−)	TMA
4	F	10.3	(−)	(−)	(−)	(+)	(+)	(−)	TMA
5	M	3.6	(−)	(−)	(−)	(±)	(−)	MCP	TMA
6	M	0.5	(−)	HUS	(−)	(±)	(−)	(−)	nd
7	F	0.3	Gastroenteritis	(−)	(+)	(−)	(−)	(−)	TMA
8	M	13.8	*Campylobacter jejuni* infection	HUS	(−)	(±)	(−)	C3, CFH	nd
9	F	0.1	*Bordetella pertussis* infection	(−)	(−)	(−)	(−)	THBD	nd
10	F	0.4	(−)	(−)	(−)	(+)	(−)	C3	nd

aHUS atypical hemolytic uremic syndrome, *M* male, *F* female, *URI* upper respiratory tract infection, *C3* complement 3, *CFH* complement factor H, *MCP* membrane cofactor protein, *THBD* thrombomodulin, *TMA* thrombotic microangiopathy, *nd* not done, *CKD* chronic kidney disease

[a] Hemolytic assay; (+) for enhanced hemolytic activity (±) for mildly enhanced hemolytic activity

[b] CFH, CFI, MCP, C3, CFB and THBD were investigated as the candidate genes for aHUS

Table 2 Summary of the eculizumab therapy in ten patients

Treatment before eculizumab therapy	
Plasma therapy; PI and/or PE	10/10 (100 %)
RRT; HD and/or PD	8/10 (80 %)
Antihypertensive agent	8/10 (80 %)
Anticoagulant therapy; rTM	2/10 (20 %)
At the administration of eculizumab	
Indication for eculizumab therapy	
Refractory to plasma therapy	7/10 (70 %)
Dependent on plasma therapy	3/10 (30 %)
Median period from onset to administration	22 days (range 3–1591)
Median age	2.2 years (range 0.2–13.8)
Laboratory data: median	
Hemoglobin	8.3 g/dL (range 4.0–11.6)
Platelet count	10.6 × 10^4/μL (range 1.4–68.6)
LDH	478 U/L (range 216–2695)
Serum creatinine ($n = 5$)[a]	1.10 mg/dL (range 0.28–6.06)
eGFR ($n = 5$)[a]	45.0 mL/min/1.73 m^2 (range 14.2–59.1)
UP/UCr ($n = 7$)	9.8 mg/mgCr (range 2.0–44.6)
Efficacy of eculizumab therapy	
Achievement of hematological remission	10/10 (100 %)
Median period to normalization or improvement	
Platelet count; >15 × 10^4/μL ($n = 6$)	5.5 days (range 4–14)
LDH ($n = 8$)	17 days (range 1–93)
Hemoglobin; ≥11 g/dL ($n = 6$)	49 days (range 6–112)
eGFR; ≥60 mL/min/1.73 m^2 ($n = 8$)	25.5 days (range 7–82)
Median period to disappearance of schistocytes ($n = 9$)	12 days (range 4–49)
Achievement of withdrawal	
Plasma therapy ($n = 9$)	9/9 (100 %)
RRT ($n = 6$)	5/6 (83 %)
Median period to withdrawal	
Plasma therapy ($n = 9$)	0 days (range 0–10)
RRT ($n = 5$)	3 days (range 2–487)
Adverse events	2/10 (20 %)[b]
At the last observation	
Median follow-up period after administration of eculizumab	202 days (range 28–958)
Laboratory data: median	
Hemoglobin	11.8 g/dL (range 9.0–15.6)
Platelet count	28.6 × 10^4/μL (range 17.7–60.4)
LDH	247 U/L (range 144–308)
Serum creatinine ($n = 8$)[a]	0.34 mg/dL (range 0.20–0.47)
eGFR ($n = 8$)[a]	78.6 mL/min/1.73 m^2 (range 63.8–149.6)
ESRD on PD	2/10 (20 %)
Hematuria and proteinuria	3/9 (33 %)[c]
Medication of antihypertensive agent	6/10 (60 %)
Relapse of TMA during eculizumab therapy	0/10 (0 %)
Eculizumab continuation	10/10 (100 %)

PI plasma infusion, *PE* plasma exchange, *RRT* renal replacement therapy, *HD* hemodialysis, *PD* peritoneal dialysis, *rTM* recombinant thrombomodulin, *LDH* lactate dehydrogenase, *eGFR* estimated glomerular filtration rate, *UP/UCr* urinary protein-creatinine ratio, *ESRD* end-stage renal disease, *TMA* thrombotic microangiopathy

[a] Data of patients on dialysis are excluded

[b] Fever, nausea, hair loss and headache ($n = 1$). Rash, wheezing and hypotension ($n = 1$)

[c] One patient was in anuria

(range 4–49), respectively. Plasma therapy was successfully discontinued in all patients, although one patient could not discontinue RRT (Patient 7). Regarding the patients who achieved the cessation of plasma therapy and RRT, the median periods to the withdrawal from plasma therapy and RRT were 0 days (range 0–10) and 3 days (range 2–487), respectively. Figure 1 shows the improvement in parameters of both TMA and renal function after the administration of eculizumab therapy. At the last observation, two patients (Patients 1, 7) had ESRD and were on chronic peritoneal dialysis and three patients (Patients 1, 2, 5) had hematuria and proteinuria. No patients relapsed with TMA after the administration of eculizumab and the regular infusion of eculizumab had been continued for all patients until the last observation.

Adverse events

Adverse events indicating causality in eculizumab infusions were observed in two patients: fever, nausea, hair loss and headache in Patient 2; rash, wheezing and hypotension in Patient 7. As these symptoms were transient and not serious, regular eculizumab therapy was continued. No patients suffered from severe infections including meningococcal infection during the follow-up period.

Discussion

The findings in this nationwide study indicate that eculizumab therapy was effective and well tolerated for Japanese pediatric aHUS patients who were refractory to or dependent on plasma therapy. Our results mostly correspond with the results of previous case reports and clinical trials of eculizumab for aHUS patients [9–16].

Before the era of eculizumab, plasma therapy was the first line and the only therapy for aHUS. Plasma therapy was assumed to be effective by providing normal

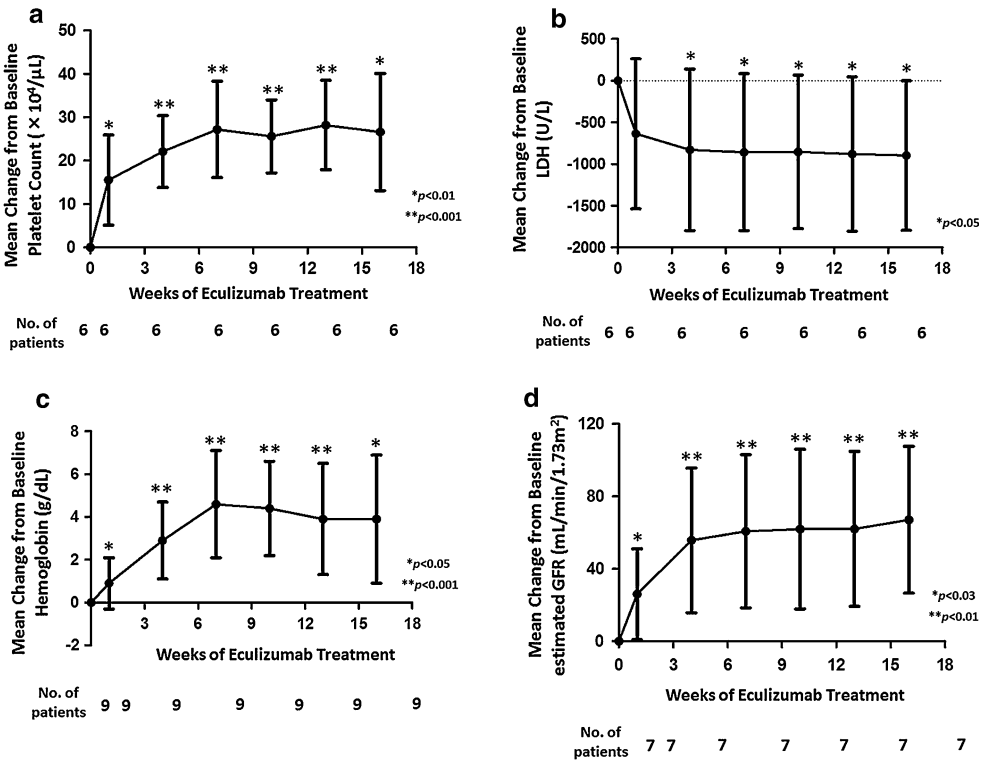

Fig. 1 The improvement of blood and renal parameters in aHUS after the administration of eculizumab therapy. **a** Platelet count ($n = 6$), **b** lactate dehydrogenase concentration ($n = 6$), **c** hemoglobin concentration ($n = 9$) and **d** estimated glomerular filtration rate ($n = 7$)

complement proteins and removing mutant abnormal proteins or auto-antibodies [7–9]. According to the guideline published by the European Paediatric Study Group for HUS in 2009, plasma therapy was recommended to be started as soon as possible (within 24 h) after the diagnosis of aHUS [22]. Nevertheless, it was reported that 29 % of children with aHUS still died or reached ESRD within one year [6]. It was also described that plasma therapy induced complete or partial remission of 63, 25, 57, 88 and 75 % in aHUS patients with CFH, CFI, C3, THBD mutations or anti-CFH autoantibodies, respectively [4]. The analysis of European pediatric aHUS patients mainly treated with plasma therapy in 2009 demonstrated that 11 % of the patients failed to achieve hematological remission and 17 % remained dialysis-dependent at day 33 [23]. These data indicate that the efficacy of plasma therapy in aHUS is limited. Moreover, the incidence of complications in plasma therapy related to vascular access in children is higher than in adults [9].

Eculizumab has become the alternative therapeutic option for aHUS since 2009. This new drug received approval for the indication of aHUS in the United States and Europe in 2012, and in Japan in 2013. The previous case series and the results of clinical trials demonstrated that eculizumab was significantly more effective than conventional plasma therapy for aHUS patients [9–16]. Zuber et al. [9] reviewed the case series of aHUS patients who were treated with eculizumab as a first-line therapy or a rescue therapy. In these cases, all the patients could achieve hematological remission, and 80 % of children and 31 % of adults showed a full recovery to baseline renal function. In a prospective phase 2 clinical trial of eculizumab for patient with aHUS over 12 years of age, who were resistant to or dependent on plasma therapy, eculizumab therapy resulted in improvement of both thrombocytopenia and renal impairment [10].

In our study, after the administration of eculizumab, hematological remission was quickly achieved and plasma therapy was also immediately discontinued in all patients. Notably, platelet count was normalized within several days after the first infusion of eculizumab in most patients. This is one of the most distinctive features of the efficacy of eculizumab [10, 11]. This quick response in the resolution of hematological abnormality strongly suggests that all patients were affected by complement-related aHUS, and it can be the appropriate indicator for therapeutic efficacy of eculizumab. It may also indicate that this therapy can rapidly stop further intravascular thrombus formation by direct blockade of downstream of abnormally activated complement cascade.

On renal outcome, renal impairment was also improved in most patients, although one patient (Patient 7) could not discontinue dialysis and two patients (Patient 1, 7) had developed ESRD at the last observation. Previous literature

suggested that earlier initiation of eculizumab therapy was associated with better improvement of renal function [9–11], although some cases experienced a significant improvement in renal function after RRT of several months [9, 24, 25]. In our study, two of the eight patients who required RRT during the course of the disease (Patients 1, 3) started eculizumab more than one month after the onset of aHUS. Patient 3 could successfully withdraw from RRT 69 days after the administration of eculizumab. Although there is not enough evidence to elucidate the mechanism of such late improvement in renal function as several months after chronic RRT, the extent of renal damage in capillary endothelial cells and interstitium before eculizumab therapy might influence the outcome of renal function. In addition, pediatric patients may have a greater potential to recover renal function than adult patients because each nephron is still in developing during the early stages of life.

There are also other advantages to this new therapy. As eculizumab blocks the downstream complement cascade at the late component C5, it preserves the early components of the cascade which play important roles in phagocytosis and opsonization of microorganisms [9]. In addition, eculizumab is a fully humanized recombinant monoclonal antibody with minimal immunogenicity. Therefore, serious infusion reactions and the development of neutralizing antibodies against the drug are rare [26]. Eculizumab has changed the strategy of management of aHUS dramatically, and it has become not only the substitute for plasma therapy but also the frontline therapy.

However, eculizumab therapy also has some serious adverse events and critical disadvantages. One of the serious adverse events is an increased susceptibility to meningococcal infection. As eculizumab causes late complement pathway deficiencies and inhibits the membrane attack complex formation, patients are at risk of severe encapsulated bacterial infections, especially by *Neisseria meningitidis* [2, 7, 9]. It is well known that individuals deficient in components of the terminal complement pathway are highly predisposed to invasive, often recurrent meningococcal infections [27]. In patients treated with eculizumab for paroxysmal nocturnal hemoglobinuria, the meningococcal infection rate was 0.42 per 100 patients per year [26]. Although annual incidence of this infection, such as bacterial meningitis or sepsis, is only approximately ten patients per year in Japan [28], vaccination against *Neisseria meningococcus* is mandatory for all the patients treated with eculizumab at least two weeks prior to the initiation of the therapy. In this study, all patients were provided with meningococcal vaccine, but they were unapproved and imported because there were no approved vaccines in Japan at that time [29].

If the meningococcal vaccine cannot be given, patients should receive antibiotic prophylaxis until at least two weeks after the vaccination [21]. However, limited-time antibiotic prophylaxis cannot be sufficient to prevent from this critical infection. Tetravalent vaccines against serotypes A, C, Y and W135 are commonly available, but they are not effective for serotype B which is major type found in Japan [30]. Moreover, serum antibody titer acquired by the vaccination can be decreased in several years. It means that we have to keep in mind the risk of meningococcal infection for all the patients treated with eculizumab even after the vaccination.

Furthermore, as the optimal duration of eculizumab treatment has not yet been established, life-long therapy is recommended to prevent relapses at this time in spite of very high-cost therapy [9]. Zuber et al. [9] reviewed five patients treated with a single infusion of eculizumab who experienced relapse mostly within one year and progressed to ESRD. Legendre et al. [10] described that five of the 18 patients who received inappropriate eculizumab doses had subsequent severe complications of TMA. However, it remains unclear whether all patients with aHUS require chronic life-long eculizumab therapy. Ardissino et al. [31] reported that seven of the ten patients could discontinue eculizumab under home monitoring of urine hemoglobin, although three patients with CFH-related aHUS relapsed after discontinuation. Therefore, the risk of relapse in aHUS patients after discontinuation of eculizumab therapy could depend on the genetic background. Better understanding of the genetic correlation and establishing useful biomarkers for monitoring aHUS disease activity are needed to address the optimal duration of this extremely expensive therapy.

Unfortunately, a portion of aHUS patients are resistant to eculizumab therapy. The lack of efficacy of eculizumab may come from a delay in starting eculizumab therapy [9–11], the pathogenesis of aHUS with non-complement-dependent mechanisms such as DGKE mutations [32], or host genetic C5 variants which inhibit the binding of eculizumab to the target epitope [33]. However, there are still some patients in whom the reason of the ineffectiveness is not clear. In this study, Patient 7 could achieve hematological remission but did not have any improvement of renal impairment even though she was administered eculizumab as early as 17 days after aHUS onset. In such cases, unknown factors or mechanisms other than complement activation may be involved in severe renal injury.

An increasing number of children with aHUS will receive this revolutionary treatment in the future. The French Study Group for aHUS/C3G suggested that eculizumab may be considered as a first-line therapy in children with a first episode of aHUS [9]. We should give careful consideration to the indication for eculizumab because some critical issues remain with this new therapy.

However, delayed initiation of eculizumab could also lead to not only irreversible renal impairment but also severe systemic multiple organ damage caused by TMA. As complement investigations take a long time and complement-related mutations have been found only in 50–70 % of patients with aHUS [1–7], identification of a genetic mutation is not necessary for clinical diagnosis and treatment initiation [9, 10]. Therefore, empirical eculizumab therapy for aHUS may be a choice in the early phase of disease after excluding STEC infection and TTP. If patients achieve hematological remission promptly, they could quite likely have aHUS related to abnormalities of complement regulatory factors.

There were some limitations to this study. Firstly, it was a retrospective study and the number of patients enrolled was small. Secondly, most patients were observed for very short periods after the administration of eculizumab. Therefore, we need to confirm the long-term efficacy and outcome of eculizumab therapy in pediatric aHUS. Finally, although immediate and definite efficacy of eculizumab was confirmed in all the patients, genetic mutations of complement-related proteins could not be detected in half of them. Even for the detected mutations, novel ones were not evaluated whether they were definitely causative or not. In fact, Patient 5 carried a novel MCP mutation, but also revealed mildly enhanced hemolytic assay suggesting aberrant CFH function. Patient 10 demonstrated enhanced hemolytic assay, but no CFH-related mutation was detected. In these patients, interacting with some other mutations or SNPs of the complement-related proteins may contribute to the onset of aHUS. We need further investigation to elucidate these discrepancies.

In conclusion, eculizumab is an efficacious and well-tolerated therapy in Japanese pediatric aHUS patients. The appropriate indication for use of this breakthrough therapy and the proper period of the treatment have yet to be determined.

Acknowledgments The authors would like to thank the following co-investigators for their contributions to this study: Kenji Ishikura (Tokyo Metropolitan Children's Medical Center), Koichi Kamei (National Center for Child Health and Development), Tomohiro Udagawa (Tokyo Medical and Dental University), Tomohito Takimoto, Masamitsu Shirozu and Manao Nishimura (Kyushu University). We also appreciate Yoko Yoshida (Nara Medical University) and Toshiyuki Miyata (National Cerebral and Cardiovascular Center) for performing hemolytic assays, anti-CFH antibody analysis and genetic mutation screening. Alexion Pharmaceuticals, Inc. provided eculizumab on compassionate grounds to seven patients in this study until eculizumab received approval for the indication of aHUS in Japan.

Conflict of interest Potential financial conflicts of interest. Patent royalties: Yoshihiro Fujimura (Alfresa Pharma), Honoraria: Shuichi Ito (Alexion Pharma), Research funding: Yoshihiro Fujimura (Alexion Pharma). The other authors have declared that no conflicts of interest exist.

References

1. Noris M, Remuzzi G. Atypical hemolytic-uremic syndrome. N Engl J Med. 2009;361:1676–87.
2. Loirat C, Fremeaux-Bacchi V. Atypical hemolytic uremic syndrome. Orphanet J Rare Dis. 2011;6:60.
3. Sellier-Leclerc AL, Fremeaux-Bacchi V, Dragon-Durey MA, Macher MA, Niaudet P, Guest G, et al. Differential impact of complement mutations on clinical characteristics in atypical hemolytic uremic syndrome. J Am Soc Nephrol. 2007;18:2392–400.
4. Noris M, Caprioli J, Bresin E, Mossali C, Pianetti G, Gamba S, et al. Relative role of genetic complement abnormalities in sporadic and familial aHUS and their impact on clinical phenotype. Clin J Am Soc Nephrol. 2010;5:1844–59.
5. Kavanagh D, Goodship T. Genetics and complement in atypical HUS. Pediatr Nephrol. 2010;25:2431–42.
6. Fremeaux-Bacchi V, Fakhouri F, Garnier A, Bienaime F, Dragon-Durey MA, Ngo S, et al. Genetics and outcome of atypical hemolytic uremic syndrome: a nationwide French series comparing children and adults. Clin J Am Soc Nephrol. 2013;8:554–62.
7. Waters AM, Licht C. aHUS caused by complement dysregulation: new therapies on the horizon. Pediatr Nephrol. 2011;26:41–57.
8. Verhave JC, Wetzels JF, van de Kar NC. Novel aspects of atypical haemolytic uraemic syndrome and the role of eculizumab. Nephrol Dial Transplant. 2014;29:iv131–41.
9. Zuber J, Fakhouri F, Roumenina LT, Loirat C, Fremeaux-Bacchi V. Use of eculizumab for atypical haemolytic uraemic syndrome and C3 glomerulopathies. Nat Rev Nephrol. 2012;8:643–57.
10. Legendre CM, Licht C, Muus P, Greenbaum LA, Babu S, Bedrosian C, et al. Terminal complement inhibitor eculizumab in atypical hemolytic-uremic syndrome. N Engl J Med. 2013;368:2169–81.
11. Fakhouri F, Delmas Y, Provot F, Barbet C, Karras A, Makdassi R, et al. Insights from the use in clinical practice of eculizumab in adult patients with atypical hemolytic uremic syndrome affecting the native kidneys: an analysis of 19 cases. Am J Kidney Dis. 2014;63:40–8.
12. Wong EK, Goodship TH, Kavanagh D. Complement therapy in atypical haemolytic uraemic syndrome (aHUS). Mol Immunol. 2013;56:199–212.
13. Gruppo RA, Rother RP. Eculizumab for congenital atypical hemolytic-uremic syndrome. N Engl J Med. 2009;360:544–6.
14. Ariceta G, Arrizabalaga B, Aguirre M, Morteruel E, Lopez-Trascasa M. Eculizumab in the treatment of atypical hemolytic uremic syndrome in infants. Am J Kidney Dis. 2012;59:707–10.
15. Besbas N, Gulhan B, Karpman D, Topaloglu R, Duzova A, Korkmaz E, et al. Neonatal onset atypical hemolytic uremic syndrome successfully treated with eculizumab. Pediatr Nephrol. 2013;28:155–8.
16. Christmann M, Hansen M, Bergmann C, Schwabe D, Brand J, Schneider W. Eculizumab as first-line therapy for atypical hemolytic uremic syndrome. Pediatrics. 2014;133:e1759–63.
17. Sawai T, Nangaku M, Ashida A, Fujimaru R, Hataya H, Hidaka Y, et al. Diagnostic criteria for atypical hemolytic uremic syndrome proposed by the Joint Committee of the Japanese Society of Nephrology and the Japan Pediatric Society. Clin Exp Nephrol. 2014;18:4–9.
18. Uemura O, Nagai T, Ishikura K, Ito S, Hataya H, Gotoh Y, et al. Creatinine-based equation to estimate the glomerular filtration rate in Japanese children and adolescents with chronic kidney disease. Clin Exp Nephrol. 2014;18:626–33.
19. Schwartz GJ, Brion LP, Spitzer A. The use of plasma creatinine concentration for estimating glomerular filtration rate in infants, children, and adolescents. Pediatr Clin North Am. 1987;34:571–90.

20. Fan X, Yoshida Y, Honda S, Matsumoto M, Sawada Y, Hattori M, et al. Analysis of genetic and predisposing factors in Japanese patients with atypical hemolytic uremic syndrome. Mol Immunol. 2013;54:238–46.
21. Administration USFaD. Prescribing information for Soliris. http://www.accessdata.fda.gov/drugsatfda_docs/label/2011/125166s172lbl.pdf.
22. Ariceta G, Besbas N, Johnson S, Karpman D, Landau D, Licht C, et al. Guideline for the investigation and initial therapy of diarrhea-negative hemolytic uremic syndrome. Pediatr Nephrol. 2009; 24:687–96.
23. Johnson S, Stojanovic J, Ariceta G, Bitzan M, Besbas N, Frieling M, et al. An audit analysis of a guideline for the investigation and initial therapy of diarrhea negative (atypical) hemolytic uremic syndrome. Pediatr Nephrol. 2014;29:1967–78.
24. Kim J, Waller S, Reid C. Eculizumab in atypical haemolytic-uraemic syndrome allows cessation of plasma exchange and dialysis. Clin Kidney J. 2012;5:34–6.
25. Povey H, Vundru R, Junglee N, Jibani M. Renal recovery with eculizumab in atypical hemolytic uremic syndrome following prolonged dialysis. Clin Nephrol. 2014;82:326–31.
26. Hillmen P, Muus P, Roth A, Elebute MO, Risitano AM, Schrezenmeier H, et al. Long-term safety and efficacy of sustained eculizumab treatment in patients with paroxysmal nocturnal haemoglobinuria. Br J Haematol. 2013;162:62–73.
27. Lewis LA, Ram S. Meningococcal disease and the complement system. Virulence. 2014;5:98–126.
28. Takahashi H, Kuroki T, Watanabe Y, Tanaka H, Inouye H, Yamai S, et al. Characterization of Neisseria meningitidis isolates collected from 1974 to 2003 in Japan by multilocus sequence typing. J Med Microbiol. 2004;53:657–62.
29. Tanimoto T, Kusumi E, Hosoda K, Kouno K, Hamaki T, Kami M. Concerns about unapproved meningococcal vaccination for eculizumab therapy in Japan. Orphanet J Rare Dis. 2014;9:48.
30. Bouts A, Monnens L, Davin JC, Struijk G, Spanjaard L. Insufficient protection by Neisseria meningitidis vaccination alone during eculizumab therapy. Pediatr Nephrol. 2011;26:1919–20.
31. Ardissino G, Testa S, Possenti I, Tel F, Paglialonga F, Salardi S, et al. Discontinuation of eculizumab maintenance treatment for atypical hemolytic uremic syndrome: a report of 10 cases. Am J Kidney Dis. 2014;64:633–7.
32. Lemaire M, Fremeaux-Bacchi V, Schaefer F, Choi M, Tang WH, Le Quintrec M, et al. Recessive mutations in DGKE cause atypical hemolytic-uremic syndrome. Nat Genet. 2013;45:531–6.
33. Nishimura J, Yamamoto M, Hayashi S, Ohyashiki K, Ando K, Brodsky AL, et al. Genetic variants in C5 and poor response to eculizumab. N Engl J Med. 2014;370:632–9.

European Journal of Human Genetics (2015), 1–5

www.nature.com/ejhg

ARTICLE

Somatic mosaicism and variant frequency detected by next-generation sequencing in X-linked Alport syndrome

Xue Jun Fu[1], Kandai Nozu*[,1], Hiroshi Kaito[1], Takeshi Ninchoji[1], Naoya Morisada[1], Koichi Nakanishi[2], Norishige Yoshikawa[2], Hiromi Ohtsubo[1], Natsuki Matsunoshita[1], Naohiro Kamiyoshi[1], Chieko Matsumura[3], Nobuaki Takagi[4], Kohei Maekawa[4], Mariko Taniguchi-Ikeda[1] and Kazumoto Iijima[1]

X-linked Alport syndrome (XLAS) is a progressive, hereditary nephropathy. Although men with XLAS usually develop end-stage renal disease before 30 years of age, some men show a milder phenotype and develop end-stage renal disease later in life. However, the molecular mechanisms associated with this milder phenotype have not been fully identified. We genetically diagnosed 186 patients with suspected XLAS between January 2006 and August 2014. Genetic examination involved: (1) extraction and analysis of genomic DNA using PCR and direct sequencing using Sanger's method and (2) next-generation sequencing to detect variant allele frequencies. We identified somatic mosaic variants in the type VI collagen, α5 gene (*COL4A5*) in four patients. Interestingly, two of these four patients with variant frequencies in kidney biopsies or urinary sediment cells of ≥ 50% showed hematuria and moderate proteinuria, whereas the other two with variant frequencies of < 50% were asymptomatic or only had hematuria. *De novo* variants can occur even in asymptomatic male cases of XLAS resulting in mosaicism, with important implications for genetic counseling. This is the first study to show a tendency between the variant allele frequency and disease severity in male XLAS patients with somatic mosaic variants in *COL4A5*. Although this is a very rare status of somatic mosaicism, further analysis is needed to show this correlation in a larger population.
European Journal of Human Genetics advance online publication, 27 May 2015; doi:10.1038/ejhg.2015.113

INTRODUCTION

Alport syndrome (AS) is a hereditary disorder of type IV collagen, characterized by chronic kidney disease progressing to end-stage renal disease (ESRD), sensorineural hearing loss, and ocular abnormalities. Approximately 85% of AS patients show X-linked inheritance (XLAS: OMIM301050) and variants in *COL4A5*, which encodes the type IV collagen α5 (α5(IV)) chain. *COL4A5* variants result in abnormal α5 (IV) expression, typically with complete absence of α5(IV) in the glomerular basement membrane (GBM) and Bowman's capsule in men, and a mosaic expression pattern in women.[1]

Male patients with XLAS can be classified as having either 'adult type', associated with mild deafness and the development of ESRD > 30 years of age, or 'juvenile type', associated with hearing loss and often with lenticonus, and an onset of ESRD < 30 years of age.[2] These two phenotypes are partially related to the genotype; for example, missense variants or in-frame variants of *COL4A5* were reported in cases of later-onset ESRD.[3–5] We recently reported that 29% of male XLAS patients expressed the α5(IV) chain in the glomerulus and showed milder clinical manifestations.[6] Interestingly, all α5(IV)-positive patients possessed non-truncating variants ($n = 13$) or somatic mosaic variants ($n = 2$) of *COL4A5*. One of these patients has been described in a previous case report.[7] This implies that men with XLAS and somatic mosaic variants show milder phenotypes; however, no case series has reported the correlation between variant frequency and disease severity in patients with somatic mosaic variants. The present study, therefore, examined the correlation between variant frequency and phenotype in a case series of male XLAS patients with somatic mosaic variants using next-generation sequencing (NGS). We provide herein the first report of an asymptomatic male XLAS case and also describe the first cases of somatic and gonadal mosaic variants in *COL4A5*.

MATERIALS AND METHODS

Ethical considerations

All procedures were reviewed and approved by the Institutional Review Board of Kobe University School of Medicine. Informed consent was obtained from all patients or their parents.

Data collection

Clinical and laboratory findings of patients with XLAS were obtained from their medical records. Patients were referred to our hospital for clinical evaluation or genetic analysis. Most patients were followed in various local hospitals in Japan. DNA and data sheets were sent to our laboratory after acceptance of the request for mutational analysis.

Estimated glomerular filtration rates (eGFRs) were measured from the data in these data sheets. eGFRs were calculated using the Schwartz formula for patients aged ≤ 19 years, and the Cockcroft–Gault formula for patients aged ≥ 20 years.[8–10]

[1]Department of Pediatrics, Kobe University Graduate School of Medicine, Kobe, Japan; [2]Department of Pediatrics, Wakayama Medical University, Wakayama, Japan; [3]Department of Pediatrics, National Hospital Organization Chiba-East Hospital, Chiba, Japan; [4]Department of Pediatrics, Hyogo College of Medicine, Hyogo, Japan
*Correspondence: Dr K Nozu, Department of Pediatrics, Kobe University Graduate School of Medicine, 7-5-1 Kusunoki-cho, Chuo, Kobe 6500017, Japan. Tel: +81 78 382 6090; Fax: +81 78 382 6099; E-mail: nozu@med.kobe-u.ac.jp
Received 8 January 2015; revised 24 April 2015; accepted 29 April 2015

Mutational analyses using Sanger sequencing

Mutational analyses of *COL4A5* were carried out using the following methods: (1) PCR and direct sequencing of genomic DNA of all exons and exon–intron boundaries and (2) reverse-transcription PCR of mRNA and direct sequencing of abnormal mRNA products when a suspected splicing-site variant was detected.

Genomic DNA was isolated from peripheral blood leukocytes, urinary sediments, kidney biopsies, skin and/or hair roots from patients, and their parents using the Quick Gene Mini 80 System (Fujifilm Corporation, Tokyo, Japan) according to the manufacturer's instructions. For genomic DNA analysis, all 51 *COL4A5* exons were amplified by PCR, as described previously.[11] PCR-amplified products were then purified and subjected to direct sequencing using a Dye Terminator Cycle Sequencing Kit (Amersham Biosciences, Piscataway, NJ, USA) with an automatic DNA sequencer (ABI Prism 3130; Perkin Elmer Applied Biosystems, Foster City, CA, USA).

Mutational analysis data were submitted to the Alport syndrome and *COL4A5* database (http://www.arup.utah.edu/database/ALPORT/ALPORT_welcome.php). For variant description, reference sequences were NC_000023.9 and NM_000495.3. Exons were numbered according to a previous report.[12]

Mutational analysis using NGS

A subset of exome-targeting genes with disease-causing variants were subjected to NGS using a commercially available kit (TruSight One, Illumina, San Diego, CA, USA) and targeted resequencing as a means of deep sequencing. Following the TruSight workflow, input genomic DNA was converted into adapter-tagged libraries by rapid Nextera (Nextera DNA Library Preparation Kit, Illumina)-based sample preparation. The libraries were then denatured into single-stranded DNA, and biotin-labeled probes specific to the targeted region were used for Rapid Capture hybridization. The pool was enriched for the desired regions by adding streptavidin beads that bound to the biotinylated probes. Biotinylated DNA fragments bound to the streptavidin beads were pulled down magnetically from the solution. The enriched DNA fragments were then eluted from the beads and hybridized for a second Rapid Capture. Sequence data generated from TruSight exome-enriched libraries were analyzed using the on-instrument MiSeq Reporter software (Illumina).

For deep sequencing of somatic mosaic variant analysis, 500-bp PCR products harboring each suspected mutation site were purified by gel extraction using the QIAquick gel extraction kit (Qiagen, Valencia, CA, USA). Each variant was then analyzed using the TruSeq PCR-free LT kit (Illumina). All procedures were conducted according to the manufacturers' instructions. The primer sequences were as follows:

COL4A5-exon25-F: 5′-CCCCAGTTGTATTCAGTA-3′ and COL4A5-exon 25-R: 5′-GAGCAAAATTAACAGTAA-3′; COL4A5-exon28-F: 5′-AAAAGCATA TGTTCCACA-3′ and COL4A5-exon28-R: 5′-GATGATTTGGGGTTAAAT-3′; COL4A5-exon44-F: 5′-ATTTATTCAGGGTAATCC-3′ and COL4A5-exon44-R: 5′-TAAAAGGTCTGCTATCAA-3′; and COL4A5-exon49-F: 5′-GGAGACA ATACTTAGCAAATG-3′ and COL4A5-exon49-R: 5′-ACACCAAGGGTAG TCAAA-3′.

To determine the limit of variant frequency detection, we made test samples containing mixtures of DNA from an XLAS patient with a hemizygous *COL4A5* c.1948+1G>A mutation and control DNA at variant frequencies of 0.5, 1, 2, 10, and 20%. Targeted resequencing was then conducted using the primer pair for *COL4A5* exon25.

RESULTS

Clinical, pathological, and mutational results are shown in Figures 1 and 2, Tables 1 and 2, and Supplementary Table 1. NGS analysis findings including the depth and forward/reverse reads are shown in Supplementary Table 1.

Patient ID14

The pedigree of patient ID14 is shown in Figure 1a. The precise clinical course of this patient has been reported previously.[7] At 16 years of age, the patient had microhematuria and moderate proteinuria with 0.74 g/g creatinine (Cr). Genetic analysis revealed the presence of an intron 43 splicing acceptor site variant (c.3998-2A>T, IVS44-2A>T). Transcriptional analysis showed that this variant caused skipping of exon44 (72 bp).

Patient ID28

A 38-year-old male was detected with microhematuria and proteinuria when he had a common cold; however, he had no urine abnormalities other than on that occasion. His pedigree is shown in Figure 1b. His older daughter also showed macrohematuria when she had a common cold at the age of 3 years, and subsequently demonstrated persistent microhematuria and mild proteinuria (0.2 g/g Cr). She underwent a kidney biopsy and was pathologically diagnosed with XLAS with a basket-weave change (BWC) on the GBM and mosaic α5(IV) expression. Genetic analysis revealed a *COL4A5* heterozygous variant at the intron 27 splicing acceptor site (c.2147-2A>G, IVS28-2A>G), which has been reported previously without precise clinical information.[13] Transcriptional analysis revealed this variant to cause skipping of part of exon28 (18 bp). Her mother was asymptomatic with no variants and her father was also asymptomatic, suggesting that she represents a sporadic case with a *de novo COL4A5* variant. However, the second daughter was also detected with hematuria at a screening test at 3 years of age, and was genetically diagnosed with XLAS with the same variant (IVS28-2A>G). Subsequent genetic testing of the father revealed the same variant with somatic mosaicism in genomic DNA extracted from leukocytes and urine sediments (Figure 2). He was confirmed to have a normal karyotype (46,XY). Because both daughters carry the same heterozygous variant, this indicates that their father also has the same variant in a mosaic state that includes germinal cells. The father was subsequently diagnosed with asymptomatic XLAS with a somatic and gonadal mosaic variant in *COL4A5*.

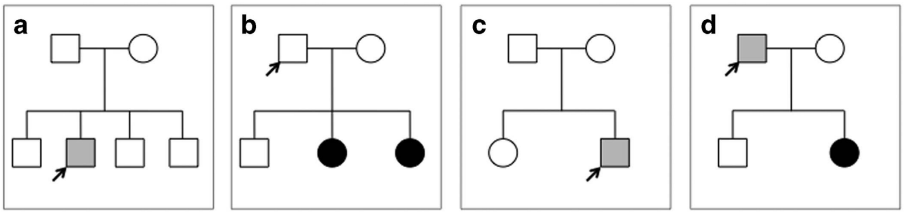

Figure 1 Patient pedigrees. (**a**) Patient ID14 possessing *COL4A5* mutation c.3998-2A>T in intron 43. This individual showed hematuria and moderate proteinuria. The parents are asymptomatic. (**b**) Patient ID28 possessing *COL4A5* mutation c.2147-2A>G in intron 27. This individual is asymptomatic although possesses a somatic and gonadal mosaic variant. One daughter has hematuria and mild proteinuria, whereas the second daughter has hematuria. (**c**) Patient ID52 possessing *COL4A5* mutation c.1912G>A in exon25. This individual has hematuria and moderate proteinuria. The parents are asymptomatic. (**d**) Patient ID 252 possessing *COL4A5* mutation c.4787G>T. This individual has hematuria without proteinuria, and the daughter has hematuria and mild proteinuria.

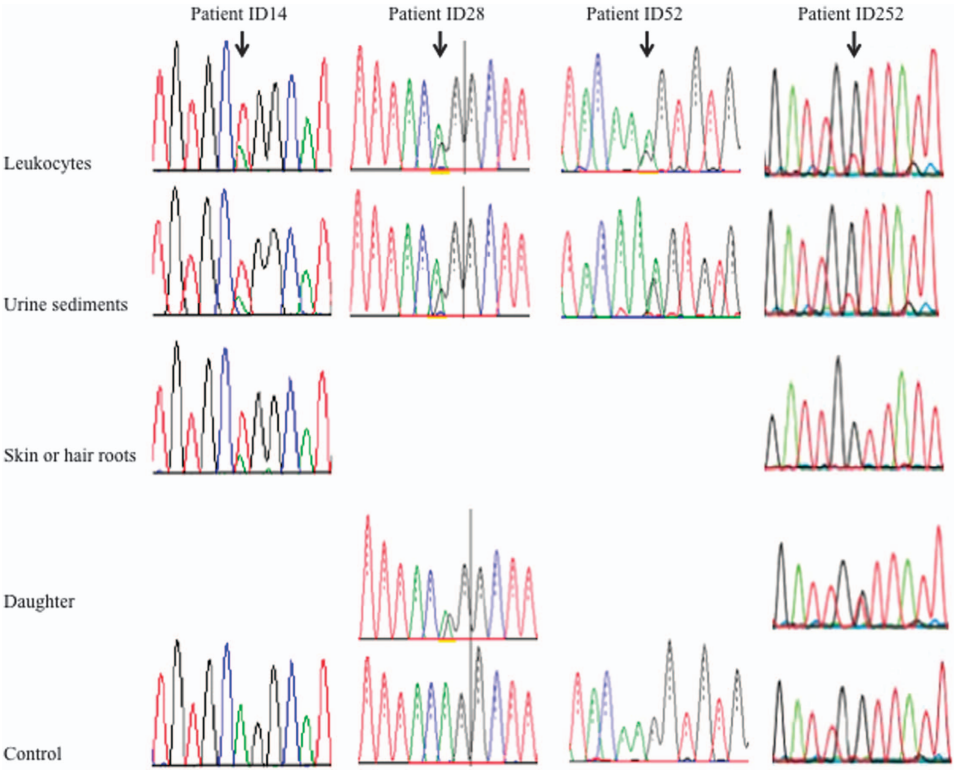

Figure 2 Direct sequencing of patients with somatic mosaic variants. Patient ID14: c.3998-2A>T, IVS44-2A>T. NGS analysis revealed variant allele frequencies of 57.1% in leukocytes, 61.3% in urinary sediment, cells and 75.3% in skin. Patient ID28: c.2147-2A>G, IVS28-2A>G. NGS analysis revealed variant allele frequencies of 31.3% in leukocytes and 33.3% in urinary sediment cells. His daughter shows heterozygous variant. Patient ID52: c.1912G>A, p.(Gly638Ser). NGS analysis revealed variant allele frequencies of 60.9% in leukocytes and 68% in urinary sediment cells. Patient ID252: c.4787G>T, p.(Gly1596Val). NGS analysis revealed variant allele frequencies of 20.6% in leukocytes, 24.1% in urinary sediment cells, and 0% in hair roots. His daughter shows heterozygous variant.

Table 1 Clinical characteristics and laboratory data

Patient ID	*Sex*	*Age (years)*	*ESRD (age)*	*Hearing loss (detected age)*	*sCr (mol/l)*	*eGFR (ml/min/1.73 m2)*	*Hematuria*	*U-P/Cr (g/g Cr)*	*EM*	*alpha-5*	*Family history*
14	M	15–20	—	—	68.9	144.7	3+	0.74	BWC	Mosaic	Sporadic
28	M	35–40	—	—	68.9	87.1	—	—	—	—	Two daughters pro/OB
52	M	15–20	—	—	80.4	125	3+	0.83	BWC	Mosaic	Sporadic
252	M	40–45	—	—	86.6	104.1	3+	—	—	—	Daughter pro/OB

Abbreviations: BWC, basket-weave change; EASRD, end-stage renal disease; eGFR, estimated glomerular filtration rate; EM, electron microscopic findings; M, male; ND, not determined; OB, occult; pro, proteinuria; blood sCr, serum creatinine levels; U-P/Cr, urinary protein–creatinine ratio.

Patient ID52

The pedigree of patient ID52 is shown in Figure 1c. He was an 18-year-old man who was first detected with hematuria and proteinuria by screening at the age of 3 years. Examination of a kidney biopsy taken at 10 years of age revealed AS with a BWC on the GBM. However, α5(IV) expression showed a mosaic pattern. His karyotype was 46,XY. Genetic analysis revealed an exon25 missense variant (c.1912G>A, p.(Gly638Ser)), which was reported previously without precise clinical information.[14] At the age of 18 years, he had microhematuria and moderate proteinuria of 0.83 g/g Cr.

Patient ID252

Patient ID252 was a 42-year-old man in whom hematuria was first detected at 6 years of age. His pedigree is shown in Figure 1d. His daughter showed macrohematuria and mild proteinuria (0.2 g/g Cr) when she was 6 years old. She underwent kidney biopsy and was pathologically diagnosed with XLAS with a BWC on GBM and mosaic α5(IV) expression. Genetic analysis revealed a heterozygous missense variant at *COL4A5* exon 49 (c.4787G>T, p.(Gly1596Val)). This amino-acid variant with a different amino-acid substitution was reported in a male patient who had not developed ESRD at the age of 19.[15] Her mother was asymptomatic with no variants, but her father showed persistent microhematuria without proteinuria and had the same variant with somatic mosaicism in genomic DNA extracted from both leukocytes and urine sediments. We confirmed his karyotype to be normal (46,XY). His daughter had the same heterozygous variant, indicating that their father also had a germline variant. The father was diagnosed with XLAS with a somatic and gonadal mosaic variant in *COL4A5*.

Table 2 *COL4A5* variants and variant allele frequencies

Patient ID	Variant position	Variants	Amino acid change	Methods	Variant frequency (%) Leukocytes	Urine sediments	Kidney	Hair roots	Skin
14	intron43	c.3998-2A>T	p.(Gly1333_Pro1356del)	Trusight One	57.1	61.3	—	—	75.3
		c.3998-2A>T		Targeted resequencing	60.8	63.0	62.9	—	64.8
28	intron27	c.2147-2A>G	p.(Gly716_Pro721del)	Trusight one	31.3	33.3	—	—	—
		r.2147_2164del		Targeted resequencing	43.7	45.5			
52	exon25	c.1912G>A	p.(Gly638Ser)	Trusight one	60.9	68.0	—	—	—
		r.(1912g>a)		Targeted resequencing	70.4	—	72.7	—	—
252	exon49	c.4787G>T	p.(Gly1596Val)	Trusight one	20.6	24.1	—	0	—
		r.(4787g>t)		Targeted resequencing	24.9	19.4	—	1.5	—

Table 3 Determining the limit of variant frequency detection

Variant frequency (%) Test sample	NGS result	Depth	Wild type Forward reads	Wild type Reverse reads	Mutant Forward reads	Mutant Reverse reads
0.5	1.1	459 772	140 068	310 841	1665	3441
1	1.9	504 779	149 572	340 835	2954	6680
2	2.6	463 811	124 329	323 702	3158	8805
10	10.7	399 956	98 220	255 492	11 222	31 623
20	19.4	440 254	350 826	118 714	26 670	58 759

Limit of variant frequency detection

Table 3 shows the results of our analysis to determine the limit of variant detection frequency. Targeted resequencing revealed that 1–2% was the lower limit of detection.

Comparison of variant frequencies between kidney biopsies and urinary sediments

We previously showed that urinary sediments can be used as an alternative cell source to kidney biopsies.[16,17] The present study compared the allele frequencies between DNA extracted from these two sources and obtained very similar findings (Table 2). Therefore, we compared the variant frequency of either kidney biopsies or urinary sediments with the phenotype in our analysis.

DISCUSSION

Male patients with XLAS sometimes show a milder, 'adult type' phenotype, with only mild deafness and an onset of renal failure >30 years old.[2] This milder phenotype is associated with unique genotypes such as missense or in-frame variants in *COL4A5*.[3–5] We previously reported a male XLAS patient with a missense *COL4A5* variant who showed only hematuria without proteinuria at the age of 33.[18] We also reported a male patient with a somatic *COL4A5* variant who showed hematuria and mild proteinuria at the age of 8 years. His kidney biopsy expressed α5(IV) mosaicism in the glomerulus, which was associated with the somatic mosaic variant.[7] To date, however, only six patients in four reports have been described with somatic mosaic variants in *COL4A5*, including our previous report (Table 4).[7,19–21] Although all six cases showed a milder phenotype and some of the female cases were asymptomatic, no asymptomatic male cases have previously been reported.

A recent publication by Beicht *et al.*[19] described an asymptomatic female XLAS patient with a somatic mosaic variant who had variant allele frequencies of 14, 7, 4, and 7% in leukocytes, urine sediments, hair roots, and oral mucosa, respectively, as shown by NGS. However, it is difficult to evaluate variant allele frequencies and phenotypes in female XLAS patients because skewed X-inactivation might affect the phenotype. The present study examined the correlation between the percentage of variant alleles in genomic DNA extracted from kidney biopsies and/or urinary sediments and renal symptoms in men with XLAS and somatic mosaic variants for the first time, revealing a tendency for an association between lower variant allele frequency and milder phenotype. Interestingly, two patients with variant frequencies in kidney biopsies and/or urinary sediment cells of ≥50% showed hematuria and moderate proteinuria, whereas two patients with frequencies <50% were asymptomatic or only had hematuria.

We recently reported a male XLAS patient with a mild phenotype caused by a unique intronic splicing variant, causing a cryptic exon in the transcript; however, mRNA extracted from the kidney showed both normal and abnormal transcripts, the former rescuing him from having the severe phenotype.[22]

The milder phenotype in men with XLAS is currently defined by the following five patterns: (1) missense variants in *COL4A5*;[4–6] (2); in-frame variants in *COL4A5*;[4,6] (3) somatic mosaic variants in *COL4A5*;[7,19–21] (4) α5(IV)-positive expression in the glomerulus;[6] and (5) aberrant splicing variants in *COL4A5*, leading to both normal and abnormal mRNAs.[22] In this study, we reported four cases with milder phenotypes: two with splice site variants (ID14 and 28) and two with missense variants (ID52 and 252). These variant types could contribute to a modulation of the phenotype. However, among these four patients, the influence of somatic mosaicism appears to be stronger because, of the two patients with missense mutations, ID252 with a lower variant frequency showed a much milder phenotype.

We previously used the techniques of semi-quantitative PCR analysis, restriction enzyme digestion, and electrophoresis to report variant frequencies for patient ID14 of 37% in leukocytes, 71% in urine sediments, and 32% in the skin.[7] Although at the time of this study (2008), we thought that our methods were highly efficient, it now appears that they were not reliable because the two techniques used in the current study (TruSight One and targeted resequencing) achieved almost identical frequencies, which differed from our previous data.

Patients ID28 and 252 of the present study also showed mosaic variants in germline cells. In these cases, we were unable to conduct an analysis of sperm cells because we were not given consent to do so. However, determining the mutation allele frequency in these cells would provide additional information about the genetic risk facing

Table 4 Previously reported cases with *COL4A5* mosaic variants

		Mosaicism							Variants		
First author	*Sex*	*Age (years)*	*Somatic cells*	*Germline cells*	*ESRD (age)*	*Urinary exam*	*Hearing loss*	*Ocular lesion*	*Exon*	*Nucleotide*	*Amino acid*
Plant KE	Female	ND	+	+	–	OB	–	–	26	c.2006G>C	p.Gly669Ala
	Female	ND	+	+	–	–	–	–	IVS12-3	c.848-3C>A	exon 12 skip
	Male	ND	+	+	43	ND	ND	–	25	c.1912G>A	p.Gly638Ser
Bruttini M	Female	ND	–	+	–	–	–	–	IVS44+1	c.4069+1G>C	exon44 skip
Krol RP	Male	8	+	ND	–	OB, mild pro	–	–	IVS44-2	c.3998-2A>T	exon44 skip
Beicht S	Female	ND	+	+	–	OB	+	Myopia	IVS30-1	c.2396-1G>A	exon 30 skip

Abbreviations: ESRD, end-stage renal disease; ND, not determined; OB: occult blood; pro: proteinuria.

offspring inheriting the mutated allele, which would be invaluable for genetic counseling.

NGS is a highly relevant tool for use in the diagnosis of AS. Moreover, early diagnosis of this disease is becoming increasingly important because AS is now a treatable disease.[23,24] The targeted resequencing technique that we used in the present study is both efficient and cost effective, and we propose that it should be adopted worldwide for the use in disease diagnosis.

The present study reports a tendency between variant allele frequency and the severity of renal symptoms in four men with XLAS with somatic mosaic variants. Although asymptomatic female cases with mosaic variants have been reported previously, the current study provides the first report of an asymptomatic male XLAS patient with a mosaic variant in *COL4A5*. We also describe the first male XLAS cases with somatic and gonadal mosaic variants in *COL4A5*. These results indicate that *de novo* variants can occur even in asymptomatic men with XLAS, and that the variant frequency may influence the severity of XLAS in patients with somatic mosaic variants. These cases highlight the fact that genetic counseling for asymptomatic parents of a child with AS should consider the possibility that one of the parents may carry a variant and show somatic and gonadal mosaicism.

CONFLICT OF INTEREST

KI received grants from Novartis Pharma K.K., Japan Blood Product Organization, Kyowa Hakko Kirion Co., Ltd, JCR Pharmaceuticals Co., Ltd, AbbVie Inc., Genzyme Japan K.K., Teijin Pharma Ltd, Daiichi Sankyo Co., Ltd, and Miyarisan Pharmaceutical Co., Ltd, and lecture fees from Kyowa Hakko Kirin Co., Ltd, Astellas Pharma Inc., Pfizer Japan Inc., Asahi Kasei Pharma Corp., Kowa Pharmaceutical Co., Ltd, Merck Sharp & Dohme Corp., Alexion, Meiji Seika Pharma Co., Ltd, and Novartis Pharma K.K.. KI is also an advisor for Zenyaku Kogyo Co., Ltd.

ACKNOWLEDGEMENTS

This study was supported by a grant from the Ministry of Health, Labour, and Welfare of Japan for Research on Rare Intractable Diseases in Kidney and Urinary Tract (H24-nanchitou (nan)-ippan-041 to KI) in the 'Research on Measures for Intractable Diseases' Project; a Grant-in-Aid for Scientific Research (KAKENHI) from the Ministry of Education, Culture, Sports, Science, and Technology of Japan (Subject ID: 25893131 to KN); and a grant from the Mother and Child Health Foundation (Subject ID: 25-7 to KN).

1 Kashtan CE: Alport syndrome and thin glomerular basement membrane disease. *J Am Soc Nephrol* 1998; **9**: 1736–1750.
2 Hudson BG, Tryggvason K, Sundaramoorthy M, Neilson EG: Alport's syndrome, Goodpasture's syndrome, and type IV collagen. *N Engl J Med* 2003; **348**: 2543–2556.
3 Bekheirnia MR, Reed B, Gregory MC *et al*: Genotype-phenotype correlation in X-linked Alport syndrome. *J Am Soc Nephrol* 2010; **21**: 876–883.
4 Gross O, Netzer KO, Lambrecht R, Seibold S, Weber M: Meta-analysis of genotype-phenotype correlation in X-linked Alport syndrome: impact on clinical counselling. *Nephrol Dial Transplant* 2002; **17**: 1218–1227.
5 Jais JP, Knebelmann B, Giatras I *et al*: X-linked Alport syndrome: natural history in 195 families and genotype- phenotype correlations in males. *J Am Soc Nephrol* 2000; **11**: 649–657.
6 Hashimura Y, Nozu K, Kaito H *et al*: Milder clinical aspects of X-linked Alport syndrome in men positive for the collagen IV alpha5 chain. *Kidney Int* 2014; **85**: 1208–1213.
7 Krol RP, Nozu K, Nakanishi K *et al*: Somatic mosaicism for a mutation of the COL4A5 gene is a cause of mild phenotype male Alport syndrome. *Nephrol Dial Transplant* 2008; **23**: 2525–2530.
8 Cockcroft DW, Gault MH: Prediction of creatinine clearance from serum creatinine. *Nephron* 1976; **16**: 31–41.
9 Schwartz GJ, Gauthier B: A simple estimate of glomerular filtration rate in adolescent boys. *J Pediatr* 1985; **106**: 522–526.
10 Schwartz GJ, Haycock GB, Edelmann CM Jr, Spitzer A: A simple estimate of glomerular filtration rate in children derived from body length and plasma creatinine. *Pediatrics* 1976; **58**: 259–263.
11 Martin P, Heiskari N, Zhou J *et al*: High mutation detection rate in the COL4A5 collagen gene in suspected Alport syndrome using PCR and direct DNA sequencing. *J Am Soc Nephrol* 1998; **9**: 2291–2301.
12 International Human Genome Sequencing Consortium: Finishing the euchromatic sequence of the human genome. *Nature* 2004; **431**: 931–945.
13 Nagel M, Nagorka S, Gross O: Novel COL4A5, COL4A4, and COL4A3 mutations in Alport syndrome. *Hum Mutat* 2005; **26**: 60.
14 Plant KE, Green PM, Vetrie D, Flinter FA: Detection of mutations in COL4A5 in patients with Alport syndrome. *Hum Mutat* 1999; **13**: 124–132.
15 Renieri A, Bruttini M, Galli L *et al*: X-linked Alport syndrome: an SSCP-based mutation survey over all 51 exons of the COL4A5 gene. *Am J Hum Genet* 1996; **58**: 1192–1204.
16 Kaito H, Nozu K, Fu XJ *et al*: Detection of a transcript abnormality in mRNA of the SLC12A3 gene extracted from urinary sediment cells of a patient with Gitelman's syndrome. *Pediatr Res* 2007; **61**: 502–505.
17 Nozu K, Iijima K, Kawai K *et al*: In vivo and in vitro splicing assay of SLC12A1 in an antenatal salt-losing tubulopathy patient with an intronic mutation. *Hum Genet* 2009; **126**: 533–538.
18 Kaneko K, Tanaka S, Hasui M *et al*: A family with X-linked benign familial hematuria. *Pediatr Nephrol* 2010; **25**: 545–548.
19 Beicht S, Strobl-Wildemann G, Rath S *et al*: Next generation sequencing as a useful tool in the diagnostics of mosaicism in Alport syndrome. *Gene* 2013; **526**: 474–477.
20 Bruttini M, Vitelli F, Meloni I *et al*: Mosaicism in Alport syndrome with genetic counselling. *J Med Genet* 2000; **37**: 717–719.
21 Plant KE, Boye E, Green PM, Vetrie D, Flinter FA: Somatic mosaicism associated with a mild Alport syndrome phenotype. *J Med Genet* 2000; **37**: 238–239.
22 Nozu K VI, Kaito H, Fu XJ *et al*. X-linked Alport syndrome caused by splicing mutations in COL4A5. *Clin J Ame Soc Nephrol* 2014; **9**: 1958–1964.
23 Kashtan CE, Ding J, Gregory M *et al*: Clinical practice recommendations for the treatment of Alport syndrome: a statement of the Alport Syndrome Research Collaborative. *Pediatr Nephrol* 2013; **28**: 5–11.
24 Savige J, Gregory M, Gross O, Kashtan C, Ding J, Flinter F: Expert guidelines for the management of Alport syndrome and thin basement membrane nephropathy. *J Am Soc Nephrol* 2013; **24**: 364–375.

Supplementary Information accompanies this paper on European Journal of Human Genetics website (http://www.nature.com/ejhg)

ORIGINAL RESEARCH ARTICLE | Genetics inMedicine

Differential diagnosis of Bartter syndrome, Gitelman syndrome, and pseudo–Bartter/Gitelman syndrome based on clinical characteristics

Natsuki Matsunoshita, MD[1], Kandai Nozu, MD, PhD[1], Akemi Shono, PhD[1], Yoshimi Nozu, MNS[1], Xue Jun Fu, MD, PhD[1], Naoya Morisada, MD, PhD[1], Naohiro Kamiyoshi, MD[1], Hiromi Ohtsubo, MD[1], Takeshi Ninchoji, MD, PhD[1], Shogo Minamikawa, MD[1], Tomohiko Yamamura, MD[1], Koichi Nakanishi, MD, PhD[2], Norishige Yoshikawa, MD, PhD[2], Yuko Shima, MD, PhD[2], Hiroshi Kaito, MD, PhD[1] and Kazumoto Iijima, MD, PhD[1]

Purpose: Phenotypic overlap exists among type III Bartter syndrome (BS), Gitelman syndrome (GS), and pseudo-BS/GS (p-BS/GS), which are clinically difficult to distinguish. We aimed to clarify the differences between these diseases, allowing accurate diagnosis based on their clinical features.

Methods: A total of 163 patients with genetically defined type III BS ($n = 30$), GS ($n = 90$), and p-BS/GS ($n = 43$) were included. Age at diagnosis, sex, body mass index, estimated glomerular filtration rate, and serum and urine electrolyte concentrations were determined.

Results: Patients with p-BS/GS were significantly older at diagnosis than those with type III BS and GS. Patients with p-BS/GS included a significantly higher percentage of women and had a lower body mass index and estimated glomerular filtration rate than did patients with GS. Although hypomagnesemia and hypocalciuria were predominant biochemical findings in patients with GS, 17 and 23% of patients with type III BS and p-BS/GS, respectively, also showed these abnormalities. Of patients with type III BS, GS, and p-BS/GS, 40, 12, and 63%, respectively, presented with chronic kidney disease.

Conclusions: This study clarified the clinical differences between BS, GS, and p-BS/GS for the first time, which will help clinicians establish differential diagnoses for these three conditions.

Genet Med advance online publication 16 April 2015

Key Words: Bartter syndrome; Gitelman syndrome; pseudo-Bartter; pseudo-Gitelman; salt-losing tubulopathy

INTRODUCTION

Bartter syndrome (BS) (OMIM #s: type I, 601678; type II, 241200; type III, 607364; type IV, 602522; type IVb, 613090) and Gitelman syndrome (GS) (OMIM # 263800) are inherited autosomal-recessive, salt-losing tubulopathies characterized by hypokalemic metabolic alkalosis. BS and GS are reportedly caused by mutations in genes encoding ion transporters or channels, leading directly or indirectly to loss of function.[1–6] These genes include *SLC12A1*, which encodes the apical furosemide-sensitive Na–K–2Cl cotransporter[2]; *KCNJ1*, which encodes the apical renal outer medullary potassium channel[3]; *CLCNKB*, which encodes the basolateral chloride channel Kb (expressed in the thick ascending limb of Henle's loop and in the distal convoluted tubule)[1,7]; and *BSND*, which encodes barttin, a subunit of chloride channels Ka and Kb. Mutations in these genes lead to types I–IV BS, respectively.[6,8] Combined mutations in both *CLCNKA* and *CLCNKB* result in type IVb BS.[9,10] By contrast, mutations in the *SLC12A3* gene, which encodes the apical thiazide-sensitive Na–Cl cotransporter (NCCT) in the distal convoluted tubule, are responsible for GS.[4] Types I, II, IV, and IVb BS (antenatal BS) usually present during the neonatal period with relatively severe symptoms, whereas type III BS (classic BS) presents during early childhood with milder symptoms. In contrast to BS, GS is usually diagnosed during late childhood or adulthood. However, phenotypic overlap frequently occurs between type III BS and GS, which are difficult to diagnose based on their clinical presentations and require genetic tests. For example, some patients with type III BS may show clinical features of GS, including hypomagnesemia and hypocalciuria, and diuretic tests may fail to differentiate between them.[7,11–13] Moreover, mutations in known disease-related genes have not been identified in some patients with clinically diagnosed BS/GS. This suggests that some acquired conditions may cause a BS/GS-like disorder, or pseudo-BS/GS (p-BS/GS), associated with loss of sodium or chloride in the urine, stool, or vomitus or with chloride-intake deficiency, resulting in clinical symptoms identical to those of BS/GS. As previously reported, p-BS/GS may be caused by a wide variety of conditions such

[1]Department of Pediatrics, Kobe University Graduate School of Medicine, Kobe, Japan; [2]Department of Pediatrics, Wakayama Medical University, Wakayama, Japan. Correspondence: Kandai Nozu (nozu@med.kobe-u.ac.jp)

Submitted 1 November 2014; accepted 17 March 2015; advance online publication 16 April 2015. doi:10.1038/gim.2015.56

as surreptitious diuretic use, laxative abuse, a chronic chloride-deficient diet, cyclic vomiting, congenital chloride diarrhea, and cystic fibrosis.[5] Despite the need for accurate diagnosis of these three diseases, the differences in their clinical characteristics have rarely been analyzed, and few useful indicators currently exist. This study aimed to clarify the clinical differences among patients with genetically defined type III BS, GS, and p-BS/GS.

MATERIALS AND METHODS

Ethical considerations

This study was approved by the institutional review board of Kobe University Graduate School of Medicine. Informed consent was obtained from all patients or their parents.

Inclusion criteria

Clinical and laboratory findings of patients with a clinical diagnosis of BS/GS were retrospectively obtained from their medical records. All patients in this study had low serum potassium concentrations and metabolic alkalosis. Hypomagnesemia was defined as a serum magnesium concentration <1.7 mg/dl. Hypocalciuria was defined as a urinary calcium–to–creatinine ratio <0.04 mg/mg. Body height, SD of body height, body weight, body mass index (BMI), serum creatinine, and estimated glomerular filtration rate (eGFR) were obtained at the time of mutational analysis. eGFR was used as an indicator of renal function and was calculated using the formula developed by Schwartz et al.[14,15] or equations designed to obtain the eGFR in Japanese individuals[16] for patients aged ≤17 and ≥18 years, respectively. Urinary electrolyte excretion was evaluated as the fractional excretion of sodium (FENa) and the fractional excretion of chloride (FECl).

Mutational analyses

Genomic DNA was isolated from peripheral blood leukocytes of the patients and their family members using a compact extraction system for DNA isolation (QuickGene-Mini80; Fujifilm, Tokyo, Japan), according to the manufacturer's instructions. All exons and exon–intron boundaries of the *CLCNKB* and *SLC12A3* genes were amplified by polymerase chain reaction and direct sequencing using previously described primer pairs.[10,17] Patients suspected to have BS/GS with no *CLCNKB* or *SLC12A3* mutations were diagnosed as having p-BS/GS. If patients suspected to have BS/GS carried only one *CLCNKB* or *SLC12A3* mutant allele, we performed additional semi-quantitative polymerase chain reaction[10,18] or multiplex ligation-dependent probe amplification using the SALSA P266-*CLCNKB* or P136-*SLC12A3* multiplex ligation-dependent probe amplification assays (MRC-Holland, Amsterdam, The Netherlands) to detect large heterozygous deletions. Total RNA from leukocytes and/or urine sediment was isolated as previously described[19,20] and analyzed to detect splicing abnormalities. Patients with type III BS and GS with homozygous or compound heterozygous mutations in *CLCNKB* or *SLC12A3* were included in this study, whereas patients with only heterozygous mutations were excluded.

Statistical analyses

Data are expressed as mean ± SD. All analyses were performed using standard statistical software (JMP version 10 for Windows; SAS Institute, Cary, NC). The clinical backgrounds of the patients were compared using the Mann–Whitney *U*-, Kruskal–Wallis, Steel–Dwass, Fisher's exact, Pearson's χ^2, and Student's *t*-tests, as appropriate. A P value <0.05 was considered statistically significant.

RESULTS

Clinical and laboratory data for 163 patients with type III BS, GS, or p-BS/GS

In total, 190 patients were referred to our hospital for mutational analysis from November 2006 to April 2014. We performed genetic tests based on the BS/GS genetic analysis algorithm proposed by Peters et al.[21] and assessed the patients' clinical findings and biochemical parameters. Among these 190 patients, 21 with genetically defined type I, II, or IV BS were excluded from this study, together with 6 patients with only one mutant allele in *CLCNKB* or *SLC12A3*. Finally, 163 patients with either type III BS (n = 30), GS (n = 90) or p-BS/GS (n = 43) were included in this study (**Figure 1**). The characteristics of the three groups are summarized in **Table 1**. Patients with type III BS had a significantly lower mean age at diagnosis than did patients with GS or p-BS/GS (4.2 ± 14.0 vs. 18.0 ± 17.1 vs. 36.7 ± 16.5 years, respectively; P < 0.001) (**Figure 2a**). Thirty-eight (88.4%) of the patients with p-BS/GS were diagnosed during adulthood (≥18 years of age), whereas 28 (93.3%) of the patients with type III BS were diagnosed during the first 3 years of life. Patients with GS had a wide range of ages at diagnosis, ranging from infancy to old age; 26 (28.9%) were diagnosed during adulthood. These results suggest that patients clinically diagnosed with BS/GS in adulthood are more likely to have p-BS/GS or GS. However, 6

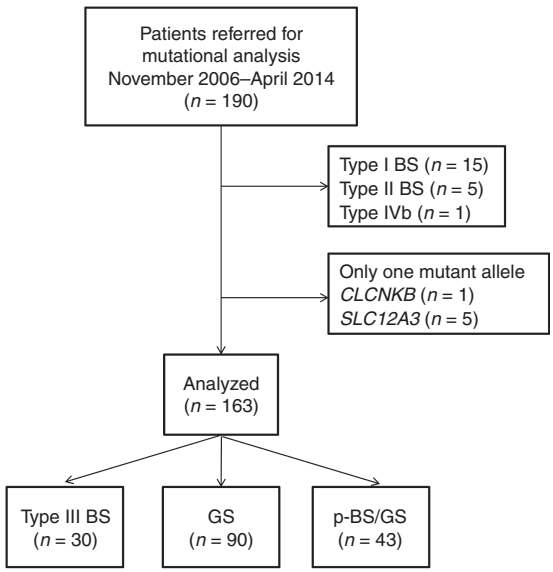

Figure 1 Flow diagram showing patient recruitment and analysis procedure. A total of 163 patients were finally enrolled in this study. BS, Bartter syndrome; GS, Gitelman syndrome.

Table 1 Clinical and laboratory data for 163 patients with type III Bartter syndrome (BS), Gitelman syndrome (GS), or pseudo-BS/GS

	Type III BS (*n* = 30)	GS (*n* = 90)	p-BS/GS (*n* = 43)	*P* value
Age at diagnosis (years)	4.2 ± 14.0	18.0 ± 17.1	36.7 ± 16.5	<0.001[a]
Male patients, *n* (%)	12 (40%)	49 (54.4%)	11 (25.6%)	0.006[b]
Blood pH	7.555 ± 0.10	7.466 ± 0.06	7.477 ± 0.06	<0.001[c]
Blood HCO_3^- concentration (mEq/l)	35.5 ± 10.7	30.8 ± 4.30	32.0 ± 7.70	0.17
Serum potassium concentration (mEq/l)	2.38 ± 0.56	2.45 ± 0.40	2.42 ± 0.41	0.74
Serum magnesium concentration (mg/dl)	1.88 ± 0.32	1.58 ± 0.35	1.95 ± 0.73	<0.001[d]
Serum creatinine concentration (mg/dl)	0.49 ± 0.38	0.48 ± 0.21	1.03 ± 0.57	<0.001[e]
eGFR (ml/min/1.73 m^2)	99.3 ± 36.2	116.9 ± 25.2	71.2 ± 38.1	<0.001[f]
Urinary calcium–to–creatinine ratio (mg/mg)	0.26 ± 0.36	0.02 ± 0.03	0.18 ± 0.40	<0.001[g]
Plasma renin activity (ng/ml/h)	100.7 ± 118.3	20.0 ± 24.8	24.8 ± 24.6	<0.001[h]
Plasma aldosterone concentration (pg/ml)	671.1 ± 676.4	238.9 ± 256.7	548.6 ± 853.8	<0.001[i]

Values are represented as mean ± SD unless otherwise indicated.

eGFR, estimated glomerular filtration rate; .

[a]Type III BS versus GS: $P < 0.001$; type III BS versus p-BS/GS: $P < 0.001$; GS versus p-BS/GS: $P < 0.001$. [b]GS versus p-BS/GS: $P = 0.002$.[c]Type III BS versus GS: $P < 0.001$; type III BS versus p-BS/GS: $P = 0.004$. [d]Type III BS versus GS: $P < 0.001$; GS versus p-BS/GS: $P = 0.002$. [e]Type III BS versus p-BS/GS: $P < 0.001$; GS versus p-BS/GS: $P < 0.001$. [f]Type III BS versus GS: $P = 0.04$; type III BS versus p-BS/GS: $P = 0.01$; GS versus p-BS/GS: $P < 0.001$.[g]Type III BS versus GS: $P < 0.001$; GS versus p-BS/GS: $P < 0.001$.[h]Type III BS versus GS: $P < 0.001$; type III BS versus p-BS/GS: $P = 0.001$. [i]Type III BS versus GS: $P < 0.001$.

patients with GS (6.7%) were diagnosed at ≤3 years of age, and 14 (15.6%) were at ≤5 years of age. Genetic testing was required to differentiate between GS and type III BS in these patients.

As expected, patients with GS had a significantly lower mean serum magnesium concentrations (1.58 ± 0.35 vs. 1.88 ± 0.32 vs. 1.95 ± 0.73 mg/dl, respectively; $P < 0.001$) (**Figure 2b**) and urinary calcium–to–creatinine ratio (0.02 ± 0.03 vs. 0.26 ± 0.36 vs. 0.18 ± 0.40 mg/mg, respectively; $P < 0.001$) (**Figure 2c**) than did patients with type III BS or p-BS/GS. Although hypomagnesemia and hypocalciuria were predominant biochemical findings in patients with GS, 5 patients with type III BS (16.7%) and 10 with p-BS/GS (23.3%) also showed hypomagnesemia and hypocalciuria (**Supplementary Figures S1 and S2** online). However, only 41 patients (45.6%) with GS presented with both hypomagnesemia and hypocalciuria (**Supplementary Figure S3** online), and 9 showed neither hypomagnesemia nor hypocalciuria. Six patients (20.0%) with type III BS and four (9.3%) with p-BS/GS presented with hypercalciuria (>0.37 mg/mg). Patients with type III BS also had significantly higher blood pH and plasma renin activity than did those with GS or p-BS/GS (**Table 1**). All three groups included some patients with a low eGFR (<90 ml/min/1.73 m^2), but the mean eGFR was significantly lower in the p-BS/GS group than in the type III BS and GS groups (71.2 ± 38.1 vs. 99.3 ± 36.2 vs. 116.9 ± 25.2 ml/min/1.73 m^2, respectively; $P < 0.001$) (**Figure 2d**). Twelve patients with type III BS (40.0%) presented with chronic kidney disease (stage II, $n = 7$; stage III, $n = 5$), compared with 11 patients (12.0%) with GS (stage II, $n = 9$; stage III, $n = 2$) and 27 (62.8%) with p-BS/GS (stage II, $n = 8$; stage III, $n = 13$; stage IV, $n = 6$).

We next aimed to identify the clinical indices that distinguish a diagnosis of GS according to age at diagnosis. We divided all 90 patients with GS into the following three groups by age at diagnosis: childhood (≤12 years of age), $n = 55$; adolescence (13–17 years of age), $n = 9$; and adulthood (≥18 years), $n = 26$. Patients with GS diagnosed during adulthood had a significantly higher urinary calcium–to–creatinine ratio (0.03 ± 0.03 mg/mg) than did patients diagnosed during childhood or adolescence (0.02 ± 0.03 vs. 0.01 ± 0.01 mg/mg, respectively; $P = 0.035$), whereas there were the no significant differences in the mean serum magnesium concentration or other parameters.

Clinical and laboratory data for adult patients with type III BS, GS, or p-BS/GS

Most patients with p-BS/GS were diagnosed during adulthood. We therefore compared adult patients with adult-diagnosed p-BS/GS and adult-diagnosed GS to adjust for the age of these two groups. The clinical features and laboratory data for these two groups are shown in **Supplementary Table S1** online.

The p-BS/GS group included a significantly higher percentage of women (76.3 vs. 44.8%; $P = 0.008$), had a lower mean BMI (17.9 ± 4.1 vs. 21.2 ± 3.5 kg/m^2; $P < 0.001$) (**Figure 3a**), and had a lower mean eGFR (65.1 ± 36.2 vs. 99.8 ± 31.2 ml/min/1.73 m^2; $P < 0.001$) (**Figure 3b**) than the GS group. Furthermore, adult patients with p-BS/GS had a significantly higher mean serum magnesium concentration (1.95 ± 0.75 vs. 1.57 ± 0.37 mg/dl; $P = 0.01$) (**Figure 3c**) and urinary calcium–to–creatinine ratio (0.07 ± 0.08 vs. 0.03 ± 0.03 mg/mg; $P = 0.008$) (**Figure 3d**) than did those with GS. Although the age at diagnosis and current age were similar in both groups, the eGFR was significantly lower in patients with p-BS/GS, suggesting the possibility of renal damage associated with hypovolemia (caused by underlying factors such as dehydration or nutritional deficiency), reflected by the higher percentage of women and lower BMI in

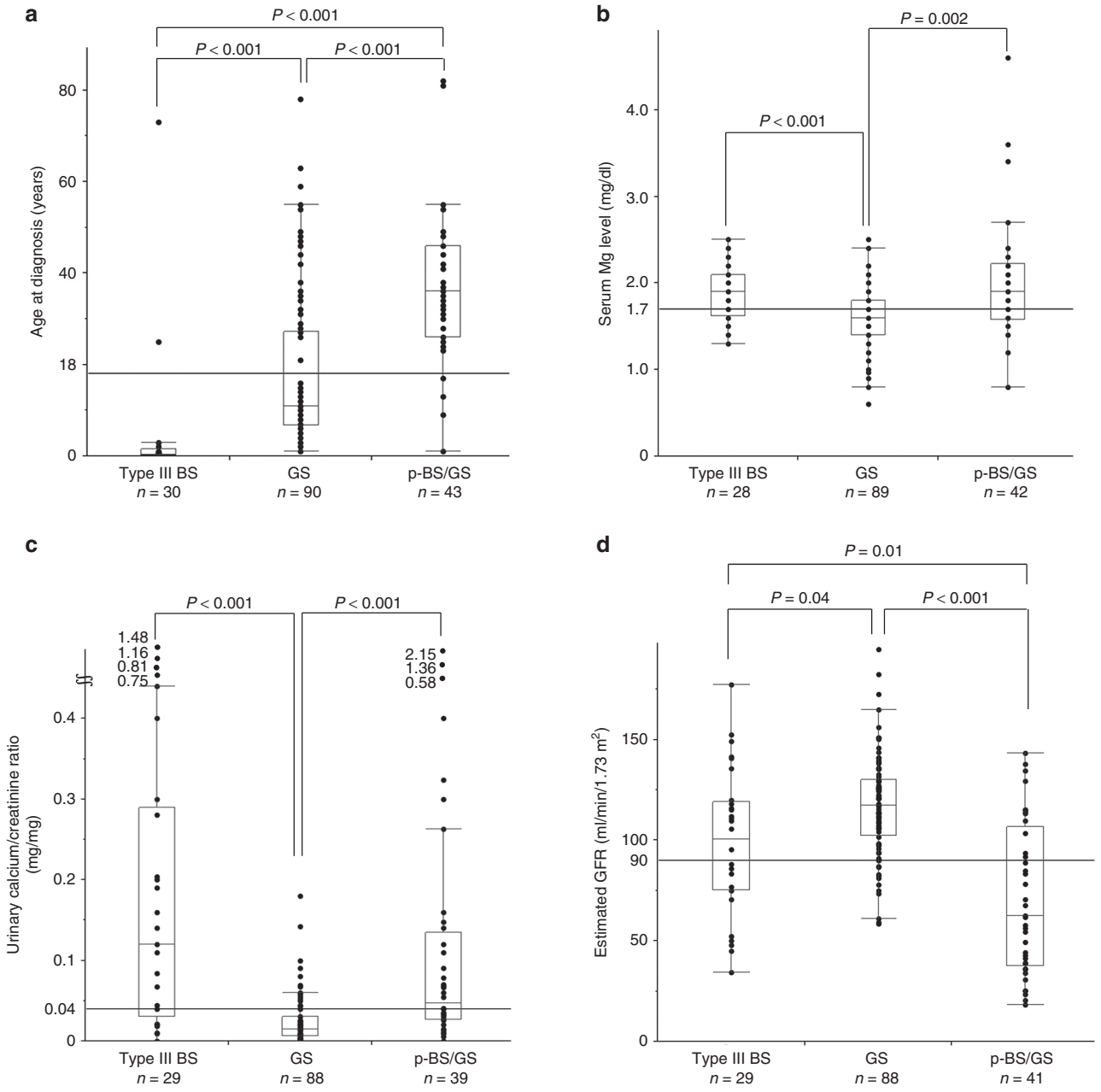

Figure 2 Selected clinical and biochemical parameters in three disorders. (**a**) Age at diagnosis. Patients with pseudo–Bartter syndrome/Gitelman syndrome (p-BS/GS) were significantly older at diagnosis than were patients with type III Bartter syndrome (BS) or Gitelman syndrome (GS) (36.7 ± 16.5 vs. 4.2 ± 14.0 vs. 18.0 ± 17.1 years, respectively; $P < 0.001$). (**b**) Serum magnesium concentrations. Patients with GS had a significantly lower mean serum magnesium concentration than patients with type III BS or p-BS/GS (1.58 ± 0.35 vs. 1.88 ± 0.32 vs. 1.95 ± 0.73 mg/dl, respectively; $P < 0.001$). Four patients lacked data. (**c**) Urinary calcium–to–creatinine ratio. Patients with GS had a significantly lower mean urinary calcium–to–creatinine ratio than patients with type III BS or p-BS/GS (0.02 ± 0.03 vs. 0.26 ± 0.36 vs. 0.18 ± 0.40 mg/mg, respectively; $P < 0.001$). Six patients lacked data. (**d**) Estimated glomerular filtration rate (eGFR). Patients with p-BS/GS had a significantly lower mean eGFR than patients with type III BS or p-BS/GS (71.2 ± 38.1 vs. 99.3 ± 36.2 vs. 116.9 ± 25.2 ml/min/1.73 m^2, respectively; $P < 0.001$). Twelve patients (40.0%) with type III BS presented with chronic kidney disease (stage II, $n = 7$; stage III, $n = 5$), compared with 11 patients (12.0%) with GS (stage II, $n = 9$; stage III, $n = 2$) and 27 (62.8%) with p-BS/GS (stage II, $n = 8$; stage III, $n = 13$; stage IV, $n = 6$). Six patients lacked data.

this group. Notably, 11 patients (12%) with GS presented with a reduced eGFR (<90 ml/min/1.73 m^2) in adulthood, though the prognosis for renal function in patients with GS is usually considered benign. When we compared the adult patients with p-BS/GS with the adult patients with type III BS to adjust for age, we found no statistically significant difference in the eGFR (**Supplementary Figure S4** online), although it was significantly lower than that of adult patients with GS (**Figure 3b**). Excluding the influence of the aging process on the eGFR evaluation, these data show that patients with p-BS/GS had more severe kidney dysfunction than patients with GS, but this difference was not observed in patients with type III BS. These

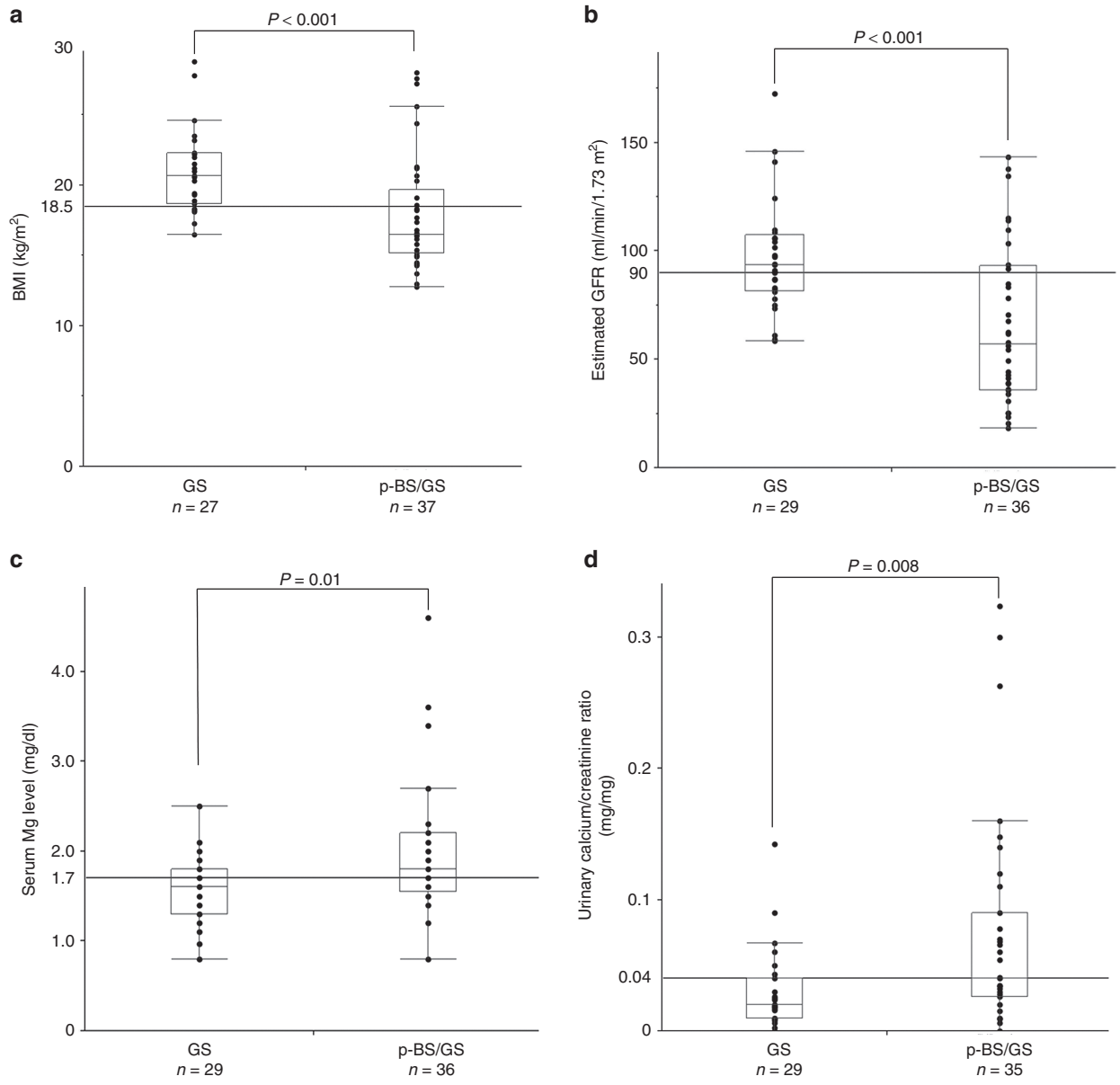

Figure 3 Selected clinical and biochemical parameters in adult Gitelman and pseudo-Bartter/Gitelman patients. (**a**) Body mass index (BMI) in patients aged ≥18 years with Gitelman syndrome (GS) and pseudo–Bartter syndrome (BS)/Gitelman syndrome (p-BS/GS). Patients with p-BS/GS had a significantly lower mean BMI than patients with GS (17.9 ± 4.1 vs. 21.2 ± 3.5 kg/m^2, respectively; $P < 0.001$). Three patients lacked data. (**b**) Estimated glomerular filtration rate (eGFR) in patients with GS or p-BS/GS aged ≥18 years. Patients with p-BS/GS had a significantly lower mean eGFR than patients with GS (65.1 ± 36.2 vs. 99.8 ± 31.2 ml/min/1.73 m^2, respectively; $P < 0.001$). Two patients lacked data. (**c**) Serum magnesium concentrations in patients with GS or p-BS/GS aged ≥18 years. Patients with p-BS/GS had a significantly higher mean serum magnesium concentration than patients with GS (1.95 ± 0.75 vs. 1.57 ± 0.37 mg/dl, respectively; $P = 0.01$). Two patients lacked data. (**d**) Urinary calcium–to–creatinine ratios in patients with GS and p-BS/GS aged ≥18 years. Patients with p-BS/GS had a significantly higher urinary calcium–to–creatinine ratio than patients with GS (0.07 ± 0.08 vs. 0.03 ± 0.03 mg/mg, respectively; $P = 0.008$). Three patients lacked data.

findings may reflect the fact that patients with type III BS often develop kidney dysfunction.[22]

Clinical and laboratory data for patients with p-BS/GS

The underlying factors in all 43 patients with p-BS/GS are shown in **Supplementary Figure S5** online. Twenty-four patients (56%) had apparent underlying causes of hypokalemia and metabolic alkalosis, including diuretic or laxative abuse ($n = 14$), severe hyperemesis gravidarum ($n = 3$), alcoholism ($n = 2$), anorexia ($n = 2$), excessive dieting ($n = 1$), a habit of taking sweat-baths (saunas) ($n = 1$), and a habit of drinking Chinese tea, which contains diuretics ($n = 1$). Consistent with the findings of a previous study,[5] most of these factors could potentially lead to hypovolemia. By contrast, no clear underlying factors were identified in the remaining 19 patients (44%) with p-BS/GS, despite detailed interviews. The 38 patients with p-BS/GS who were aged ≥18 years were divided into two groups according to the presence or absence of underlying

factors. The clinical differences between these groups are shown in **Supplementary Table S2** online. The only significant difference was in height, which was significantly shorter in the group without underlying factors. This suggests that p-BS/GS in patients without obvious underlying factors might be partially caused by genetic factors different from those responsible for BS or GS because a short stature reflects underlying factors that existed during the growth phase.

We focused on the patients with p-BS/GS caused by laxative abuse because laxative abuse is the most common cause of p-BS/GS (**Supplementary Table S3** online, **Supplementary Figure S6** online). Eleven patients had p-BS/GS caused by laxative abuse, including seven who used magnesium oxide laxatives and four who used laxatives that did not contain magnesium (sennoside, $n = 3$; Japanese traditional medicine, $n = 1$). Four of the five patients with p-BS/GS with markedly high serum magnesium concentrations (>2.5 mg/dl) had a history of chronic use of a magnesium oxide laxative preparation. Unexpectedly, none of the patients who used laxatives that did not contain magnesium had hypomagnesemia (**Supplementary Figure S6** online). On the basis of these results we can say that patients with pseudo-BS/GS caused by laxatives tend to have normal or high serum magnesium concentrations.

We also compared the 11 patients with p-BS/GS caused by laxative abuse with the 29 adult patients with GS (**Supplementary Table S3** online). As expected, the patients with p-BS/GS caused by laxative abuse had a lower mean BMI (18.7 ± 4.8 vs. 21.2 ± 3.5 kg/m^2, respectively; $P = 0.02$) and a lower mean eGFR (64.8 ± 25.8 vs. 99.8 ± 31.2 ml/min/1.73 m^2, respectively; $P = 0.005$) than the adult patients with GS. Notably, the patients with p-BS/GS caused by laxative abuse had significantly higher plasma renin activity (26.2 ± 17.9 vs. 15.9 ± 9.9 ng/ml/h, respectively; $P = 0.03$) and plasma aldosterone concentrations (617.4 ± 655.8 vs. 273.4 ± 333.8 pg/ml, respectively; $P = 0.02$) than adult patients with GS, reflecting the marked activation of the renin–aldosterone system secondary to chronic diarrhea. Furthermore, patients with p-BS/GS caused by laxative abuse had a significantly higher mean urinary calcium–to–creatinine ratio than patients with GS (0.09 ± 0.06 vs. 0.03 ± 0.03 mg/mg, respectively; $P = 0.04$). These results may clarify the characteristics of p-BS/GS caused by laxative abuse.

Four patients with p-BS/GS had hypercalciuria. Among them, one (a 1-year-old girl) was being given a Chinese tea containing a diuretic, possibly a loop diuretic, by her parents. The other three patients were relatively young (two were 9 years old and one was 13 years old), which might suggest that they had a hereditary disorder other than BS/GS. None of the patients in our cohort were taking loop diuretics for medical purposes.

FENa and FECl

Impaired tubular reabsorption of sodium chloride, resulting in urinary loss, is a common pathophysiological mechanism of BS/GS. We therefore compared FENa and FECl among the patients with BS, GS, and p-BS/GS with available urine sodium and/or chloride concentration data. Patients with type III BS had a significantly higher mean FENa (1.62 ± 0.79% vs. 0.69 ± 0.44% vs. 0.32 ± 0.28%, respectively; $P < 0.001$) (**Figure 4a**) and FECl (2.80 ± 1.44% vs. 1.10 ± 0.68% vs. 0.44 ± 0.45%, respectively; $P < 0.001$) (**Figure 4b**) than patients with GS and p-BS/GS. These results suggest that patients with genetically defined BS/GS show more severe defects in the tubular reabsorption of sodium chloride than patients with p-BS/GS.

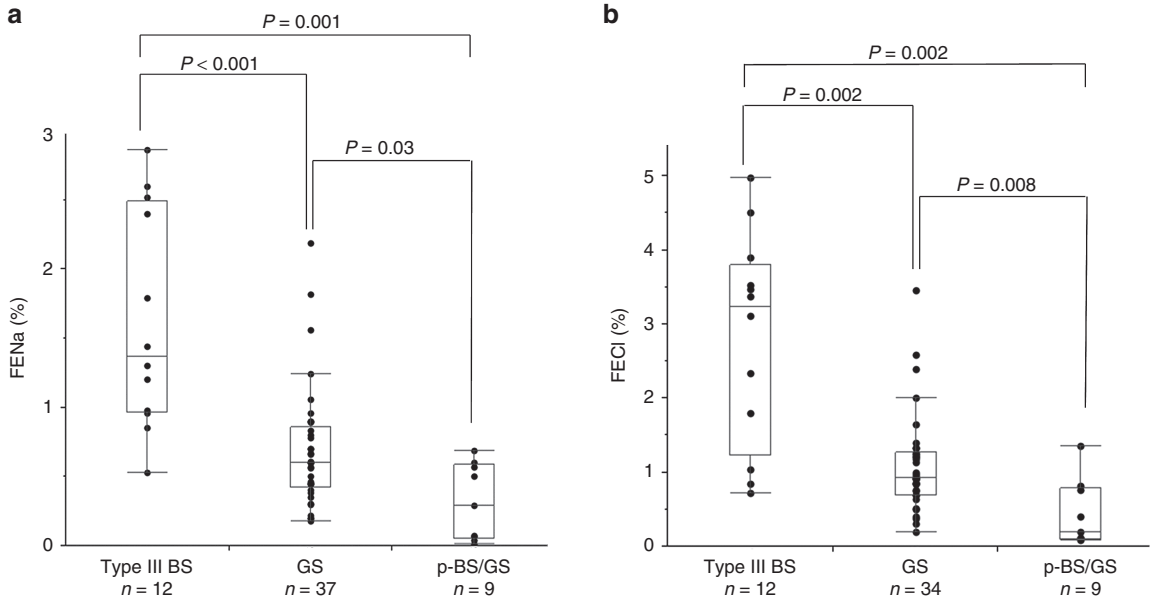

Figure 4 Fractional excretion of sodium and chloride in three disorders. (**a**) Fractional excretion of sodium (FENa). Patients with type III Bartter syndrome (BS) had a significantly higher FENa than patients with Gitelman syndrome (GS) or pseudo-BS/GS (p-BS/GS) (1.62 ± 0.79% vs. 0.69 ± 0.44% vs. 0.32 ± 0.28%, respectively; $P < 0.001$). (**b**) Fractional excretion of chloride (FECl). Patients with type III BS had a significantly higher FECl than patients with GS or p-BS/GS (2.80 ± 1.44% vs. 1.10 ± 0.68% vs. 0.44 ± 0.45%, respectively; $P < 0.001$).

DISCUSSION

This study demonstrates for the first time the clinical distinctions among patients with genetically defined type III BS, GS, and p-BS/GS. The results provide useful and novel clinical information about these three diseases, which are usually difficult to differentiate and are frequently confused with one another in the clinical setting.

BS and GS have been divided into three main categories according to age at onset: antenatal BS (types I, II, IV, and IVb), classic BS (type III BS), and GS. Antenatal BS is usually easy to diagnose because patients present with typical symptoms, such as polyhydramnios, low birth weight, or failure to thrive, during the antenatal or neonatal period.[5,21] By contrast, the clinical manifestations of type III BS and GS may vary and resemble each other.[7,11–13] Furthermore, p-BS/GS is difficult to distinguish from type III BS or GS because its clinical features match those of the latter two diseases. Correctly distinguishing these three diseases based on their clinical characteristics is thus important. We therefore analyzed and compared the clinical data for 163 Japanese patients with genetically defined type III BS, GS, and p-BS/GS.

Age at diagnosis differed significantly among patients with the three diseases. A previous report suggested that patients with type III BS often presented with the disease during childhood, whereas patients with GS were usually diagnosed during late childhood or adulthood.[23] In this study most patients with type III BS (93%) were diagnosed before the age of 3 years, whereas most patients with p-BS/GS (88%) were diagnosed during adulthood. About one-third (29%) of patients with GS were diagnosed during adulthood. These findings suggest that age at diagnosis may be useful for differentiating among these three diseases. Distinguishing between infantile-onset GS and type III BS remains problematic, however, and genetic testing is required to determine the nature of the disease in these patients.

We also found that patients in all three groups demonstrated varying degrees of progressive renal impairment, as previously reported.[22,24–26] Tseng et al.[24] reported that 7 of 117 patients (6%) with genetically diagnosed GS developed chronic kidney disease (stage III or IV). In this study 12 of 30 patients (40.0%) with type III BS, 11 of 90 (12.0%) with GS, and 27 of 43 (62.8%) with p-BS/GS presented with stage II–IV chronic kidney disease. Thus caution is necessary when establishing a list of differential diagnoses because both hypokalemic metabolic alkalosis and renal impairment are common to all three diseases.

We further clarified the differences between adult patients with p-BS/GS and adult patients with GS to adjust for the age of these two groups and found that p-BS/GS was more common among adult women with a lower BMI and eGFR. Previous reports demonstrated that dehydration caused by anorexia and diuretic or laxative abuse causes renal hypoperfusion, resulting in a reduced glomerular filtration rate.[27,28] These reports support our current data, given that anorexia and diuretic and laxative abuse are generally recognized to be more common among women.

The results of this study also confirmed the significant phenotypic overlap in serum magnesium concentrations and urinary calcium–to–creatinine ratios among the three diseases. Some cases of type III BS were previously reported to show features similar to those of GS, including hypomagnesemia and hypocalciuria.[7,11–13] In addition, one report published in 2003 showed that, in a large consanguineous family, both the BS and GS phenotypes were present with the same *CLCNKB* mutation.[13] In the same year a review article pointed out the phenotypic overlaps between type III BS and GS.[29] In this study 16.7% of patients with type III BS and 23.3% with p-BS/GS had hypomagnesemia and hypocalciuria, as in GS. Interestingly, only 47% of patients with GS typically presented with hypomagnesemia and hypocalciuria. These data demonstrate the difficulty of distinguishing among these disorders on the basis of the absence or presence of hypomagnesemia and hypocalciuria.

We also attempted to identify the underlying factors contributing to the development of p-BS/GS. Among the 43 patients with p-BS/GS, more than half (56%) had contributing factors, including diuretic or laxative abuse in 33%. The remainder (44%), however, had no clear contributing factors. Although the acquisition of a detailed history has been considered to allow for discernment between GS and p-BS/GS, the limited value of this approach was demonstrated by the low detection rate of underlying factors in this study. Veldhuis et al.[30] reported that measurement of the urinary chloride concentration is useful for differential diagnosis based on urinary or fecal chloride loss. We therefore evaluated urinary electrolyte excretion (FENa and FECl). In this study patients with type III BS and GS had significantly higher mean FENa and FECl values than patients with p-BS/GS. These findings suggest that FENa and FECl may be useful parameters for differentiating among these three diseases.

There are several possible reasons for the failure to identify underlying factors. We may have failed to detect mutations in the *CLCNKB* or *SLC12A3* gene; however, that we would have missed both mutations on the paternal and maternal alleles is unlikely. We failed to detect two mutations in only six patients, and if our strategy was inadequate, we expect this number would have been much larger. Some patients with p-BS/GS also may have presented with inherited disorders other than BS/GS. Choi et al.[31] recently reported that *SLC26A3* gene mutations were responsible for congenital chloride diarrhea in 5 of 39 patients with clinically diagnosed BS. As reported previously, however, we failed to detect any *SLC26A3* gene mutations in patients with p-BS/GS with no detectable underlying factors.[32] Our findings suggest that *SLC26A3* mutations may have been quite rare in our cohort. We also demonstrated that adult patients with p-BS/GS with no underlying factors had a significantly shorter stature than those with underlying factors. This suggests the possible existence of unidentified inherited disorders in patients with p-BS/GS. In fact, some researchers doubt the existence of new loci other than those on genes already identified for these phenotypes.[29,31] Identification of defects in other transporter genes may significantly improve

our understanding of the underlying mechanisms of renal salt homeostasis. Next-generation sequencing, in addition to functional studies and in vivo analysis using transgenic animals, is needed to characterize these undiagnosed cases. This new technology will also reduce the burden of genetic analysis and allow for the detection of unidentified mutations.

In this study five patients were heterozygous carriers of NCCT mutations. We could not detect the other mutation despite performing several types of genetic analyses. For accurate phenotyping of GS, we excluded these patients from this study. However, some previous reports have indicated the possibility that a single loss-of-function mutation of the NCCT gene can result in a phenotype similar to that of patients treated by low-dose thiazide diuretics.[33] Recent large cohort studies also showed that about 8% of patients with GS have only heterozygous mutations in the NCCT gene; that GS occurs by heterozygous mutations in NCCT-gene haploinsufficiency or dominant-negative effects by hypomorphic alleles remains possible.[12,24] Further study is needed to answer this long-standing question.

This study had several limitations. First, we diagnosed p-BS/GS based on negative genetic results for *CLCNKB*, *SLC12A3*, and *SLC26A3* mutations, and we may have failed to detect mutations in these genes. However, it is very unlikely that we missed mutations in both alleles, as required for autosomal recessive inheritance, as discussed above. The second limitation is that we observed the patients' clinical courses for only a relatively short period of time. Long-term follow-up is necessary to clarify their prognoses, including their renal prognoses.

In conclusion, we provided herein the first criteria for establishing clinical distinctions among genetically diagnosed type III BS, GS, and p-BS/GS. Our results indicate that p-BS/GS is particularly common among adult women with lower BMIs and eGFRs. These results suggest that age at diagnosis, sex, BMI, and renal function, in addition to the serum magnesium concentration and urinary calcium–to–creatinine ratio, should be taken into consideration for the differential diagnosis of type III BS, GS, and p-BS/GS.

SUPPLEMENTARY MATERIAL

Supplementary material is linked to the online version of the paper at http://www.nature.com/gim

ACKNOWLEDGMENTS

This study was supported by a grant from the Ministry of Health, Labour and Welfare, Japan, for Research on Rare Intractable Diseases in Kidney and Urinary Tract (H24-nanchitou (nan)-ippan-041 to Kazumoto Iijima) in the "Research on Measures for Intractable Diseases" Project; a Grant-in-Aid for Scientific Research (KAKENHI) from the Ministry of Education, Culture, Sports, Science and Technology of Japan (subject ID: 25893131 to K.N.); and a grant from the Mother and Child Health Foundation (subject ID: 25–7 to K.N.).

DISCLOSURE

The authors declare no conflict of interest.

REFERENCES

1. Simon DB, Bindra RS, Mansfield TA, et al. Mutations in the chloride channel gene, CLCNKB, cause Bartter's syndrome type III. *Nat Genet* 1997;17:171–178.
2. Simon DB, Karet FE, Hamdan JM, DiPietro A, Sanjad SA, Lifton RP. Bartter's syndrome, hypokalaemic alkalosis with hypercalciuria, is caused by mutations in the Na-K-2Cl cotransporter NKCC2. *Nat Genet* 1996;13:183–188.
3. Simon DB, Karet FE, Rodriguez-Soriano J, et al. Genetic heterogeneity of Bartter's syndrome revealed by mutations in the K+ channel, ROMK. *Nat Genet* 1996;14:152–156.
4. Simon DB, Nelson-Williams C, Bia MJ, et al. Gitelman's variant of Bartter's syndrome, inherited hypokalaemic alkalosis, is caused by mutations in the thiazide-sensitive Na-Cl cotransporter. *Nat Genet* 1996;12:24–30.
5. Seyberth HW, Schlingmann KP. Bartter- and Gitelman-like syndromes: salt-losing tubulopathies with loop or DCT defects. *Pediatr Nephrol* 2011;26:1789–1802.
6. Birkenhäger R, Otto E, Schürmann MJ, et al. Mutation of BSND causes Bartter syndrome with sensorineural deafness and kidney failure. *Nat Genet* 2001;29:310–314.
7. Nozu K, Iijima K, Kanda K, et al. The pharmacological characteristics of molecular-based inherited salt-losing tubulopathies. *J Clin Endocrinol Metab* 2010;95:E511–E518.
8. Estévez R, Boettger T, Stein V, et al. Barttin is a Cl- channel beta-subunit crucial for renal Cl- reabsorption and inner ear K+ secretion. *Nature* 2001;414:558–561.
9. Schlingmann KP, Konrad M, Jeck N, et al. Salt wasting and deafness resulting from mutations in two chloride channels. *N Engl J Med* 2004;350:1314–1319.
10. Nozu K, Inagaki T, Fu XJ, et al. Molecular analysis of digenic inheritance in Bartter syndrome with sensorineural deafness. *J Med Genet* 2008;45:182–186.
11. Lee BH, Cho HY, Lee H, et al. Genetic basis of Bartter syndrome in Korea. *Nephrol Dial Transplant* 2012;27:1516–1521.
12. Vargas-Poussou R, Dahan K, Kahila D, et al. Spectrum of mutations in Gitelman syndrome. *J Am Soc Nephrol* 2011;22:693–703.
13. Zelikovic I, Szargel R, Hawash A, et al. A novel mutation in the chloride channel gene, CLCNKB, as a cause of Gitelman and Bartter syndromes. *Kidney Int* 2003;63:24–32.
14. Schwartz GJ, Haycock GB, Edelmann CM Jr, Spitzer A. A simple estimate of glomerular filtration rate in children derived from body length and plasma creatinine. *Pediatrics* 1976;58:259–263.
15. Schwartz GJ, Gauthier B. A simple estimate of glomerular filtration rate in adolescent boys. *J Pediatr* 1985;106:522–526.
16. Matsuo S, Imai E, Horio M, et al.; Collaborators developing the Japanese equation for estimated GFR. Revised equations for estimated GFR from serum creatinine in Japan. *Am J Kidney Dis* 2009;53:982–992.
17. Fukuyama S, Okudaira S, Yamazato S, Yamazato M, Ohta T. Analysis of renal tubular electrolyte transporter genes in seven patients with hypokalemic metabolic alkalosis. *Kidney Int* 2003;64:808–816.
18. Nozu K, Fu XJ, Nakanishi K, et al. Molecular analysis of patients with type III Bartter syndrome: picking up large heterozygous deletions with semiquantitative PCR. *Pediatr Res* 2007;62:364–369.
19. Kaito H, Nozu K, Fu XJ, et al. Detection of a transcript abnormality in mRNA of the SLC12A3 gene extracted from urinary sediment cells of a patient with Gitelman's syndrome. *Pediatr Res* 2007;61:502–505.
20. Nozu K, Iijima K, Kawai K, et al. In vivo and in vitro splicing assay of SLC12A1 in an antenatal salt-losing tubulopathy patient with an intronic mutation. *Hum Genet* 2009;126:533–538.
21. Peters M, Jeck N, Reinalter S, et al. Clinical presentation of genetically defined patients with hypokalemic salt-losing tubulopathies. *Am J Med* 2002;112:183–190.
22. Bettinelli A, Borsa N, Bellantuono R, et al. Patients with biallelic mutations in the chloride channel gene CLCNKB: long-term management and outcome. *Am J Kidney Dis* 2007;49:91–98.
23. Shaer AJ. Inherited primary renal tubular hypokalemic alkalosis: a review of Gitelman and Bartter syndromes. *Am J Med Sci* 2001;322:316–332.
24. Tseng MH, Yang SS, Hsu YJ, et al. Genotype, phenotype, and follow-up in Taiwanese patients with salt-losing tubulopathy associated with SLC12A3 mutation. *J Clin Endocrinol Metab* 2012;97:E1478–E1482.

25. Knoers NV, Levtchenko EN. Gitelman syndrome. *Orphanet J Rare Dis* 2008;3:22.
26. Calò LA, Marchini F, Davis PA, Rigotti P, Pagnin E, Semplicini A. Kidney transplant in Gitelman's syndrome. Report of the first case. *J Nephrol* 2003;16: 144–147.
27. Boag F, Weerakoon J, Ginsburg J, Havard CW, Dandona P. Diminished creatinine clearance in anorexia nervosa: reversal with weight gain. *J Clin Pathol* 1985;38:60–63.
28. Lowinger K, Griffiths RA, Beumont PJ, Scicluna H, Touyz SW. Fluid restriction in anorexia nervosa: a neglected symptom or new phenomenon? *Int J Eat Disord* 1999;26:392–396.
29. Zelikovic I. Hypokalaemic salt-losing tubulopathies: an evolving story. *Nephrol Dial Transplant* 2003;18:1696–1700.
30. Veldhuis JD, Bardin CW, Demers LM. Metabolic mimicry of Bartter's syndrome by covert vomiting: utility of urinary chloride determinations. *Am J Med* 1979;66:361–363.
31. Choi M, Scholl UI, Ji W, et al. Genetic diagnosis by whole exome capture and massively parallel DNA sequencing. *Proc Natl Acad Sci USA* 2009;106:19096–19101.
32. Ishimori S, Kaito H, Matsunoshita N, et al. SLC26A3 gene analysis in patients with Bartter and Gitelman syndromes and the clinical characteristics of patients with unidentified mutations. *Kobe J Med Sci* 2013;59:E36–E43.
33. Fava C, Montagnana M, Rosberg L, et al. Subjects heterozygous for genetic loss of function of the thiazide-sensitive cotransporter have reduced blood pressure. *Hum Mol Genet* 2008;17:413–418.

4 Vervaet BA, Verhulst A, D'Haese PC, De Broe ME. Nephrocalcinosis: New insights into mechanisms and consequences. *Nephrol. Dial. Transplant.* 2009; **24**: 2030–35.
5 Morimoto M, Yu Z, Stenzel P *et al*. Reduced elastogenesis: A clue to the arteriosclerosis and emphysematous changes in Schimke immune-osseous dysplasia? *Orphanet J. Rare Dis.* 2012; **7**: 70. doi:10.1186/1750-1172-7-70.
6 Ozdemir N, Alpay H, Bereket A *et al*. Membranous nephropathy in Schimke immuno-osseous dysplasia. *Pediatr. Nephrol.* 2006; **2**: 870–72.
7 Santangelo L, Gigante M, Netti GS *et al*. A novel SMARCAL1 mutation associated with a mild phenotype of Schimke immune-osseous dysplasia (SIOD). *BMC Nephrol.* 2014; **15** (1): 41. doi:10.1186/1471-2369-15-41.
8 Balogun RA, Adams ND, Palmisano J, Yamase H, Chughtai I, Kaplan AA. Focal segmental glomerulosclerosis, proteinuria and nephrocalcinosis associated with renal tubular acidosis. *Nephrol. Dial. Transplant.* 2002; **17**: 308–10.
9 Yamazaki H, Nozu K, Narita I *et al*. Atypical phenotype of type I Bartter syndrome accompanied by focal segmental glomerulosclerosis. *Pediatr. Nephrol.* 2009; **24**: 415–18.
10 Schmidt B, Christen HJ, Henkenrath P, Benz-Bohm G, Müller Berghaus J, Querfeld U. Cerebral complications in Schimke immuno-osseous dysplasia. *Eur. J. Pediatr.* 1997; **156**: 789–91.

Autoimmune-type atypical hemolytic uremic syndrome treated with eculizumab as first-line therapy

Masataka Hisano,[1] Akira Ashida,[2] Eiji Nakano,[1] Mamiko Suehiro,[1] Yoko Yoshida,[3] Masanori Matsumoto,[3] Toshiyuki Miyata,[4] Yoshihiro Fujimura[3] and Motoshi Hattori[5]

[1]*Department of Nephrology, Chiba Children's Hospital, Chiba,* [2]*Department of Pediatrics, Osaka Medical College, Takatsuki,* [3]*Department of Blood Transfusion Medicine, Nara Medical University, Kashihara,* [4]*Department of Molecular Pathogenesis, Research Institute National Cerebral and Cardiovascular Center, Suita and* [5]*Department of Pediatric Nephrology, Tokyo Women's Medical University, Tokyo, Japan*

Abstract We report a case of atypical hemolytic uremic syndrome (aHUS) in a 4-year-old boy. Although the patient had the typical triad of aHUS (microangiopathic hemolytic anemia, thrombocytopenia, and acute kidney injury), urgent dialysis was not indicated because he had neither oliguria nor severe electrolyte abnormality. He was given eculizumab as first-line therapy, which led to significant clinical improvement, thus avoiding any risk of complications associated with plasma exchange and central venous catheterization. Retrograde functional analysis of the patient's plasma using sheep erythrocytes indicated an increase in hemolysis, suggesting impairment of host cell protection by complement factor H. The use of eculizumab as first-line therapy in place of plasma exchange might be reasonable for pediatric patients with aHUS.

Key words atypical hemolytic uremic syndrome, eculizumab, plasma exchange.

Hemolytic uremic syndrome (HUS) is defined by the typical triad of microangiopathic hemolytic anemia, thrombocytopenia, and acute renal injury. More than 90% of cases in children are secondary to infection with enterohemorrhagic *Escherichia coli* (EHEC) which produces Shiga toxin. The remaining 10% of cases, however, are classified as atypical hemolytic uremic syndrome (aHUS). aHUS has a poor prognosis with a high mortality rate and a high rate of progression to end-stage renal failure.[1] Plasma exchange (PE) has been recommended as first-line rescue therapy for such aHUS episodes, and for prevention of relapse.[2,3] This treatment, however, has some problems in terms of long-term acceptance, and its efficacy is controversial. Also, vascular access carries risk of complications, including bleeding and vascular injury. Eculizumab (Soliris®; Alexion Pharmaceuticals, Cheshire, CT, USA) is a humanized monoclonal anti-C5 antibody that inhibits the terminal complement pathway and hinders the generation of pro-inflammatory C5a and C5b-9 (membrane attack complex: MAC). Recent reports have indicated the efficacy and safety of eculizumab in patients with aHUS.[4,5] In Japan, it was approved for the treatment of aHUS in September 2013.

Here we describe the clinical features of a child with aHUS due to autoantibody against complement factor H (CFH), who was treated successfully with eculizumab as first-line therapy.

Correspondence: Akira Ashida, MD PhD, Department of Pediatrics, Osaka Medical College, 2-7 Daigakumachi, Takatsuki, Osaka 569-8686, Japan. Email: ped006@poh.osaka-med.ac.jp

Received 22 April 2014; revised 19 June 2014; accepted 18 July 2014.
doi: 10.1111/ped.12469

Case report

The patient was a 4-year-old Japanese boy who was the second child of non-consanguineous parents. He had an elder brother and a younger sister, both of whom were healthy. He had been brought to his family physician with a 2 day history of headache,

nausea, appetite loss, and low-grade fever. Given that anemia, thrombocytopenia, and acute kidney injury were evident, he was tentatively diagnosed as having HUS, and referred to hospital for intensive care. The clinical course is summarized in Figure 1. On admission his complexion was pale and slightly icteric. Other physical data included bodyweight, 14.9 kg; body temperature, 37.5°C; pulse rate, 144 beats/min; and blood pressure, 106/60 mmHg. Neither hepatosplenomegaly nor enlargement of superficial lymph nodes was found. The laboratory findings on admission are summarized in Table 1. Among them, severe anemia, thrombocytopenia, hyperbilirubinemia, elevated lactate dehydrogenase, elevation of serum renal function markers including creatinine, and low C3, were remarkable. Both the direct and indirect Coomb's tests were negative. Hemostatic tests showed that prothrombin time and activated partial thromboplastin time were both within the normal range, but that fibrin/fibrinogen degradation products were elevated. Furthermore, red blood cell (RBC) fragmentation was found in a peripheral blood smear. Stool culture failed to identify Shiga toxin-producing EHEC, or both Shiga toxins 1 and 2. Although the patient had macrohematuria, moderate proteinuria, and elevation of serum renal function markers, he did not fall into the category of oliguria or severe electrolyte abnormality. For this reason, urgent dialysis was not initiated. On the following day (hospital day [HD] 2), fresh frozen plasma (FFP; 23 mL/kg) was infused in order to supply normal complement regulatory factors under a tentative diagnosis of aHUS, given that diarrhea was absent. On the third day (HD 3), however, the patient's clinical symptoms worsened, and RBC concentrates were therefore transfused. Given that plasma a disintegrin-like and metalloproteinase with thrombospondin type I motifs, number 13 (ADAMTS13) activity was 120% on the night of HD 3, the patient was definitively diagnosed as having aHUS, and given eculizumab at a dose of 600 mg. On the second day after eculizumab treatment (HD 5), the macrohematuria dramatically resolved, and thereafter hematology showed gradual improvement. On HD 10, the patient started to receive eculizumab at the maintenance dose (300 mg) by injection every 2 weeks. The patient was vaccinated against *Neisseria meningococcus* and *Streptococcus pneumonia* on HD 29 and HD37, respectively, and received prophylactic antibiotic therapy with cefditoren pivoxil until 2 weeks after vaccination for meningococcus. He was discharged with no sequelae on HD32, and thereafter received an injection of eculizumab at the maintenance dose (300 mg) every 2 weeks. There were no adverse events associated with eculizumab treatment, including infusion reaction or infection, in the whole period of observation, or any further recurrence of aHUS.

Retrograde analysis including hemolytic assay, and Western blotting for detection of anti-CFH antibody and complement factor H-related protein 1/3 (CFHR 1/3) were performed using the patient's plasma, which had been obtained before plasma infusion using the method reported previously.[6,7] Comprehensive gene mutation analysis of CFH, complement factor I (CFI), complement factor B (CFB), C3, membrane cofactor protein (MCP), and thrombomodulin, was also performed as described previously.[6] The patient's plasma enhanced the hemolysis of sheep erythrocytes and this effect was suppressed by addition of purified CFH, indicating impairment of host cell protection by CFH (Fig. 2). Anti-CFH antibody was detected in the patient's plasma, but no deficiency of the protein encoded by CFHR 1/3 was observed (Fig. 2).[8] Additionally, there were no mutations of CFH, CFI, CFB, C3, MCP, or thrombomodulin. Therefore, the patient was diagnosed as having aHUS due to autoantibody against CFH without CFHR 1/3 protein deficiency.

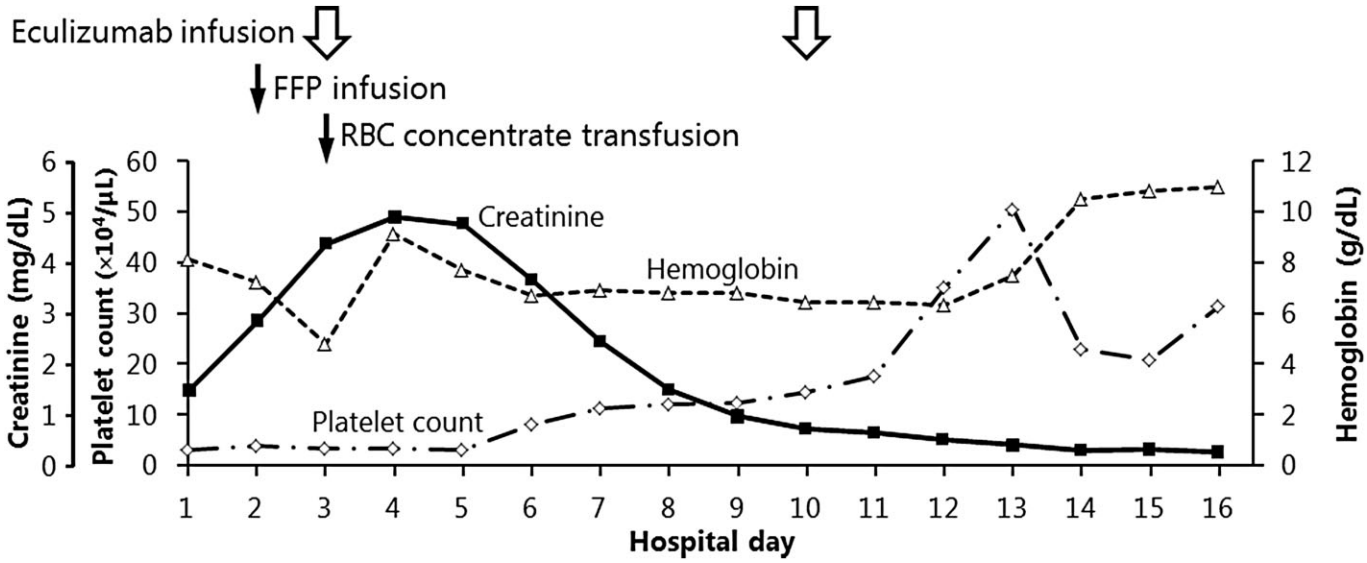

Fig. 1 Clinical course of treatment for atypical hemolytic uremic syndrome. Although fresh frozen plasma (FFP; 23 mL/kg) and red blood cell (RBC) concentrate were transfused on hospital days 2 and 3, laboratory findings including creatinine and platelet count worsened. After initiation of eculizumab, however, all of the laboratory parameters improved.

Table 1 Laboratory findings on admission

Peripheral blood		Stool culture	
WBC	9500 /μl	Normal flora	
RBC	300×10^4 /μl	EHEC	(–)
Hb	8.1 g/dL	Shiga-toxin	(–)
Ht	23.2%		
Platelet	1×10^4 /μl	Chemistry	
RBC fragmentation	(+)	TP	6.1 g/dL
		Alb	3.1 g/dL
Hemostatic test		Total bilirubin	2.6 mg/dL
PT	11.2 s	Indirect bilirubin	2.2 mg/dL
PT-INR	1.06	AST	101 IU/L
APTT	27.1 s	ALT	27 IU/L
Fibrinogen	278 mg/dL	LDH	3,570 IU/L
FDP	11.8 μg/mL	BUN	48.7 mg/dL
		UA	9.3 mg/dL
Urinalysis		Cr	1.51 mg/dL
Urine color	Light red	CRP	3.55 mg/dL
Occult blood	(4+)	Na	136 mmol/L
Protein	(2+)	K	3.8 mmol/L
Sediment		Cl	102 mmol/L
RBC	10–15/HPF	CK	403 IU/L
WBC	1–4/HPF	Haptoglobin	<10 mg/dL
Epithelium		Coombs test	
Epithelial cast	1+	Direct	(–)
		Indirect	(–)
Complement activity			
CH50	32.2 IU/L	Serological test	
C3	30.8 mg/dL	Total ANA	<40
C4	21.8 mg/dL	PR3-ANCA	<1.0
		MPO-ANCA	<1.0
ADAMTS13 activity	120%	ss-DNA antibody	<1.0
		ds-DNA antibody	<1.0

ADAMTS13, a disintegrin-like and metalloproteinase with thrombospondin type 1 motifs 13; ANCA, anti-neurophil cytoplasmic antibody; APTT, activated partial thromboplastin time; EHEC, enterohemorrhagic *Escherichia coli*; FDP, fibrin/fibrinogen degradation products; INR, international normalized ratio; MPO, myeloperoxidase; PR3, proteinase 3; PT, prothrombin time.

Discussion

Atypical hemolytic uremic syndrome is a rare disease characterized by hemolytic anemia, thrombocytopenia, and acute renal failure secondary to thrombotic microangiopathy. In recent years, aHUS has been found to be associated with dysregulation of the complement alternative pathway. In more than half of patients with aHUS, mutations in genes encoding complement-regulating protein including CFH, CFI, and MCP, have been reported.[1] Additionally, functional CFH deficiency due to autoantibodies against CFH has been reported, and this is highly associated with polymorphic homozygous deletion of genes encoding CFHR proteins 1 and 3.[1] The present patient had had no diarrhea, and neither EHEC nor Shiga toxin had been found in his stools. ADAMTS13 activity was 120%, which was within the normal range. aHUS associated with anti-CFH autoantibody was diagnosed on the basis of additional examinations including gene mutation analysis and Western blot analysis for anti-CFH antibody and proteins encoded by CFHR1/3.

Plasma exchange has been recommended as a first-line therapy for aHUS based on expert opinion rather than clinical trials.[2,3] For management of aHUS associated with anti-CFH autoantibodies, PE with FFP has been done for the purpose of removing anti-CFH autoantibodies and simultaneously supplying the circulating CFH pool. Although combination therapy with immunosuppressants has also been used, the rate of remission in response to short-term PE is 70–80%, and the rate of death or end-stage renal disease as a long-term outcome is 30–40% in patients with anti-CFH autoantibodies.[1] Additionally, it is difficult to determine whether the disease activity is stable and leads to remission, because no international standard for determining anti-CFH antibody and the levels of autoantibodies leading to disease relapse or exacerbation has been established.

In contrast, previous case reports have suggested that eculizumab is effective for treatment of aHUS.[4,5] Additionally, Legendre *et al*. noted the efficacy and safety of long-term eculizumab for thrombotic microangiopathy in aHUS patients, via two prospective phase 2 trials lasting 62–64 weeks.[9] Although reduction of the antibody load plays a very important role in aHUS associated with anti-CFH autoantibodies, eculizumab can effectively block the terminal complement cascade and stop further damage in the presence of anti-CFH autoantibodies. Noone *et al*. reported two cases of CFH autoantibody-positive HUS treated with eculizumab and proposed that eculizumab should be used in the acute phase for arresting the complement-mediated damage.[10]

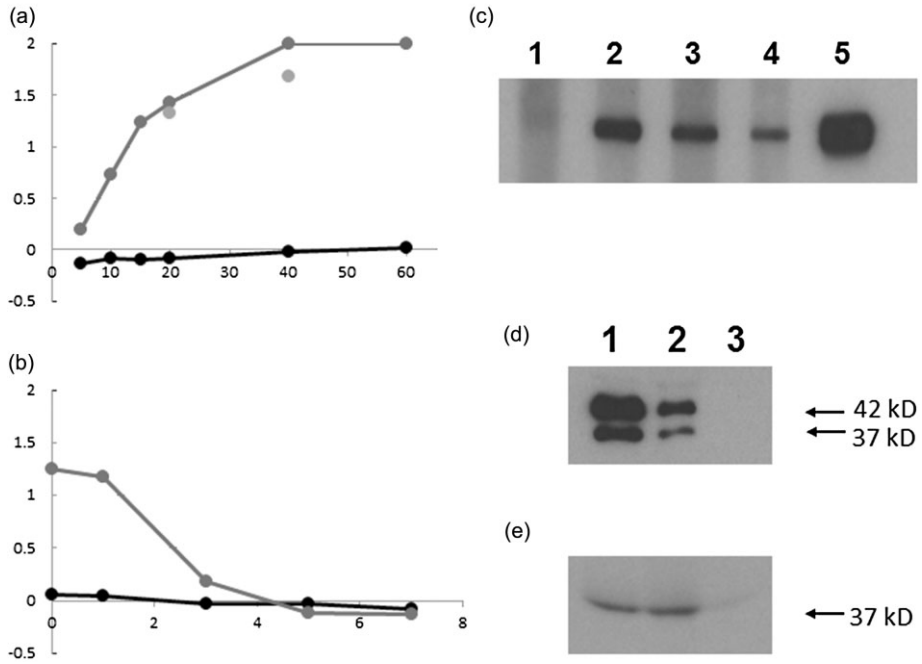

Fig. 2 (a,b) Hemolytic test and (c–e) Western blot analysis for detection of (c) anti-complement factor H (anti-CFH) autoantibodies and (d,e) protein encoded by *complement factor-H related protein CFHR1* and 3. (a) Lysis of sheep erythrocytes by addition of patient plasma. (a) OD_{414} titer sheep erythrocytolysis as a function of patient plasma. Plasma samples ranging from 5 µL to 60 µL were used. (b) Inhibition of enhanced hemolysis with 20 µL of plasma by adding purified CFH in amounts ranging from 0 µg to 7 µg. (—●—) Normal plasma ; (—●—) patient plasma; (●) normal plasma plus purified anti-CFH antibody. (c) Western blot analysis for detection of anti-CFH autoantibody. Lane 1, normal plasma; lane 2, patient plasma in the acute phase (hospital day [HD] 2); lane 3, patient plasma in the chronic phase (HD 31); lane 4, plasma of 3-year-old Japanese boy diagnosed with aHUS associated with anti-CFH autoantibody;[8] lane 5, CFH monoclonal antibody. (d,e) Western blot analysis for (d) CFHR 1 and (e) 3 proteins. (d) Plasma samples from a normal control, the present patient, and a patient who had been previously diagnosed as having deficiency of CFHR plasma proteins and autoantibody-positive HUS (DEAP-HUS)[8] were electrophoresed on a 12.0% SDS-polyacrylamide gel and transferred to a polyvinylidene fluoride membrane. After blocking with 5% dried milk, the membrane was incubated for 1.5 h at room temperature with mouse anti-human CFHR1 monoclonal antibody, the concentration of which was adjusted to 1 µg/mL. Then, 10 000-fold-diluted horseradish peroxidase (HRP)-labeled goat anti-mouse IgG antibody was used as the secondary antibody, and bound mouse monoclonal antibody was visualized using enhanced chemiluminescence substrate (Western Lightning-ECL; Perkin Elmer, Yokohama, Japan). (e) Western blot analysis for detection of CFHR 3 protein was done using the same method as for CFHR 1, with 1500-diluted rabbit anti-human CFHR 3 polyclonal antibody as the first antibody and 20 000-diluted HRP-labeled goat anti-rabbit IgG antibody as the secondary antibody. Lane 1, normal control; lane 2, present patient; lane 3, DEAP-HUS patient.[8]

Given that the present patient had neither oliguria nor electrolyte abnormalities including hyperkalemia, urgent dialysis was not necessary. Therefore, the patient received eculizumab as first-line therapy and was able to avoid the risk of complications associated with these maneuvers. Therapy with eculizumab was very effective, and no adverse events occurred. Zuber *et al*. proposed the use of eculizumab as first-line therapy for all episodes of aHUS in children because of its efficacy and safety, and for avoiding any potential complications of PE.[4]

Conclusion

The present study has demonstrated the efficacy and short-term safety of eculizumab as first-line therapy in the acute phase for aHUS associated with anti-CFH autoantibodies in a pediatric patient.

Acknowledgments

Yoshihiro Fujimura serves as a consultant to Alexion Pharmaceuticals and Alflessa Corporation. The other authors have no conflicts of interest.

References

1 Waters AM, Licht C. aHUS caused by complement dysregulation: New therapies on the horizon. *Pediatr. Nephrol.* 2011; **26**: 41–57.
2 Ariceta G, Besbas N, Johnson S *et al*. The European Pediatric Study Group for HUS. Guideline for the investigation and initial therapy of diarrhea-negative hemolytic uremic syndrome. *Pediatr. Nephrol.* 2009; **24**: 687–96.
3 Taylor CM, Machin S, Wigmore SJ, Goodship THJ, on behalf of a working party from the Renal Association, the British Committee for Standards in Haematology and the British Transplantation Society. Clinical Practice Guidelines for the management of atypical Haemolytic Uraemic Syndrome in the United Kingdom. *Br. J. Haematol.* 2009; **148**: 37–47.
4 Zuber J, Fakhouri F, Roumenina LT, Loirat C, Frémeaux-Bacchi V, on behalf of the French Study Group for aHUS/C3G. Use of eculizumab for atypical haemolytic uraemic syndrome and C3 glomerulopathies. *Nat. Rev. Nephrol.* 2012; **8**: 643–57.
5 Zuber J, Quintrec ML, Krid S *et al*. for the French Study Group for Atypical HUS. Eculizumab for atypical hemolytic uremic syndrome recurrence in renal transplantation. *Am. J. Transplant.* 2012; **12**: 3337–54.

6 Fan X, Yoshida Y, Honda S *et al*. Analysis of genetic and predisposing factors in Japanese patients with atypical hemolytic uremic syndrome. *Mol. Immunol.* 2013; **54**: 238–46.
7 Sánchez-Corral P, González-Rubio C, Rodríguez de Córdoba S *et al*. Functional analysis in serum from atypical hemolytic uremic syndrome patients reveals impaired protection of host cells associated with mutations in factor H. *Mol. Immunol.* 2004; **41**: 81–4.
8 Dragon-Durey MA, Sethi SK, Bagga A *et al*. Clinical features of anti-factor H autoantibody associated hemolytic uremic syndrome. *J. Am. Soc. Nephrol.* 2010; **21**: 2180–87.
9 Legendre CM, Licht C, Muus P *et al*. Terminal complement inhibitor eculizumab in atypical hemolytic-uremic syndrome. *N. Engl. J. Med.* 2013; **368**: 2169–81.
10 Noone D, Waters A, Pluthero FG *et al*. Successful treatment of DEAP-HUS with eculizumab. *Pediatr. Nephrol.* 2014; **29**: 841–51.

Stenosing ureteritis in Henoch–Schönlein purpura: Report of two cases

Katsuaki Kasahara, Osamu Uemura, Takuhito Nagai, Satoshi Yamakawa, Masaru Nakano and Naoyuki Iwata
Department of Pediatric Nephrology, Aichi Children's Health and Medical Center, Aichi-ken, Japan

Abstract Stenosing ureteritis (SU), a rare complication of Henoch–Schönlein purpura (HSP), typically presents with severe symptoms. We report the cases of two HSP patients presenting with gross hematuria, blood clotting, and colicky flank pain, followed by purpura on the lower extremities. Early-stage ultrasonography indicated hydronephrosis, thickened renal pelvic mucous membrane, and ureteral dilatation (UD), suggesting HSP complicated with SU. After early SU treatment with prednisolone, kidney function, thickened renal pelvic mucous membrane, and UD progressively normalized and the pain gradually disappeared. Regular ultrasonography of HSP patients from the onset of gross hematuria can be useful to detect early SU and facilitate conservative therapy with prednisolone. Diagnosis of SU can be easily missed by assuming HSP nephritis, particularly owing to the non-specific symptoms. Common characteristics as well as treatment methods and prognosis of SU are given in the literature review.

Key words gross hematuria, Henoch–Schönlein purpura, Henoch–Schönlein purpura nephritis, hydronephrosis, stenosing ureteritis, ultrasonography.

Henoch–Schönlein purpura (HSP) is the most common childhood systemic small-vessel vasculitis and can cause serious complications such as stenosing ureteritis (SU).[1,2] SU symptoms may be masked by gastrointestinal and renal symptoms and, in some cases, it may be diagnosed incidentally.[2–5] Depending on the course, various reports have stated the necessity of surgical treatment for SU, but the benefits of steroid monotherapy have also been noted.[2,6,7] We report the cases of two HSP patients presenting with ureteral stenosis, gross hematuria, and colicky flank pain that improved with prednisolone (PSL) therapy. Although an extensive literature review found >30 cases reports on the clinical spectrum of the complications, only seven English-language case reports published during 1997–2013 have been included (Table 1).[2–10]

Correspondence: Katsuaki Kasahara, MD, Department of Pediatric Nephrology, Aichi Children's Health and Medical Center, 1-2 Osakata, Morioka-chou, Oobu-shi, Aichi-ken 474-8710, Japan. Email: katsukasa@nifty.com

Received 11 March 2014; revised 24 June 2014; accepted 31 July 2014.
doi: 10.1111/ped.12471

Case reports

Patient 1

A 6-year-old boy, diagnosed with gastroenteritis by a local general practitioner, presented with a 3 day history of colicky flank pain and gross hematuria. The patient had a history of severe sinusitis and bilateral vesicoureteral reflux (stage III at 4 years of age), but no history of urinary tract infection (UTI) after 4 years of age. At presentation, he was afebrile and normotensive; on physical examination, tenderness was observed around the navel, with no evidence of purpura or joint pain.

Blood test results were as follows: white blood cell (WBC) count, 19 570/μL; platelet count, 35.0×10^4/μL; creatinine (Cr), 0.39 mg/dL; C-reactive protein (CRP), 7.6 mg/dL (normal, <0.5 mg/dL); complement component 3 (C3), 118 mg/dL (normal, 86–160 mg/dL); and D-dimer, 5.2 μg/mL (normal, <1.0 μg/dL). Urinary test results were as follows: urine protein, 300 mg/dL; urine sediment, 281/μL (normal, <5/μL) and 4865/μL (normal, <5/μL) for WBC and red blood cells (RBC; non-glomerular), respectively. Urine biochemistry was as follows: calcium/Cr ratio (Ca/Cr), 0.1 (normal, <0.31); and β-2 microglobulin (β2MG), 301 μg/L (normal, <230 μg/L). To exclude urolithiasis and colitis, ultrasonography and abdominal